JOURNAL OF GEOPHYSICAL RESEARCH

The continuation of

TERRESTRIAL MAGNETISM AND ATMOSPHERIC ELECTRICITY
(1896-1948)

An International Quarterly

VOLUME 60 September, 1955 NUMBER 3

CONTENTS

(Contents concluded on outside back cover)

Published at

THE WILLIAM BYRD PRESS, INC.

P. O. BOX 2-W, SHERWOOD AVE. AND DURHAM ST.

RICHMOND 5, VIRGINIA

Address all correspondence to

JOURNAL OF GEOPHYSICAL RESEARCH

5241 BROAD BRANCH ROAD, NORTHWEST

WASHINGTON 15, D.C., U.S.A.

SIX DOLLARS A YEAR SINGLE NUMBERS, TWO DOLLARS

JOURNAL OF GEOPHYSICAL RESEARCH

The continuation of

Terrestrial Magnetism and Atmospheric Electricity

(1896-1948)

An International Quarterly

Founded 1896 by L. A. BAUER *Continued 1928-1948 by* J. A. FLEMING

Fields of Interest

Terrestrial Magnetism
Atmospheric Electricity
The Ionosphere
Solar and Terrestrial Relationships
Aurora, Night Sky, and Zodiacal Light
The Ozone Layer
Meteorology of Highest Atmospheric Levels
The Constitution and Physical States of the Upper Atmosphere
Special Investigations of the Earth's Crust and Interior, including experimental seismic waves, physics of the deep ocean and ocean bottom, physics in geology
And similar topics

This Journal serves the interests of investigators concerned with terrestrial magnetism and electricity, the upper atmosphere, the earth's crust and interior by presenting papers of new analysis and interpretation or new experimental or observational approach, and contributions to international collaboration. It is not in a position to print, primarily for archive purposes, extensive tables of data from observatories or surveys, the significance of which has not been analyzed.

Forward *manuscripts* to one of the Associate Editors, or to the editorial office of the Journal at 5241 Broad Branch Road, Northwest, Washington 15, D. C., U. S. A. It is preferred that manuscripts be submitted in English, but communications in French, German, Italian, or Spanish are also acceptable. A brief abstract, preferably in English, must accompany each manuscript. A *publication charge* of $8 per page will be billed by the Editor to the institution which sponsors the work of any author; private individuals are not assessed page charges. Manuscripts from outside the United States are invited, and should not be withheld or delayed because of currency restrictions or other special difficulties relating to page charges. Costs of publication are roughly twice the total income from page charges and subscriptions, and are met by subsidies from the Carnegie Institution of Washington and international and private sources.

Back issues and *reprints* are handled by the Editorial Office, 5241 Broad Branch Road, N.W. Washington 15, D.C., U.S.A.

Subscriptions are handled by the Editorial Office, 5241 Broad Branch Road, N.W., Washington 15, D.C., U.S.A.

Entered as second-class matter at the Post Office at Richmond, Virginia, under the act of March 3, 1879.

Journal of

GEOPHYSICAL RESEARCH

The continuation of

Terrestrial Magnetism and Atmospheric Electricity

VOLUME 60 SEPTEMBER, 1955 No. 3

GEOMAGNETIC DISTORTION OF THE *F*2 REGION ON THE MAGNETIC EQUATOR

BY MOTOKAZU HIRONO AND HIROSHI MAEDA

Geophysical Institute, Kyoto University, Kyoto, Japan

(Received March 7, 1955)

ABSTRACT

The direct relation between the geomagnetic S_q-variation and the vertical electron drift of the *F*2 region on the magnetic equator is examined.

It is shown that the electric field in the *F*2 region accompanied by S_q electric current produces the vertical drift which is sufficient to interpret the main features of the anomaly of the *F*2 region on the equator. It is to be noticed that the main term of the drift velocity is diurnal. The daily variations of the maximum electron density and its height in the *F*2 region are calculated under consideration of the vertical electron drift for the reasonable distribution of decay coefficient with altitude inferred by observed results. The calculated *F*2 daily variations have a striking resemblance with those observed near the magnetic equator. When the ion production takes its maximum value at about 200 km, there appears a lower secondary maximum of electron density which agrees well with the observed *F*1 layer.

The change of characteristics of daily variations of the *F*2 region with the sunspot-cycle is likely to be accounted for by a slight shift of the phase of the drift.

1. INTRODUCTION

Analyses of ionospheric data and theoretical researches by Martyn [see 1 of "References" at end of paper], Mitra [2], and Weiss [3] have established the existence of solar semi-diurnal components of tidal origin in the maximum electron concentration N_m of the $F2$ region and its height h_m , and further studies have been made by K. Maeda [4].

We tried to find a direct relation between the daily variation of the earth's magnetic field and the vertical electron drift in the $F2$ region on the magnetic equator.

McNish and Gautier [5] have attacked a similar problem, and an interesting relation between these data is shown. Their theoretical consideration, however, is confined to the vertical drift due to the electric field induced by the daily variation of the magnetic field, whereas the drift due to the electrostatic field is not taken into account. According to our results, the latter is so much greater than the former that we disregarded the drift due to electromagnetic induction.

2. OBSERVED DATA OF F REGION NEAR THE EQUATOR

The world-wide distribution of $N_m(F2)$, which is closely related with the earth's magnetic field, was studied by Uyeda and others [6] and by Appleton [7]. Further studies have been made by Bailey [8], Uyeda [9], and Aono [10]. According to their results, for noon conditions, there is a belt of low values of $N_m(F2)$ circling the earth and centered roughly on the magnetic equator, and the maximum value of $N_m(F2)$ is attained roughly at about the 20° north and south geomagnetic latitudes. The data analyzed in detail came from Huancayo, close to the magnetic equator (geomag. 0°.6 south, 6°.2 west, dip 2°), and from Maui, at about 20° geomagnetic latitudes (geomag. 20.°9 north, 88°.1 west, dip 40°). All information was extracted from "Ionospheric Data" of the Central Radio Propagation Laboratory, National Bureau of Standards, Boulder, Colorado.

The values of $N_m(F2)$ are calculated from f^oF2 and h_m from the value of $(M\ 3{,}000)F2$, which will be denoted by M, using a formula by Shimazaki [11], that is,

$$h_m = -176 + 1490/M \qquad \text{(km)}$$

Various daily-variation curves are shown in Figure 1.

For Huancayo, the daily variations are averaged from one year; and for Maui, the N curves are averaged from the northern solstice of May, June, July, and August, the E curves from the equinoctial months of March, April, September, and October, and the S curves from the southern solstice of November, December, January, and February. For Huancayo, $h'F2$, $h'F1$, and $N_m(F1)$ are illustrated as well, and the average daily variations for 1942-44 obtained by Martyn [1] are shown in addition.

It can be seen from the C.R.P.L. data that the daily variations at stations close to the magnetic equator bear a good resemblance; moreover they are very similar to those observed at summer conditions in the middle and high latitudes. The values of $N_m(F2)$ and $N_m(F1)$ at noon of sunspot maximum at Huancayo are about 2.4 and 1.6 times those of sunspot minimum. The forenoon maximum of

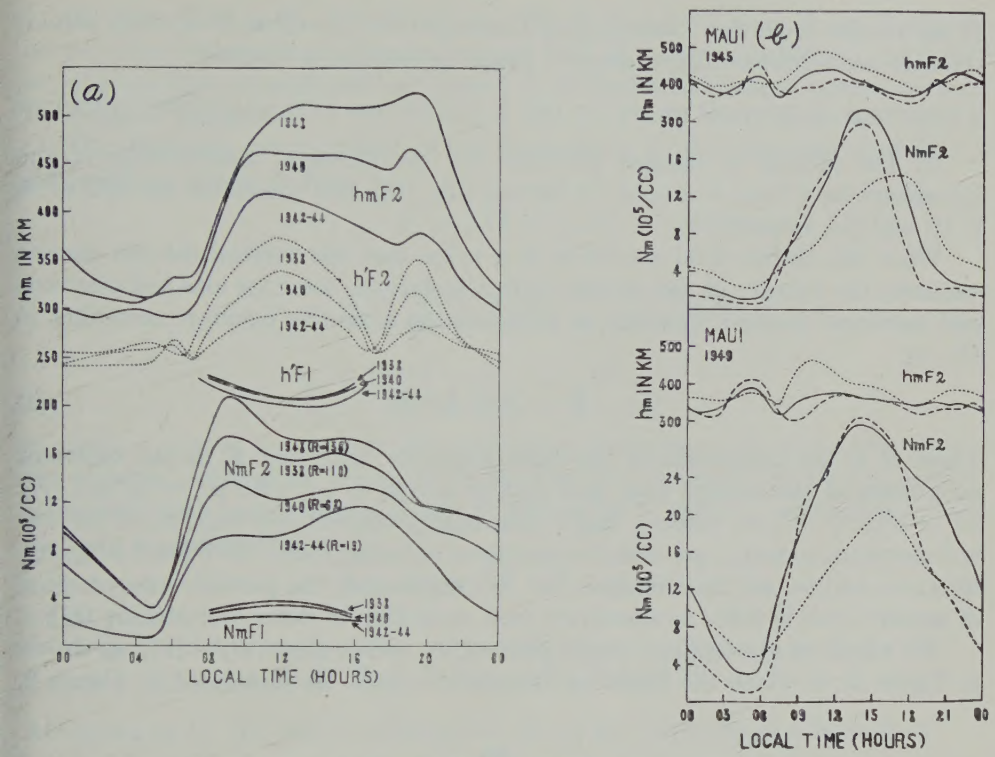

FIG. 1—(*a*) Daily variations of $N_m(F2)$, $h_m(F2)$, $h'(F2)$, $N_m(F1)$, and $h'(F1)$ at Huancayo in years of different sunspot-numbers

(*b*) Daily variations of $N_m(F2)$ and $h_m(F2)$ at Maui; dotted lines refer to the northern solstice, dashed lines to the southern solstice, and full lines to the equinox

$N_m(F2)$ is smaller than the afternoon maximum of $N_m(F2)$ for the sunspot-minimum period. The former increases in relation to the latter with the increase of sunspot-number.

The daily variations of h_m at Huancayo and Maui were subjected to a harmonic analysis, and the amplitudes P_n and phases t_n when maximum value was attained for nth term are shown in Table 1.

TABLE 1

Station	Year	Season	P_0	P_1	t_1	P_2	t_2	P_3	t_3
			km	*km*	*hr*	*km*	*hr*	*km*	*hr*
Huancayo	1942–44	Mean	350	61.9	14.2	15.3	10.7	14.6	3.2
	1940	Mean	394	87.8	14.9	13.7	9.7	16.0	3.2
	1948	Mean	429	110.6	15.7	16.8	9.4	8.0	2.3
Maui	1945	*N*	327	28.0	12.0	30.1	0.6	4.6	4.6
	1945	*E*	306	9.2	9.6	21.7	10.9	16.8	5.3
	1945	*S*	294	14.2	6.3	8.6	10.7	25.6	5.6

It can be seen from this Table that at Huancayo the diurnal term is much greater than the semi-diurnal one, whereas at Maui the relation is reversed.

3. VERTICAL ELECTRON DRIFT OF THE *F* REGION ON THE MAGNETIC EQUATOR

(i) The motion of charged particles and the electrical conductivity of the ionosphere have been discussed by Hirono [12], [13], [14] (hereafter referred to as I, II, and III, respectively).

When the electric field attains such a value that the vertical electric current vanishes, the velocity of the vertical drift, which is the same for ions and electrons and measured positive upwards, is given on the magnetic equator, according to III, by

$$W = f(h) \cdot E_y/H \quad \ldots\ldots\ldots\ldots\ldots\ldots\ldots\ldots\ldots\ldots (1)$$

where H is the magnitude of the main magnetic field, and E_y is the eastward component of the electric field, and $f(h) \simeq p_i/(p_i + p_e)$ with $p_r = (1/m_r)\{\nu_r/(\nu_r^2 + \omega_r^2)\}$, $(r = i, e)$, where ν_i and ν_e are roughly the collision frequencies for ions and electrons, ω_i and ω_e are their frequencies of spiraling round the lines of magnetic force; m_i and m_e are their masses. For this expression, the particle concentration of negative ions is taken as effectively zero, according to Bates and Massey [15].

We adopt an atmospheric model inferred by rocket observation [16], as shown in Figure 2, to which the following calculations refer. As illustrated in Figure 2,

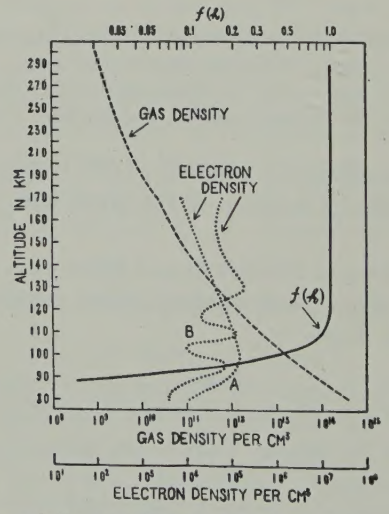

FIG. 2—Atmosphere model, variations of electron density and $f(h) = W/(E_y/H) \simeq p_i/(p_i + p_e)$ with altitude; curve A denotes the Chapman layer, and curve B is inferred from rocket observations [21]

$f(h)$ is nearly unity above the height of about 120 km and decreases rapidly in the lower region. When the vertical current is not much greater than the horizontal one, equation (1) holds approximately for the vertical electron drift in the F region.

(ii) According to the dynamo theory, the electromotive force of the S_q-current on the magnetic equator is the electrostatic field. It is shown in II from the theory of potential that the eastward component E_y of this field is almost constant between the E and F regions.

The electrical conductivity of the ionosphere in the east-west direction is expressed, as shown in I, by

$$\sigma_3 = \sigma_1(1 + \sigma_2^2/\sigma_1^2)$$

where

$$\sigma_1 = e^2\left(\frac{n_e}{m_e}\cdot\frac{\nu_e}{\nu_e^2+\omega_e^2} + \frac{n_i}{m_i}\cdot\frac{\nu_i}{\nu_i^2+\omega_i^2}\right)$$

$$\sigma_2 = \frac{n_e\cdot e}{H}\left(\frac{\omega_e^2}{\nu_e^2+\omega_e^2} - \frac{\omega_i^2}{\nu_i^2+\omega_i^2}\right)$$

in which n_e and n_i are particle concentrations of electrons and ions, and e denotes the absolute value of the charge of an electron. Let the eastward electric currents integrated with height in the E and F regions be I_1 and I_2 , respectively. Then we have approximately

$$I_1 = K_1\cdot E_y\,, \qquad I_2 = K_2\cdot E_y \ldots\ldots\ldots\ldots\ldots\ldots (2)$$

where

$$K_1 = \int_E \sigma_3\,\mathrm{d}h, \qquad K_2 = \int_F \sigma_3\,\mathrm{d}h$$

According to II, III, and H. Maeda [17], $K_1 \gg K_2$; therefore, it follows that

$$I_1 \gg I_2$$

Put $I_1 + I_2 = I$, and let the magnetic variation due to I at the lower edge of the E region be δH. Then we have

$$\delta H = 2\pi I \simeq 2\pi I_1 \ldots\ldots\ldots\ldots\ldots\ldots\ldots\ldots (3)$$

Considering the fact that about 80 per cent of the daily magnetic variation ΔH on the ground is caused by I, and that this magnetic field due to I increases upwards and the amount of the increase will be about 20 per cent at the lower edge of the E region [18], we have approximately

$$\Delta H \simeq \delta H \simeq 2\pi K_1\cdot E_y \ldots\ldots\ldots\ldots\ldots\ldots\ldots\ldots (4)$$

When the values of ΔH and K_1 are known, we can determine the value of E_y using this relation.

(iii) M. Hasegawa and H. Maeda [19] have estimated the daily variations of electrical conductivity of the S_q-layers (mainly the E layer), and as result of this analysis the daily variations of electric field and the zero-level (C_0) of the S_q-variations have also been estimated. Further, H. Maeda [20] has made his calculations on Huancayo's geomagnetic data for a period of 12 years, and the results for the mean states of sunspot-minimum years and of sunspot-maximum years are as follows in units of 10^{-5} emu:

$$\Delta H = C_0 + \sum_n C_n \sin(n\lambda + \epsilon_n) \ldots\ldots\ldots\ldots\ldots\ldots (5)$$

Years	Average sunspot-number (R)	C_0	C_1	ϵ_1	C_2	ϵ_2	C_3	ϵ_3
				°		°		°
1922,23,32,33	8 (min)	15.1	32.5	280.2	15.8	108.4	5.8	306.0
1926,27,28,29	71 (max)	24.3	52.4	274.1	25.7	103.9	10.9	302.2

$$K_1 = K_0\{1 + \sum_n \gamma_n \cos(n\lambda + \delta_n)\} \quad \text{(emu)} \ldots\ldots\ldots\ldots (6)$$

γ_1	δ_1	γ_2	δ_2
1.15	180°	0.42	0°

(Almost independent of sunspot-number)

where λ is the local time in angular measure from midnight and ΔH is measured positive northwards. The daily variation of K_1/K_0 is shown in Figure 3.

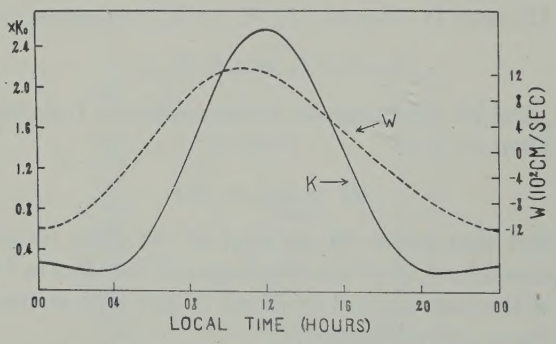

FIG. 3—Daily variations of electrical conductivity in units K_0 , and of vertical electron-drift velocity W for sunspot-minimum at a height of 300 km referred to curve A in Fig. 2

On the magnetic equator, Hall conductivities σ_{xy} and σ_{yx} vanish and Ohm's law holds in its original form, so that the results estimated by the method of the above authors are theoretically adequate. The noon value of integrated conductivity of the E layer, calculated as a simple Chapman layer of scale height = 10 km, maximum electron density at noon = 1.5×10^5/cc (for sunspot-minimum), height of maximum ion production = 100 km as shown by curve A in Figure 2, is 3.4×10^{-7} emu, so that from relation (6) K_0 becomes 1.3×10^{-7} emu. For the sunspot-maximum period mentioned above, we take $K_0 = 1.65 \times 10^{-7}$ emu, corresponding to the maximum electron density of 1.9×10^5/cc for the E layer.

The electrostatic field E_y expressed in Fourier series does not include a constant

term, since this is derived from the potential. Therefore, we have the following expression of E_y and Table 2 in connection with relations (4), (5), and (6), using the value of K_0 estimated above:

$$E_y = y_1 \sin(\lambda + \theta_1) + y_2 \sin(2\lambda + \theta_2) \quad \text{(emu)} \ldots\ldots\ldots\ldots (7)$$

TABLE 2

Years	y_1	θ_1	y_2	θ_2
		°		°
Sunspot-minimum	3.34×10^2	280	0.36×10^2	176
Sunspot-maximum	4.19×10^2	265	0.81×10^2	171

If we take the value of $H = 0.27$ gauss at the height of the F region over Huancayo, from (1) and (7), we have the following drift velocity:

$$W = f(h)\{W_1 \sin(\lambda + \theta_1) + W_2 \sin(2\lambda + \theta_2)\} \ldots\ldots\ldots\ldots (8)$$

where

$$\left.\begin{array}{l} W_1 = 1.24 \times 10^3 \text{ cm/sec} \\ W_2 = 0.13 \times 10^3 \text{ cm/sec} \end{array}\right\} \text{for sunspot-minimum period}$$

$$\left.\begin{array}{l} W_1 = 1.55 \times 10^3 \text{ cm/sec} \\ W_2 = 0.30 \times 10^3 \text{ cm/sec} \end{array}\right\} \text{for sunspot-maximum period} \quad \ldots\ldots\ldots (9)$$

The daily variation of W for sunspot-minimum at an altitude of 300 km is shown in Figure 3. The value of K_0 is influenced to some extent by the assumed electron-density distribution with altitude. If the electron density above 100 km is 1.5×10^5/cc and that below is the same as the above-mentioned Chapman layer, K_0 is increased by about 10 per cent. This variation is very small.

On the other hand, when we adopt an electron-density distribution with altitude inferred by rocket observation [21], as shown by curve B in Figure 2, K_0 takes one-half of the above-mentioned values, that is, 6.5×10^{-8} emu for sunspot-minimum and 8.3×10^{-8} emu for sunspot-maximum. If these values of K_0 are used, the electric field E_y and drift velocity W become twice as great as those represented by (8) and (9).

Effective conductivity σ_3 is obtained under the assumption that the electric and magnetic fields are completely uniform; therefore, if they are not completely so, the effective conductivity in the E-W direction may be slightly less than σ_3. Then the decrease in K_0 will give slightly greater values for W in any case.

4. SOLUTION OF THE CONTINUITY EQUATIONS

Let units of height $\mathfrak{H}$ be 50 km and $z = (h - h_0)/\mathfrak{H}$, and let $z = 0$ at an altitude of 300 km. In the F region, the local scale-height of the atmosphere $\mathfrak{H}(F)$ is taken to be the same as $\mathfrak{H}$, but in the E region the local scale-height is taken to be a function of altitude, which may be deduced from Figure 2.

The equation of motion for an electron is $dh/dt = W$, which may be transformed to

$$\frac{dz}{d\lambda} = 1.37 \times 10^4 \frac{W}{\mathfrak{X}} \quad \text{.....(10)}$$

The solution of this equation for a prescribed value of W may be written

$$z = z(z_0 , \lambda) \quad \text{.....(11)}$$

with z_0 fixed by initial conditions at $\lambda = \lambda_0$.

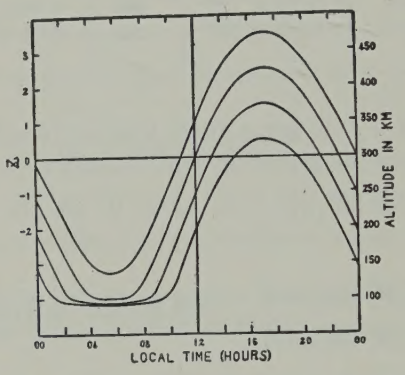

FIG. 4—Solutions of the subsidiary equation $dh/dt = W$ for some initial values of h

In Figure 4, several curves emerging from (11), derived from (8) and (9) for the sunspot-minimum period, are illustrated for some values of z_0 . According to this Figure, it was found that a part of the electrons in the $F2$ region descends at night and enters into the E region. In a later section, however, the results of calculation show that the electron density in the cell, which descends below 300 km, rapidly decreases because of a great recombination coefficient in the lower region, tending to be several times 10^4/cc, and the electron density of the E region does not seem to be appreciably influenced. Thus, $h_m(F2)$ does not descend much below the 300-km level.

Theoretical discussion of the effect of the vertical electron drift upon an ionized region, necessitates a consideration of the equation of continuity

$$\frac{\partial N}{\partial t} = I - \alpha N^2 - \frac{\partial}{\partial h}(N \cdot W) \quad \text{.....(12)}$$

where N stands for electron density per cc, I for ion production per cc per second, and α for the recombination coefficient. This equation is to be solved subject to the subsidiary condition (11) imposed by the drift.

In the F region, W is estimated to be almost independent of altitude, so that we have

$$\frac{dN}{dt} = [I]_z - [\alpha]_z N^2 \quad \text{.....(13)}$$

where d/dt stands for a derivative "following the motion." In this equation, I and α are to be evaluated at the height z, which is obtained from (11) as a function of z_0 and t. It is shown by Bates and Massey [22] that $\alpha = 8 \times 10^{-11}$cc/sec in the $F2$ region and $\alpha = 4 \times 10^{-9}$ cc/sec in the $F1$ region (independent of pressure) in the daytime. For the $F2$ region at night, Ratcliffe [23] obtained a recombination coefficient of the same order of magnitude as the above daytime value, in the absence of the vertical drift influence. Therefore, we take $\alpha = \alpha_0\ \xi(z)$, where $\xi(z)$ is taken to be unity for $z \geq 0$ and 50 for $z \leq -1$, as illustrated in Figure 5. For the electrons which have descended into the E region at night, a third term

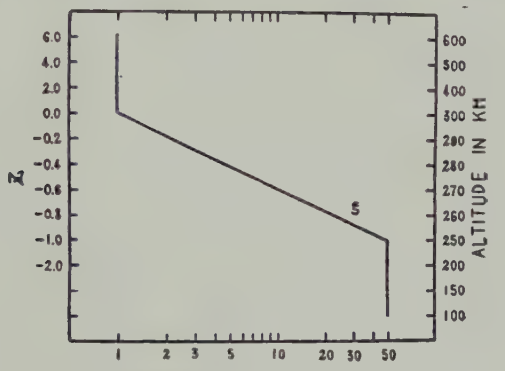

FIG. 5—Variation of $\xi(z) = \alpha(z)/\alpha_0$ with altitude

including the vertical gradient of W appears on the right-hand side of (13). In the following calculation, this term is neglected. According to the study by Weiss [3] on the variation of electron density at night, this neglection will be justified when we confine our attention to the daily variation of electron concentration in the F region. For the distribution of ion production, the following two types (a) and (b) are considered:

(a) *The maximum of ion production at noon is located at* 300 *km*

According to S. Chapman [24],

$$I = I_0 F(z, \chi)$$

where

$$F(z, \chi) = \exp\{1 - z - \exp(-z) Ch(R + z, \chi)\}$$

and $Ch(R + z, \chi)$ is a complicated function of R and the solar zenith-angle χ, $R = 150$ being used here. After some transformation of (13) and by putting $N_0(a) = (I_0/\alpha_0)^{\frac{1}{2}}$ and $\nu = N/N_0$, we get

$$\sigma_a \frac{d\nu}{d\lambda} = [F]_z - [\xi]_z \nu^2 \qquad (14)$$

where

$$1/\sigma_a = 1.37 \times 10^4 (I_0 \alpha_0)^{1/2}.$$

(b) *The maximum of ion production at noon is located at* 200 *km*

Bradbury [25], Mohler [26], and Bates [27] suggested that the $F1$ and $F2$

layers are produced by the same atoms or molecules ionized by the same ultraviolet, and the two layers are separated by a rapid change of the recombination coefficient with altitude. To examine the effect of the drift upon an ionized region under such conditions, we take $I = I_0 F(z + 2, \chi)$. Putting $N_0(b) = \{I_0 F(2, 0)/\alpha_0\}^{\frac{1}{2}}$, $\nu = N/N_0$, and $F' = F(z + 2, \chi)/F(2, 0)$, and after some transformation of (13), we get

$$\sigma_b \frac{d\nu}{d\lambda} = [F']_z - [\xi]_z \nu^2 \quad \ldots\ldots\ldots\ldots\ldots\ldots\ldots\ldots (15)$$

where

$$1/\sigma_b = 1.37 \times 10^4 \{I_0 F(2, 0)\alpha_0\}^{1/2}.$$

5. DISTORTION OF THE F REGION BY DRIFT SUBJECT TO S_q-CURRENT

To evaluate the effect of S_q drift on the F region on the equator, we solved equations (14) and (15) following the motion subject to the subsidiary condition (11), using the method of Millington [28]. Numerical integration is made at an interval of 10° of local time λ, but between the height $-1 < z < 0$ the interval was taken to be 5°. Using these solutions, the maximum electron density ν_m in units of N_0 and its height h_m ($= z_m \cdot \mathcal{H} + 300$ km) are illustrated in Figure 6. The details of the cases calculated are summarized in Table 3.

TABLE 3

Case	Continuity equation used	Drift velocity				Curve in Figure 6 illustrating
		W_1	θ_1	W_2	θ_2	
		(cm/sec)		(cm/sec)		
1	(14) with $\sigma_a = 1$	1.24×10^3	280° ($11^h.3\uparrow$)	0.13×10^3	176°	(a), Curve A
2	(14) with $\sigma_a = 1$	2.48×10^3	280° ($11^h.3\uparrow$)	0.26×10^3	176°	Curve B
3	(15) with $\sigma_b = 1$	1.24×10^3	280° ($11^h.3\uparrow$)	0.13×10^3	176°	(b), Curve A
4	(15) with $\sigma_b = 1$	2.48×10^3	280° ($11^h.3\uparrow$)	0.26×10^3	176°	Curve B
5	(14) with $\sigma_a = 1$	1.24×10^3	0° ($6^h.0\uparrow$)	0	.....	(c), Curve A
6	(14) with $\sigma_a = 1$	1.24×10^3	180° ($18^h.0\uparrow$)	0	.....	Curve B
7	(15) with $\sigma_b = 1/1.5$	3.10×10^3	265° ($12^h.3\uparrow$)	0	.....	(d)
8	(15) with $\sigma_b = 1$	2.48×10^3	250° ($13^h.3\uparrow$)	0	.....	(e)

(*i*) In the $F2$ region, it is estimated that σ_a and σ_b in (14) and (15) are close to unity. Therefore, the cases 1 to 4 in Table 3 are calculated. In any case, the corresponding values ν_{0m} and h_{0m} for the static Chapman layer are shown in the same Figure, but by dotted lines.

The variations of ν_m and h_m of these four cases are very similar to those observed at Huancayo at the period of minimum and moderate sunspot-numbers. In general, ν_m is smaller than ν_{0m}, and at noon the decrease $\delta\nu_m$ from ν_{0m} is between 40 and 60

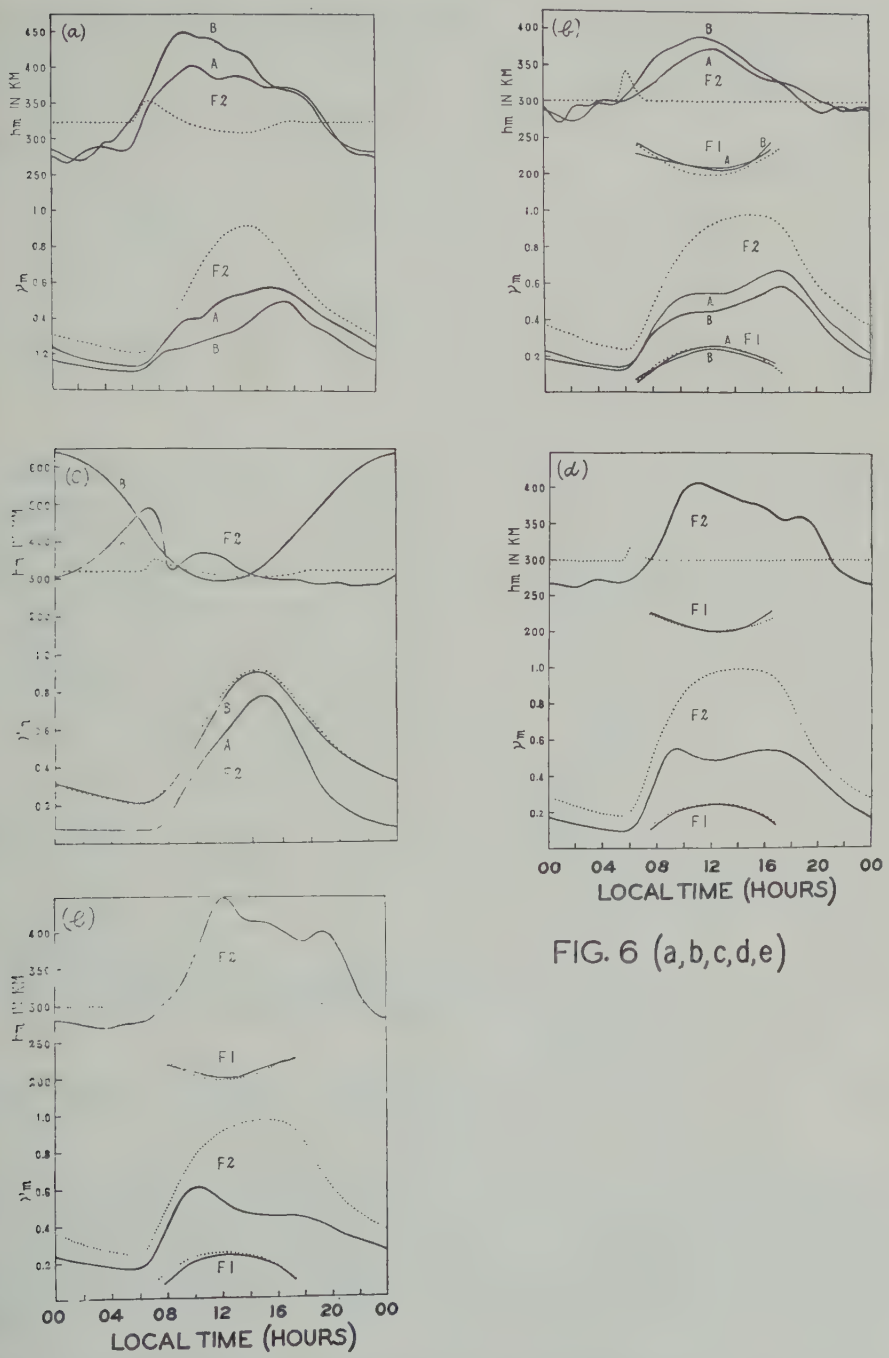

FIG. 6 (a,b,c,d,e)

FIG. 6—Calculated daily variations of $\nu_m(F2) = N_m(F2)/N_0$, $h_m(F2)$, $\nu_m(F1) = N_m(F1)/N_0$, and $h_m(F1)$ for static (dotted lines) and moving (full lines) regions; every curve is obtained under the conditions shown in Table 3

per cent, and the maximum of ν_m is attained in the afternoon. The daily variations of h_m are subjected to harmonic analysis, and amplitudes P_n and phases t_n of the terms are shown in Table 4.

TABLE 4

Case	P_0	P_1	t_1	P_2	t_2	P_3	t_3
	km	*km*	*hr*	*km*	*hr*	*km*	*hr*
1	338	62.5	13.3	7.9	9.1	13.4	1.8
2	347	82.4	12.4	15.9	10.2	8.3	2.3
3	321	36.1	12.6	9.3	0.2	6.4	2.7
4	326	51.3	12.0	10.7	11.1	2.1	7.6

Comparing these values with those calculated from the observed data at Huancayo (1942-44), as shown in section 2, it is to be noticed that cases 1 and 4 fit well with those observed. However, so far as ν_m is concerned, cases 3 and 4 are in better agreement with those observed; moreover, in the two cases, there appears a lower secondary maximum of electron density which may be termed as $\nu_m(F1)$.

The daily variations of $\nu_m(F1)$ and its height $h_m(F1)$ do not show appreciable departures from the static Chapman norm because of a great recombination coefficient and ion production in the altitudes. At noon, we have $\nu_m(F1)N_0(b) = 2.5 \times 10^5$/cc, if we take $N_0(b) = 10^6$/cc, and at the same time $h_m(F1) \simeq 200$ km. Thus, the lower layer is very similar to the observed $F1$ region.

(*ii*) The question may arise whether or not the drift W with other phases than those derived from (7) have similar effects upon the ionized region. To answer this question, cases 5 and 6 have been calculated. The variations of h_m in these cases do not resemble those observed near the magnetic equator. The variations of ν_m do not show appreciable departures from the static Chapman norm ν_{0m}, and, especially in case 6, we see that $\nu_m \simeq \nu_{0m}$. If the value of W appropriately takes less value in case 6, ν_m will be greater than ν_{0m} by about ten per cent, since in this case the motion of a cell is in phase throughout the day with the motion of the level of maximum ion production.

(*iii*) As shown in Table 2, the phase θ_1 of the diurnal term of E_y for the sunspot-maximum period is 265° instead of 280° for sunspot-minimum. The range of errors for the phases may be several degrees at the present stage of calculation and much significance may not be attached to the difference of phases until further confirmed. Moreover, the value of E_y in the E and F regions may not be strictly the same, and the difference may be 10 or 20 per cent. To find the change of characteristics of daily variations with the anticipated phase-shift of E_y and hence of W, cases 7 and 8 (shown in Table 3) were calculated for the phases of W ($12^h3\uparrow$) and ($13^h3\uparrow$).

As before, in these cases, two maxima of ν_m appear in the forenoon and afternoon. The forenoon maximum is of an order of magnitude almost comparable with the afternoon maximum for case 7, and the former is greater than the latter for case 8. Moreover, for case 8, after sunset, rapid increase of h_m appears for about

one hour and is followed by gradual decrease. These characteristics in the daily variations of v_m and h_m are very similar to those observed at sunspot-maximum at Huancayo.

The courses of the electron-density contours *vs* altitude throughout the 24-hour period for cases 4 and 7 are illustrated in Figure 7.

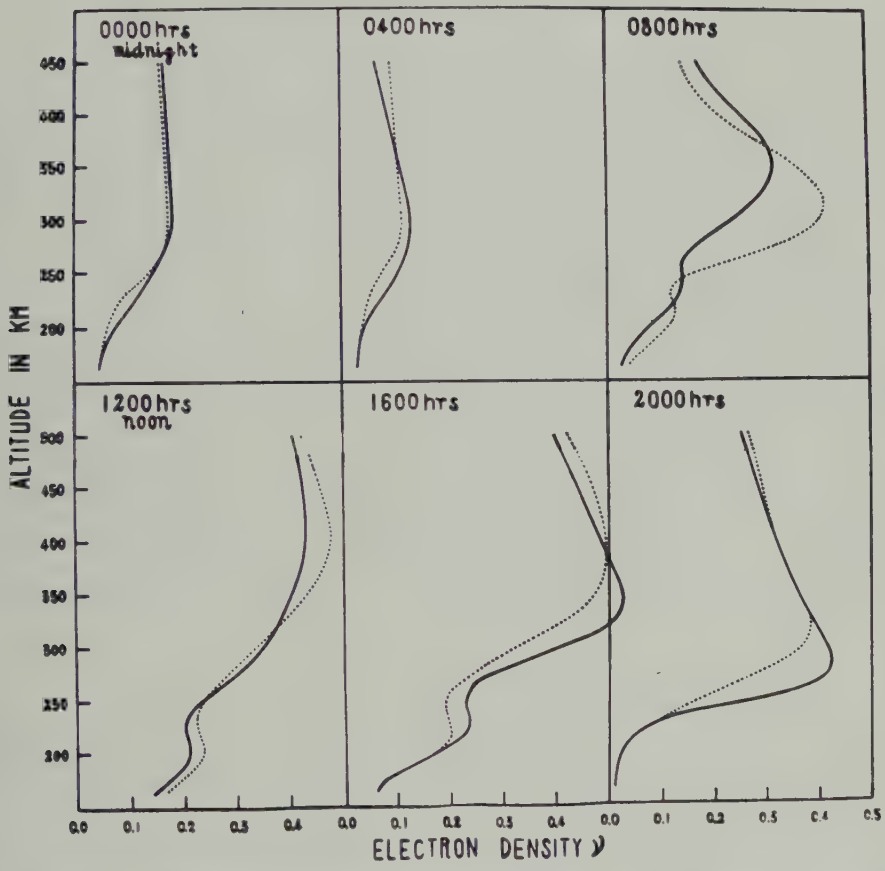

FIG. 7—Electron-density contours *vs* altitude for case 4 (full lines) and case 7 (dotted lines) shown in Table 3

(*iv*) For cases 1 to 4, the phase of W is ($11^h.3\uparrow$) and the daily variation of the calculated $F2$ region is very similar to those observed under summer conditions in middle latitudes, and for case 6 the phase of W is ($18^h.0\uparrow$) and the daily variations are very similar to those observed under winter conditions in middle latitudes, if semi-diurnal variations are not taken into consideration. These characteristics will hold for the (*b*)-type of ion-production distribution as well. The seasonal variation of the $F2$ region in middle and high latitudes might thus be produced, if the diurnal drift velocity changes with season and the ion production assumes appropriate forms.

6. DISCUSSION OF THE RESULTS

(*i*) To discuss the variation of h_m , Martyn [1] neglects the first and second terms of the right-hand side of (12) and uses the equation $\partial N/\partial t = -\partial(N \cdot W)/\partial h$. Therefore, if use is made of $W = W_n \sin(n\lambda + \theta_n)$, which is independent of altitude, the following equation is obtained:

$$\Delta h_m = (W_n/n\omega) \sin(n\lambda + \theta_n - \pi/2) \quad \ldots\ldots\ldots\ldots\ldots\ldots (16)$$

where $\omega = 7.3 \times 10^{-5}$.

If, as in the present treatment, $W_1 = 1.24 \times 10^3$ cm/sec is taken, the amplitude of Δh_m equals $W_1/\omega \simeq 170$ km. On the other hand, according to calculated results, the amplitude of Δh_m is about 60 km, and is much less than that calculated by (16). Thus, if one uses (16) to obtain the drift velocity from the observed data, a fairly large error will be introduced.

(*ii*) The distribution with altitude of recombination coefficient used in section 4 may be somewhat different from the real one in detail, so that the present calculation shows only a rough order of magnitude.

(*iii*) The electrical conductivity of the E region and its variation mentioned in section 3 seem to be plausible to fit the estimation by radio observation [29], but observations of the electron density of the E region at night are still too meager to confirm this situation.

For the electric field E_y obtained by H. Maeda [20], the diurnal term is about seven times that of the semi-diurnal one. This result is quite different from Martyn's conclusion [1] that the main term of the electric field for S_q is semi-diurnal. The variations of ν_m and h_m obtained here based on (8) agree well with observed results. On the other hand, the results calculated by Weiss [3], based on the semi-diurnal drift, do not resemble those observed on the equator.

7. CONCLUDING REMARKS

From the foregoing analysis, the following conclusion may be drawn: The eastward component of the electric field producing the S_q-current on the magnetic equator produces the vertical drift of the $F2$ region at the same time; the main term of the drift velocity is diurnal. The calculated daily variations of the $F2$ region, under consideration of this drift, have a striking resemblance to those observed near the magnetic equator.

8. ACKNOWLEDGMENTS

The authors wish to express their heartfelt thanks to Prof. M. Hasegawa of Kyoto University for his continued interest and advice, and to Prof. K. Maeda of Kyoto University and Prof. T. Nagata of Tokyo University for their valuable discussions.

References

[1] D. F. Martyn, Proc. R. Soc., A, **189**, 241 (1947); **190**, 273 (1947); **194**, 429 and 445 (1948).
[2] A. P. Mitra, J. Atmos. Terr. Phys., **1**, 286 (1951).
[3] A. A. Weiss, J. Atmos. Terr. Phys., **3**, 20 (1953).
[4] K. Maeda, J. Geomag. Geoelectr., **4**, 20 and 83 (1952); Rep. Ionosphere Res. Japan, **7**, 81 (1953).

[5] A. G. McNish and T. N. Gautier, J. Geophys. Res., **54**, 181 (1949).
[6] K. Maeda, H. Uyeda, and H. Shinkawa, Rep. Res. Phys. Inst. Rad. Waves, Nos. 1, 2, and 3 (1942).
[7] E. V. Appleton, Nature, **157**, 691 (1946); J. Atmos. Terr. Phys., **1**, 106 (1950).
[8] D. K. Bailey, Terr. Mag., **53**, 35 (1948).
[9] H. Uyeda, Rep. Res. Phys. Inst. Rad. Waves, No. 8 (1948).
[10] Y. Aono, Rep. Ionosphere Res. Japan, **6**, 69 (1952); **7**, 30 (1953).
[11] T. Shimazaki, J. Radio Res. Lab. Japan, **2**, 85 (1955).
[12] M. Hirono, J. Geomag. Geoelectr., **2**, 1 (1950); **2**, 113 (1950).
[13] M. Hirono, J. Geomag. Geoelectr., **4**, 7 (1952).
[14] M. Hirono, J. Geomag. Geoelectr., **5**, 22 (1953).
[15] D. R. Bates and H. S. W. Massey, J. Atmos. Terr. Phys., **2**, 1 (1951).
[16] R. J. Havens, R. T. Koll, and H. E. LaGow, J. Geophys. Res., **57**, 59 (1952).
[17] H. Maeda, J. Geomag. Geoelectr., **5**, 94 (1953).
[18] S. F. Singer, E. Maple, and W. A. Bowen, J. Geophys. Res., **56**, 265 (1951).
[19] M. Hasegawa and H. Maeda, Rep. Ionosphere Res. Japan, **5**, 167 (1951). H. Maeda, Rep. Ionosphere Res. Japan, **6**, 155 (1952).
[20] H. Maeda, Rep. Ionosphere Res. Japan, **9**, No. 3 (in press).
[21] W. W. Berning, Rocket exploration of the upper atmosphere, London, Pergamon Press, Ltd., p. 261 (1954). J. R. Lien, R. J. Marcou, J. C. Ulwick, J. Aarons, and D. R. McMorrow, *ibid.*, p. 223 (1954).
[22] D. R. Bates and H. S. W. Massey, Proc. R. Soc., A, **187**, 261 (1946).
[23] J. A. Ratcliffe, Mixed Commission on Ionosphere, International Council of Scientific Unions, Proc. Third Meeting, Canberra, Aug. 24-26, 1952, p. 30 (1953).
[24] S. Chapman, Proc. Phys. Soc., **43**, 26 and 483 (1931); **66**, 710 (1953).
[25] N. E. Bradbury, Terr. Mag., **43**, 55 (1938).
[26] F. L. Mohler, J. Res., Nation. Bur. Stand., Washington, D.C., **25**, 507 (1940).
[27] D. R. Bates, Proc. R. Soc., A, **196**, 562 (1949).
[28] G. Millington, Proc. Phys. Soc., **44**, 580 (1932).
[29] J. M. Watts and J. N. Brown, J. Geophys. Res., **59**, 71 (1954).

DOUBLE-DOPPLER RADAR INVESTIGATIONS OF AURORA

BY A. G. MCNAMARA*

Physics Department, University of Saskatchewan, Saskatoon, Canada

(Received March 8, 1955)

ABSTRACT

A pulsed double-Doppler radar technique has been employed to study the 90.7 Mc/sec signals reflected from auroral ionization. A spectrum analyzer was used in conjunction with the radar to measure the power spectra of the auroral echoes. The Doppler data are compared with observations of the visible aurora and with simultaneous echoes on 56 and 106 Mc/sec non-coherent high-resolution radar equipment. An interpretation of the Doppler data is given, and several theoretical models of the reflection mechanism are examined in terms of their effect on the observed spectra.

1. INTRODUCTION

Some of the earliest evidence of the rapid flutter imparted to radio waves returned by aurora was obtained by amateur radio operators. Later, these reports were examined in detail by Moore [see 1 of "References" at end of paper], and it was shown that the frequency of the fading increases approximately proportional to the radio frequency of the transmission, suggesting a Doppler origin. Bowles [2] has measured the fading rate of 50 Mc/sec continuous-wave transmissions and found the power spectrum. However, coherent (Doppler) radar does not appear to have been used for extensive study of aurora prior to the investigations at Saskatoon.

2. DOPPLER RADAR PRINCIPLES

A Doppler radar is designed to detect the frequency shift of the reflected signal relative to the transmitted signal. The general principle of operation is to supply a reference signal at the receiver which is coherent with the transmitted wave, that is, of the same frequency and related in phase. A moving target will produce a Doppler shift which is given by the formula

$$f_D = \frac{2v}{\lambda}$$

where f_D = the Doppler shift, v = the radial component of the target velocity, and λ = the wave-length of the transmitted wave.

*Now with the Radio and Electrical Engineering Division, National Research Council, Ottawa, Canada.

The Doppler radar (Fig. 1) used in these investigations was a pulsed system, operating at a radio frequency of 90.7 Mc/sec, and hence $f_D = 0.605\ v$ when v is expressed in meters per second. Besides simplifying the equipment considerably,

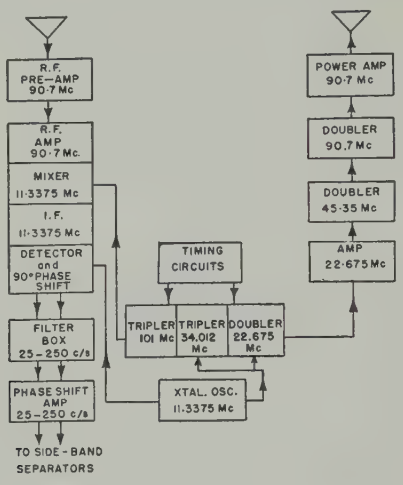

Fig. 1—Block diagram of the 90.7 Mc/sec double-Doppler radar transmitter and receiver

the pulsed Doppler system has several advantages over a continuous-wave system: interfering echoes from local objects and terrain are eliminated, and some degree of range measurement and of target discrimination can be achieved. On the other hand, pulsed Doppler suffers some limitations when used for auroral investigations. The amplitude modulation (pulsing) of the transmitter produces a discrete spectrum, consisting of the radio frequency f_0 and a number of side-bands $f_0 \pm nF$, where F is the pulse repetition frequency (PRF). In the presence of a moving target, the radio frequency and each harmonic have associated with them, at a frequency f_D removed, a component due to the moving target. When a reference frequency is injected into a coherent detector, the output audio spectrum consists of dc, the Doppler frequency, the PRF and its harmonics, and the Doppler components associated with each harmonic. Usually most of the signal power is concentrated in the interval of the first few harmonics by the use of a large duty ratio in the transmitter. All extraneous frequencies (the PRF, its harmonics, and the associated Doppler-shifted components) are eliminated by a band-pass filter occupying the lower half of the frequency interval between zero and the pulse repetition frequency. However, if the target velocities are sufficient to produce Doppler frequencies greater than one-half the value of the PRF, then the harmonic components may appear within the pass-band and an ambiguous value of the Doppler shift will be indicated. In order to permit a fairly wide band of Doppler frequencies to be recorded, a correspondingly high PRF is required. This introduces some range ambiguity, which can however be largely eliminated through the use of simultaneous observations with ordinary pulse radars.

For auroral investigations, it is highly desirable to be able to distinguish positive and negative Doppler shifts. This is achieved through the use of the "double-

Doppler" technique [3]. This system utilizes dual coherent detectors to separate the positive Doppler shifts (the upper side-band, USB) from the negative Doppler shifts (the lower side-band, LSB). The reference voltages to the coherent detectors differ in phase by 90°, with the result that the two outputs are the two quadrature rectangular components of the audio frequency signal. Their resultant is a vector, which rotates in one direction if the Doppler shift is positive, but rotates in the opposite sense if the shift is negative. A band-pass filter (25 to 250 cps) removes the pulsing harmonics nF and other extraneous components. To provide a convenient method of registering the direction of the Doppler shift, the two audio components of the signal are passed through a broad-band audio phase-shifter, which produces a 90° differential phase shift over the interval 25 to 250 cps. Hence, the two output components are in-phase or out-of-phase, depending upon whether the Doppler shift is positive or negative. Doppler shifts of 25 to 250 cps correspond to radial motion of the targets at velocities of 41 to 415 m/sec.

TABLE 1—*Double-Doppler radar specifications*

1	Transmitter frequency	90.7 Mc/sec
2	Average transmitted power	0.30 kw
3	Antenna gain	9 db over a λ/2-dipole
4	Antenna height above ground	2.39 λ
5	Polarization	Horizontal
6	Beam width	50°
7	Pulse repetition frequency (PRF)	500 to 570
8	Transmitter duty ratio	0.2
9	Transmitter pulse length	400 μsec
10	Receiver gate length	1,000 μsec
11	Doppler frequency pass-band	25 to 250 cps

The specifications of the Doppler radar are given in Table 1. The high-resolution non-coherent pulse radars with which simultaneous observations were made transmitted 35 μsec pulses at peak powers of 25 kw on 56 and 106 Mc/sec at a PRF of approximately 50 cps.

3. THE SPECTRUM ANALYZER

The auroral echoes were anticipated to have a more-or-less continuous spectrum of both positive and negative Doppler shifts, and a spectrum that might change radically within a few seconds. To meet these requirements, the spectrum analyzer of Figure 2 was designed. A side-band separator circuit discriminates between the positive and negative Doppler components, and diverts them to the upper and lower side-band channels. Five tuned amplifiers (twin-T feedback type) in each channel accept narrow bands (10 cps wide) of frequencies centered nominally at 50, 100, 150, 200, and 250 cps. The outputs of the tuned amplifiers are rectified, integrated with 0.2 second time-constants, and fed to cathode followers which drive milliammeters. The 10 meters and a clock are photographed (1 to 2 second exposure) at the discretion of the operator with a single-frame 16-mm camera. Individual

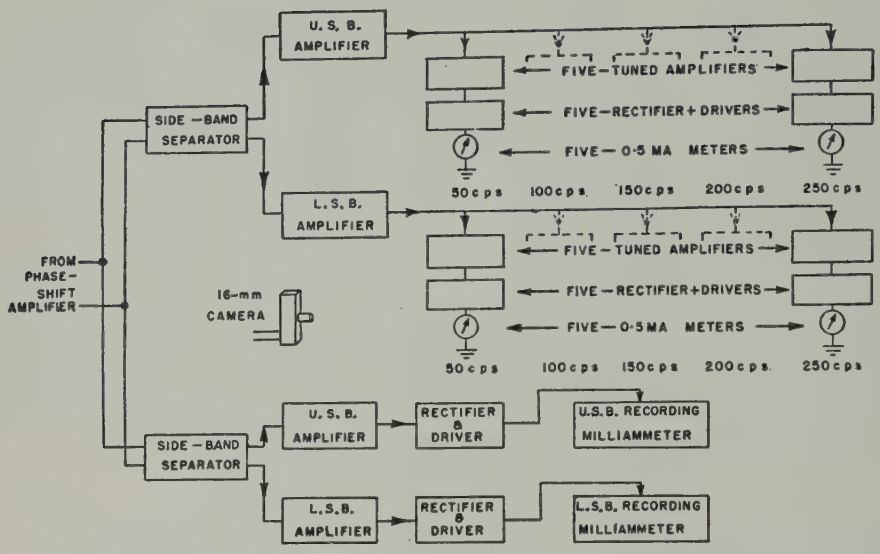

FIG. 2—Block diagram of the Doppler spectrum analyzer

control of the signal amplitude into the tuned amplifiers permits equalization of all spectrum-analyzer meter readings on random receiver noise, which was assumed to be uniform across the audio band. Two duplicate circuits, less the tuned amplifiers, drive pen-and-ink recorders that register continuously the variations of the total side-band outputs (25 to 250 cps) with time. A paper speed of one foot per hour is used.

Proper adjustment and periodic checks of the radio frequency and audio frequency phasing and the side-band separation were facilitated by the construction of a special signal generator derived from a matched auxiliary crystal oscillator. The over-all Doppler sense discrimination was found to be at least 20 decibels across the pass-band. Observation of the spectrum analyzer meters disclosed negligible signals registered on the other meters as the signal generator was tuned to each meter in turn at full scale deflection.

4. OBSERVATIONS AND INTERPRETATIONS

Auroral echoes were recorded with the Doppler equipment on many occasions during 1953 and 1954. Some representative records have been selected and are discussed in this section in order to illustrate the characteristics of the echoes and their spectra. Complete correlation of the relative occurrence of echoes on the coherent and non-coherent types of radar was difficult because of the lack of adequate Doppler range determination, and because of the blind spots in the range coverage of the Doppler radar which resulted from the high PRF and the receiver gate. There were, however, almost always echoes present during the periods in which 56 Mc/sec echoes were received. Echoes on the 106 Mc/sec radar were relatively few, but when present there were also echoes on the Doppler frequency.

One group of Doppler echoes is reproduced in Figure 3 from the records of July 27, 1953. The deflections of the recorders are proportional to the total signal

voltage in each side-band. The group of echoes is seen to consist of two subgroups of echoes, which occur approximately five minutes apart. The first subgroup is stronger in the USB (positive Doppler shifts) than in the LSB, whereas the reverse is true for the subgroup occurring five minutes later. A similar effect was recorded about 15 minutes later on the same night, and was also observed on other nights.

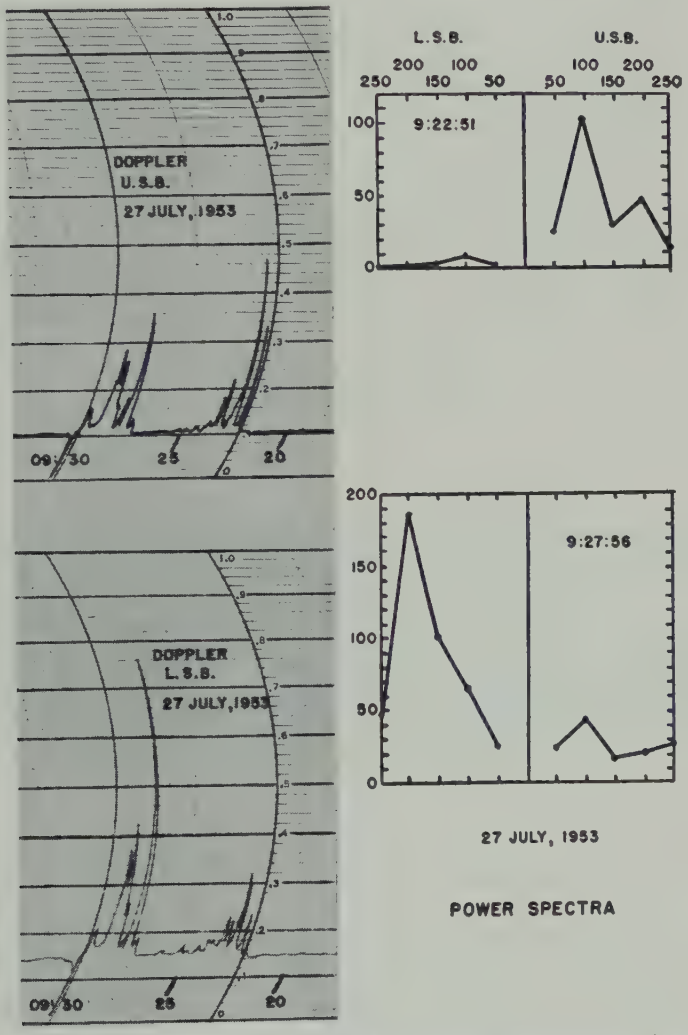

FIG. 3—Sample records of Doppler radar echoes and their power spectra, from the aurora of July 27, 1953

On one occasion when good visual observations of auroral movements were possible, a bright auroral arc was observed at a high angle in the period between the echo subgroups, after which the aurora began to recede northward and a few minutes thereafter the second subgroup of echoes appeared with the signal predominantly in the LSB. The power distributions in the side-bands at two instants are shown

by the sample spectra in Figure 3. The power spectra are obtained by plotting on a linear scale the squares of the meter readings recorded by the spectrum analyzer.

The Doppler echoes of August 11, 1953, are shown in Figure 4, together with the simultaneous echoes obtained on the 56 and 106 Mc/sec radars. (The thin black line across the 56 Mc/sec record is due to a flaw on the face of the cathode-ray tube.) The Doppler signal was continuously present for a period of nearly one hour. The sharp drop in signal level at 09^h05^m was due to a reduction of receiver gain in order to bring the pen back on scale. Two of the 64 power spectra which were taken during this hour are reproduced. The spectra remained fairly constant in shape throughout long periods; from 08^h53^m to 09^h06^m the spectra were relatively flat, and from 09^h07^m to 09^h45^m there was an increase in power at the lower frequencies.

The records and power spectra of Doppler signals obtained on March 17, 1954, are reproduced in Figures 5 and 6. Simultaneous echoes on 56 Mc/sec were also recorded. The brief echo occurring at 11^h50^m will be discussed first. The 56 Mc/sec range-time record shows a single discrete echo and is not complicated by an extended series of echoes with different relative motions. The echo appears at 850 km, moves in with a velocity estimated to be roughly 7,000 to 9,000 m/sec for several seconds, and then turns and moves out in range at approximately 3,500 m/sec for some 15 seconds or more before disappearing. The initial approach was not recorded by the Doppler radar, either because the signal was not within the pass-band or because the duration was too short to build up a response. The receding portion of the echo shows distinctly as a negative Doppler shift.

Power spectra of the echoes were obtained between 09^h20^m and 09^h35^m, and some of these are plotted in Figure 6. Simultaneous 56 Mc/sec records show that at times there were many separate ionized regions contributing to this group of echoes. The echoing regions often appear to move independently, even moving oppositely in range at the same time. From $09^h24^m30^s$ to $09^h26^m30^s$, an echo is clearly seen to move out in range on the 56 Mc/sec record; at $09^h25^m30^s$, another echo starts to move in and crosses the "path" of the other at 09^h26^m.

In general, many features of the Doppler records may be correlated with the data from the non-coherent radars and with the movements of the visible aurora. Both positive and negative Doppler shifts are observed, and often the energy distribution in the side-bands is not symmetrical. Examination of the power spectra suggests the following interpretation. In many cases, the returned signal is coherent or nearly coherent, that is, the power spectrum is quite narrow, although the tails may extend to a considerable distance. Most of the reflected signal appears to occur from almost stationary targets, or from targets moving collectively in range, and the frequency spread produced by relative movement of the individual targets is small. The width of the spectrum may be estimated when it is observed that the peak representing the gross movement of the aurora is equivalent to the zero frequency and very low frequency Doppler components (which cannot otherwise be recorded), all shifted *en masse* in frequency. When the velocity of translation is such as to place the signal within the pass-band, the shape of the central region of the spectrum is exhibited (see Fig. 6, $09^h25^m15^s$).

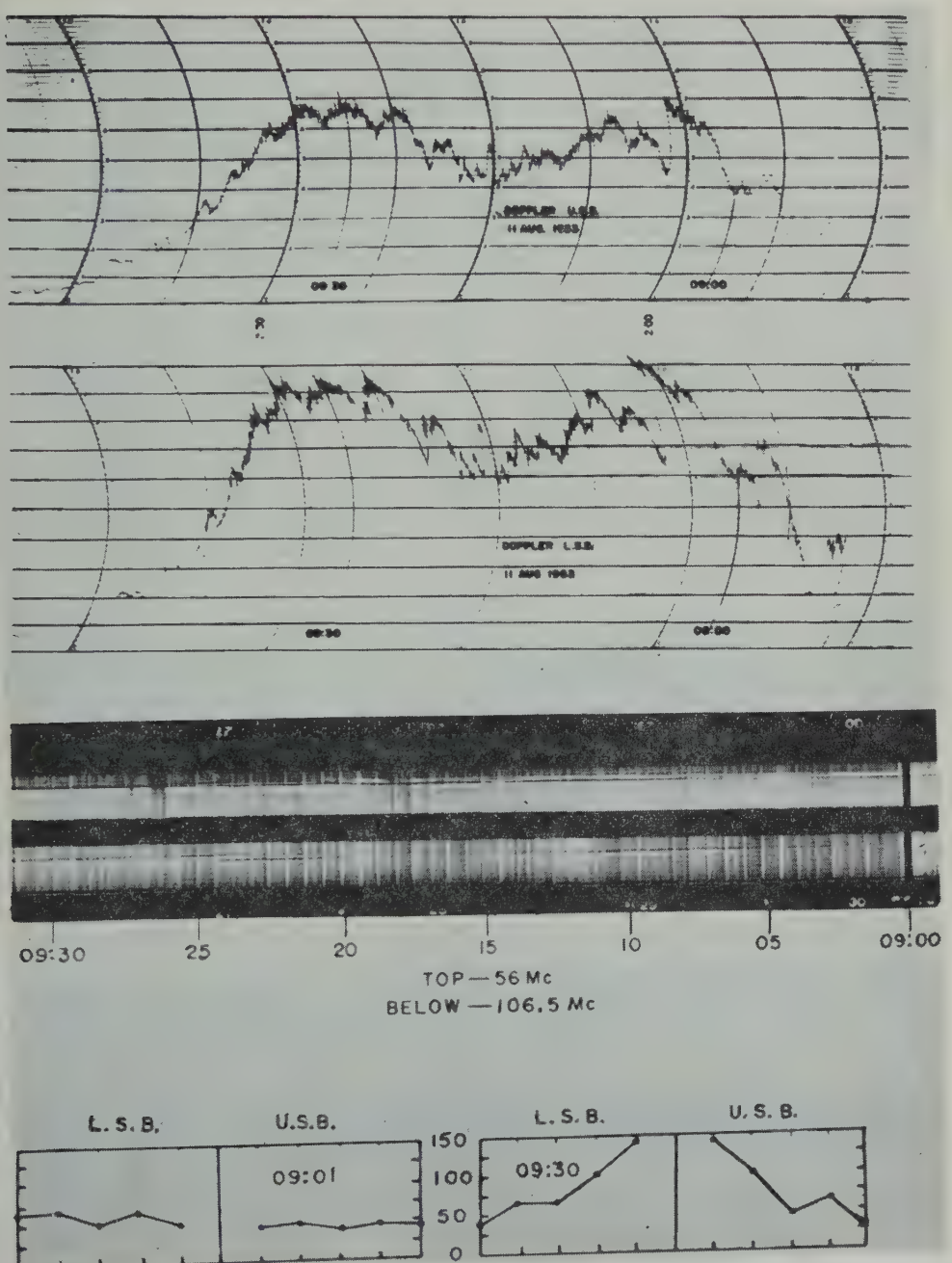

FIG. 4—Doppler radar echoes and simultaneous 56 and 106 Mc/sec high-resolution pulse radar echoes of August 11, 1953

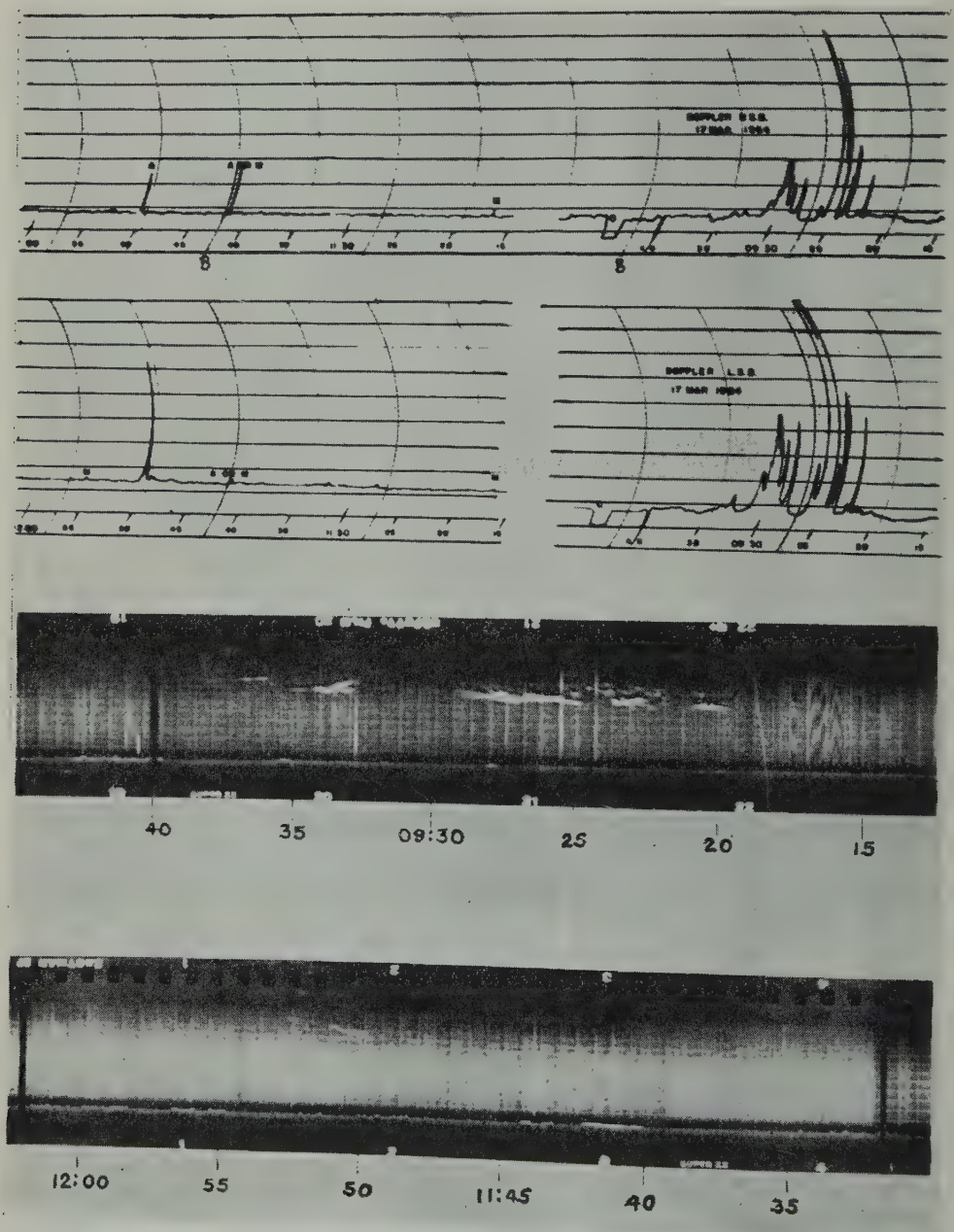

Fig. 5 –Simultaneous 90.7 Mc/sec Doppler and 56 Mc/sec high-resolution radar echoes of March 17, 1954

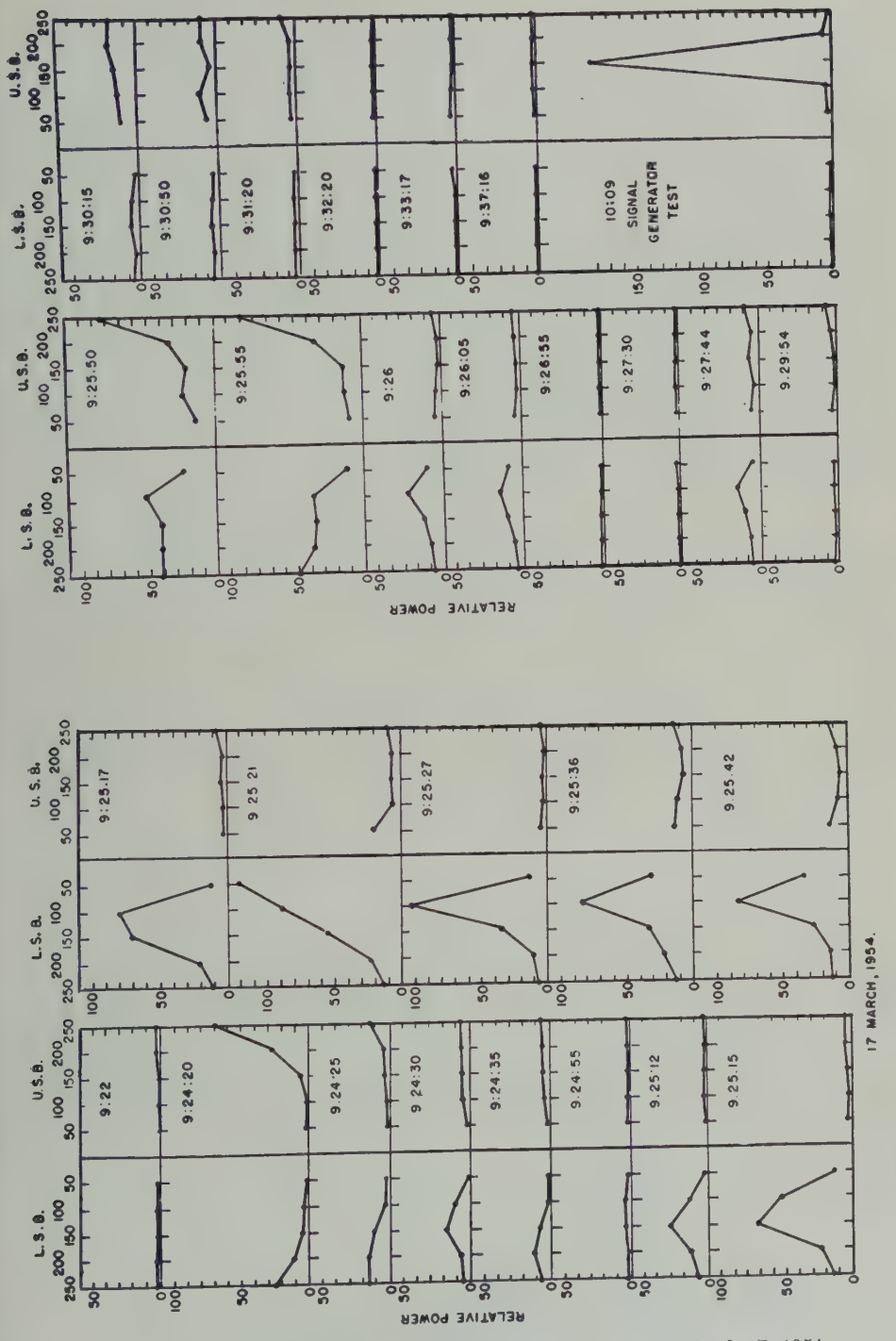

FIG. 6—Doppler radar power spectra of the echoes obtained on March 17, 1954

For a very narrow spectrum, this shape, of course, is distorted, due to channel spacing and the width of the filters. However, a rough estimate of the frequency spread may be made, and a half-power width of approximately 50 to 100 cps (total width about the central maximum) is often observed. The "zero frequency" peak is quite prominent.

At times, a relatively flat type of spectrum is observed, as in Figure 4. This may arise in one of the following ways: (1) If the relatively flat portion of the spectrum, far out on the tail of the curve, lies within the pass-band, the exhibited portion of the spectrum will appear flat. (2) If the signal is the resultant of several partially overlapping peaks which occur when the auroral ionization is complex and extended in range and the echoes come from several regions moving with different velocities, then the indicated spectrum could appear relatively flat. Pulsed radiation reduces the probability of this situation arising and herein lies one of the great advantages of the pulsed radar systems. (3) It may be one of the flat type of spectra described by Bowles [2] (see section 5*b*).

5. THEORETICAL MODELS AND THEIR SPECTRA

(*a*) *Spectra of randomly moving targets*—When the received signal is the resultant reflection from a number of randomly moving targets, it has been shown [4,5] that the power spectrum has the shape of the Gaussian function. This may be expressed [5] in the form

$$p(f)\,\mathrm{d}f = p_0 \exp\left\{-\frac{\lambda^2(f - f_0)^2}{8\overline{v^2}}\right\}\mathrm{d}f$$

Then the root-mean-square (rms) velocity of the targets is given by

$$\overline{v^2} = 0.42\lambda(\Delta f)_{3\mathrm{db}}$$

where $(\Delta f)_{3\mathrm{db}} \equiv (f - f_0)_{3\mathrm{db}}$ = the frequency deviation at which the power spectrum is down to one-half of its maximum value.

When observations are made with a coherent radar system, the spectrum of the random movement will be superimposed upon that produced by the mass movement or drift of the ensemble of scatterers. This model reproduces some of the spectral characteristics observed with the Doppler radar, but the resolution in the observed spectra is not sufficient to determine whether the shape is Gaussian. If the Gaussian spectrum is assumed, the narrower spectra observed will correspond to rms target velocities of approximately 50 m/sec; the wider spectra indicate the occurrence of velocities several times greater than this value.

(*b*) *The proton trail theory*—Moore [6] has proposed a theory of auroral reflection based upon coherent scattering from long trails of ionization produced by protons, and upon the data of Bowles [2] on the fading rate of 50 Mc/sec continuous-wave transmissions. The theory predicts a spectrum of nearly constant strength out to 100 or 200 cps and beyond this cut-off frequency a $1/f^2$ decay of power.

The data obtained from the 90.7 Mc/sec Doppler radar do not suggest such spectra in most cases. Often a sharp peak at "zero frequency" is indicated. The coherent pulse system permits observations to be made through "zero frequency,"

positive and negative frequency shifts are separated, and some degree of target resolution is obtained.

(*c*) *Diffusion and recombination of ionized volumes*—If overdense ionized regions occur within aurora [7,8], reflections from the moving surfaces of these regions will produce Doppler shifts. Development of the ambipolar diffusion theory for the ionosphere [9,10] permits calculation of possible ionization characteristics, durations, and dimensions. Two simple models of the auroral ionized volumes will be considered: spherical concentrations and cylindrical columns of equal numbers of positive ions and electrons formed within a very small radius at time $t = 0$. The reflection of radio waves is assumed to occur from the surface at which the electron density is equal to the critical value for the radio frequency employed ($n_c = 1.02 \times 10^8$ e/cc at 90.7 Mc/sec). This surface starts at a very small value at $t = 0$, expands to a maximum radius, and then shrinks to zero. For $r > \lambda/2\pi$, geometrical optics may be applied, and the projected area of the critical density surface approximates the radar cross-section. The quantity dr/dt gives the radial velocity of the reflecting surface and the Doppler shift, $(2/\lambda)\ (dr/dt)$, will be positive during the expansion and negative during the collapse.

The basic diffusion equations are [9,10]:

$$n = \frac{N}{(4\pi Kt)^{d/2}} \cdot \exp\left\{-\frac{r^2}{4Kt}\right\}$$

where n = the electron density at time t at radius r and K = the ambipolar diffusion coefficient. For a spherical concentration, N = the total number of electrons formed initially and $d = 3$, while for a cylindrical column, N = the number of electrons per unit length of column initially and $d = 2$.

In the case of auroral ionization, the ions are the air molecules and recombination can be important. Assuming a recombination coefficient of $\alpha = 10^{-8}$ cm^3/sec, the effects of both processes are given approximately for the cylindrical case by [10], as follows:

$$n \approx \frac{N}{t[4\pi K + \frac{1}{2}N\alpha \ln (t/t_0)]} \cdot \exp\left\{-\frac{r^2}{4Kt}\right\}$$

The results of a typical calculation for a cylindrical concentration of $N = 10^{15}$ e/cm, using data appropriate to a height of about 100 km [11], are shown in Figure 7. The effects of ambipolar diffusion alone (curve *A*) and of diffusion plus recombination (curve *B*) are illustrated. For a spherical concentration which will produce an ambipolar diffusion curve of dimensions comparable to the cylindrical example, a total number $N = 10^{18}$ electrons is required. Such diffusion and recombination characteristics will result in Doppler shifts which have a power spectrum sharply peaked at zero frequency and only slightly asymmetrical about zero. The duration and effective radial velocity of the overdense surface are functions of the radio frequency employed.

Moreover, even if the densities are insufficient to form a critically reflecting surface, a frequency spread of any scattered signal will be produced by the transient nature of the target. The half-power width will be approximately equal to the inverse of the target duration.

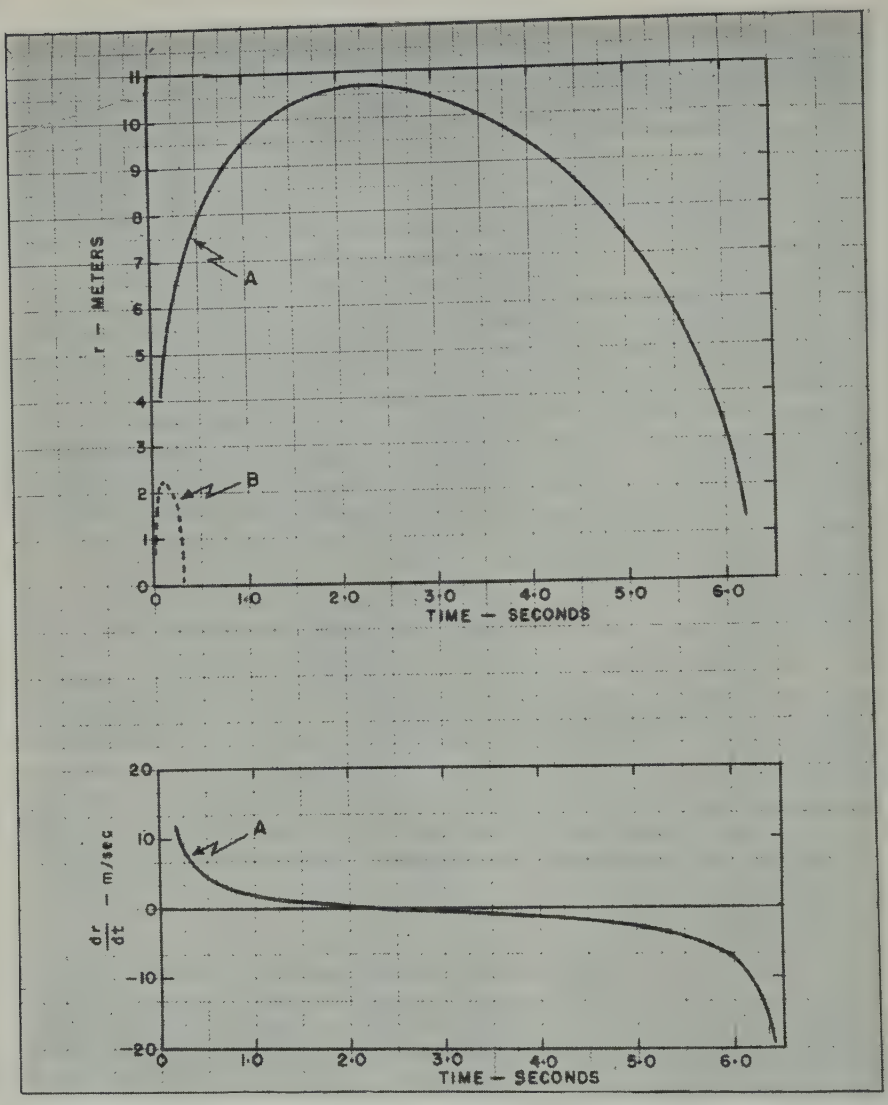

Fig. 7—Curves showing the instantaneous radius and the velocity of the critically dense surface of a cylindrical concentration containing 10^{15} electrons per centimeter of length, formed at time $t = 0$ at altitude of 100 km (curve A shows the behavior due to ambipolar diffusion alone; curve B includes the effect of recombination)

(*d*) *General motion and turbulence in the ionosphere*—Motions attributed to ionospheric winds have been measured by a number of workers, particularly in the field of meteors. Typical drift values are of the order of 50 m/sec, and velocity gradients of 1 to 10 m/sec/km have been found. Radar observations of aurora indicate apparent changes in range over wide limits and values as high as several thousands of meters per second are not uncommon. These should be regarded, not as a movement of a definite volume of ionization, but rather as a displacement of

the point of precipitation of the ionizing agent. The apparent motion, however, can constitute an important part of the Doppler shift in a coherent radar system.

6. CONCLUSIONS

Many of the features of the Doppler radar echoes can be correlated with the visible aurora and with the movements of echoing regions observed on high-resolution pulsed radars. The power spectra of the echoes are influenced by the spatial shift of the reflecting region due to changes in the point of precipitation of the ionizing agent, and by the relative motion of the individual reflecting centers within the region. Many of the observed spectra are much narrower than those previously reported as typical of auroral signals and appear to be sharply peaked at "zero frequency," the Doppler frequency corresponding to the gross movement of the entire reflecting region. Several theoretical models of the ionized region are considered and the types of spectra which should be observed are discussed. At times, however, a flat, wide type of spectrum is observed. Some possible explanations of this type of spectrum are suggested.

7. ACKNOWLEDGMENTS

This work was made possible through generous financial assistance from the Radio Physics Laboratory of the Defense Research Board of Canada, who also supplied the Doppler radar transmitter for the project. The author is grateful for the assistance of Prof. B. W. Currie of the Physics Department, who directed the auroral work at Saskatoon, and to Dr. P. A. Forsyth of the Radio Physics Laboratory for his assistance in obtaining equipment and for many valuable discussions.

References

[1] R. K. Moore, J. Geophys. Res., **56**, 97 (1951).
[2] K. Bowles, J. Geophys. Res., **57**, 157 (1952).
[3] L. A. Manning, O. G. Villard, and A. M. Peterson, J. Geophys. Res., **57**, 387 (1952).
[4] D. E. Kerr, Propagation of short radio waves, Vol. 13, M.I.T. Radiation Laboratory Series, McGraw-Hill Book Co., Inc., New York (1951).
[5] J. A. Ratcliffe, Nature, **162**, 9 (1948).
[6] R. K. Moore, Trans. Inst. Radio Eng., Prof. Group on Antennas and Propagation, No. 3, 217 (Aug. 1952).
[7] B. W. Currie, P. A. Forsyth, and F. E. Vawter, J. Geophys. Res., **58**, 179 (1953).
[8] P. A. Forsyth, J. Geophys. Res., **58**, 53 (1953).
[9] L. G. H. Huxley, Aust. J. Sci. Res., A, **5**, 10 (1952).
[10] T. R. Kaiser, Adv. Phys., **2**, 495 (1953).
[11] A. G. McNamara and B. W. Currie, J. Geophys. Res., **59**, 279 (1954).

DAY SKY BRIGHTNESS TO 220 KM

By Otto E. Berg

United States Naval Research Laboratory, Washington 25, D.C.

(Received March 15, 1955)

ABSTRACT

The brightness of the daytime sky has been measured using rocket-borne stereocameras. An upper limit of 0.0075 candle/ft^2 was found for the brightness at altitudes ranging from 80 to 220 km. This limit is consistent with the brightness being due entirely to Rayleigh scattering. No evidence of high altitude clouds was found.

INTRODUCTION

During the past few years, experiments have been conducted for the purpose of determining the brightness of the daytime sky at high altitudes. The principal point in question was whether the emission by the upper atmosphere could be explained as chiefly Rayleigh scattering by air molecules, or whether there were, in addition, strong emissions due to resonance radiation, and perhaps scattering by extremely high altitude particles and noctilucent clouds.

This paper presents the techniques and results of a recent rocket-borne photographic investigation of the daytime sky in the altitude range of 80 to 220 km. These results showed that the daytime sky at high altitudes did not have brightness in excess of that expected from Rayleigh scattering alone, and also that sunlight scattered from gas and material emanating from the rocket may have contributed to the high value reported by Miley [see 1 of "References" at end of paper].

As corroboration of statements made in this paper, series of pictures are presented in the appendix showing the sensitivity and validity of the stereoscopic system and the effects of scattered sunlight.

PAST MEASUREMENTS

Photometric measurements made by Teele [2] from the stratosphere balloon-flight of 1935 (*Explorer II*) indicate a linear relationship between atmospheric pressure and sky brightness to 72,000 feet. This linear relationship is just that expected on the basis of the sky brightness being due to Rayleigh scattering alone and is reproduced in Figure 1. The lower portion of the curve, of course, is an extrapolation. An altitude scale based on the Rocket Panel standard atmosphere [3] has been added for convenience in computing sky brightness for altitudes corresponding to those of rockets.

In a series of investigations using high altitude rockets as the transport laboratory, H. A. Miley, *et al.* [1], recently reported new and high values of the day sky brightness at high altitudes. They used photomultipliers and found a brightness

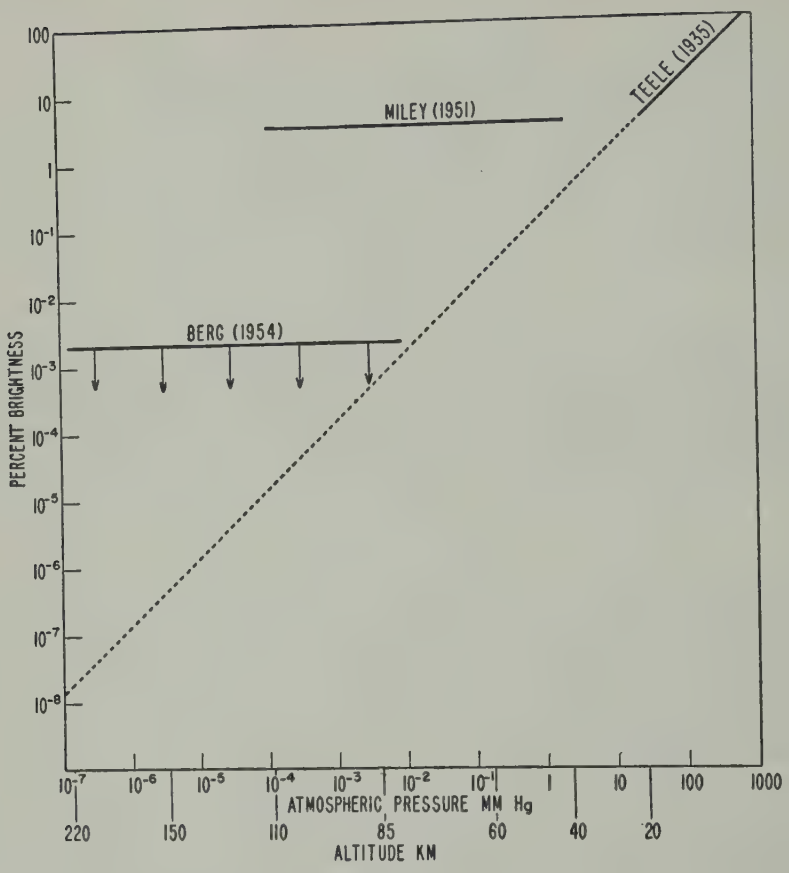

FIG. 1—Per cent sea-level sky brightness *vs* atmospheric pressure and altitude

of nearly a constant three per cent of the sea-level value for altitudes of from 40 to 130 km. Their measurement is included in Figure 1. The sky brightness predicted from Rayleigh scattering alone at these respective levels can be seen from Figure 1 to range from 0.3 per cent to 10^{-4} per cent of sea-level brightness.

Included in Miley's report are interesting photographs of overhead clouds of some sort taken on one flight at 70 km with a 16-mm camera operating at 6.67 frames per second. The exposure was 1/400 second at F/4.5 on Eastman Linagraphic film. These he interpreted to be true clouds of the noctilucent type and were thought to be associated with the high recorded sky brightness.

PURPOSE AND EXPERIMENTAL PROCEDURE

A simple photographic experiment was designed to investigate sky brightness at high altitudes. The four objectives of the experiment were as follows:

(1) To record, photographically, the brightness of the sky at known points in the sky during flight

(2) To take stereophotographs of any high-altitude cloud formations in order to determine their proximity to the rocket

(3) To determine, by comparison of photographs taken through red and blue filters, whether the clouds were of large particles and scattered neutrally, or whether they were of very small particles and scattered like the sky itself
(4) To determine whether the light from the clouds and sky was polarized or not, since, if not, the explanation of the clouds would lie in scattering by large particles or a true airglow emission, rather than Rayleigh scattering by air molecules and small particles

Figure 2 shows the unit assembled and ready for flight. It comprises two modified and armored 16-mm GSAP gun cameras, mechanically interconnected

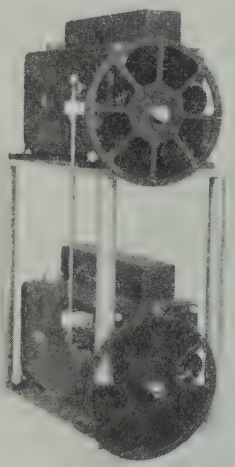

FIG. 2—Day sky stereoscopic unit

and synchronized, and mounted in stereoposition, one foot apart, with axes parallel. The one-inch F/1.5 lenses shot pictures through revolving disks, each having eight filters (Fig. 3) rotating at about 2 rpm. The camera mechanism was modified to transport 4.8 frames per second, or about 150 frames per revolution of the filter disk. The effective exposure was 1/20 second at F/1.5 on Eastman Super XX film. In each case, the film was developed in a high-speed developer, which doubled the ASA rating. The filters were Wratten Nos. 23A and 47, selected for their transmittance characteristics in red and blue, respectively. The Polaroid screen was of optical quality and oriented as shown in Figure 3.

The cameras were mounted in the forward instrument section in a position perpendicular to the rocket axis. Since the rocket was deliberately programmed to to roll after peak with its axis parallel to the earth's surface, the cameras alternately photographed the earth and the sky. The angular position of the photographed area with respect to the earth or the sky was determined by reference to data from an aspect camera.

The camera-film-filter combination was calibrated by exposures to the sky at ground-level on a very clear day. Film densities ranging from 0 to 2.0 were obtained by attenuating the sky brightness with two crossed Polaroid filters, and photometering each brightness.

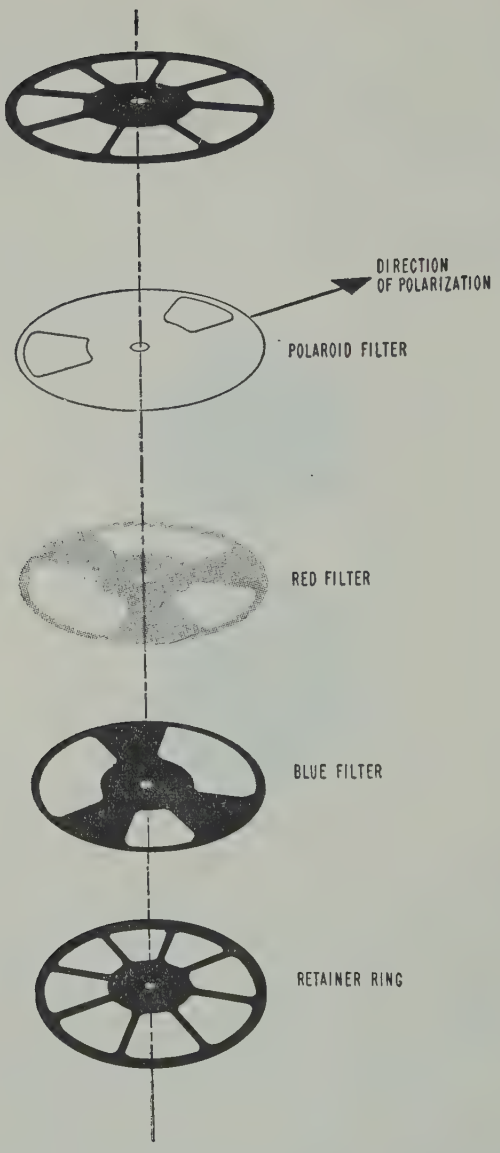

FIG. 3—Exploded view of filter disk showing orientation and assembly of filters and Polaroid

RESULTS

Since there were no true clouds observed during this flight, the remainder of this paper will be concerned with only the first of the four experimental objectives listed, namely: To record photographically the brightness of the sky at known points in the sky during flight.

In view of the many obstacles to rocket-borne sky-brightness measurements and the complex nature of scattered sunlight, the author is of the opinion that

any value assigned to sky brightness at any particular angular distance from the sun can only represent an upper limit. In this investigation, the minimum measurable brightness was determined by the sensitivity of the film. Sky brightness values assigned from this experiment are based on exposures made through the no filter-no Polaroid sections of the filter disk (see sketch, Fig. 3). Exposures made during ascent while the rocket axis was vertical were excluded from this study, since they contained obvious evidence of considerable reflection from the earth into the optical system. Only those frames were selected which were exposed as the camera aimed toward the sky and away from the sun while the rocket was rolling in a horizontal position. A total of 13 exposures were made in each camera while thus oriented. These occurred during the rocket descent from 220 to 80 km. Densitometer readings on these 13 frames showed no density above normal background density. In other words, the sensitivity of the film was not sufficient to record the brightness at this altitude range, and it can only be said that the sky brightness in this range was below a certain value.

Referring then to the calibration film, for a ground-level sky brightness of 380 candles/ft^2, the least exposure which produced a readable density above normal background density was 1/200 second at F/16 with a sky attenuation of 40 (refer to paragraph on calibration). This is equivalent to an exposure of 1/8,000 second at F/16.

A study of the above exposures—1/20 second at F/1.5 for the day sky unit and 1/8,000 second at F/16 for the calibration film— gives a ratio of 1:51,000 between the day sky brightness in the region from 80 to 220 km to that at sea-level. Or in terms of percentage, the day sky brightness from 80 to 220 km is less than 0.002 per cent of sea-level brightness. In absolute values, this represents a maximum brightness of 0.0075 candle/ft^2.

DISCUSSION OF RESULTS

It can be seen from Figure 1 that the measured upper limit for the day sky brightness is consistent with an extrapolation of the results of Teele. It can be seen that the present results are in marked disagreement with those of Miley. A possible explanation for this discrepancy is that Miley's high recorded brightness and clouds were caused by sunlight scattered from clouds of gas and particles blowing out of the rocket. This explanation is supported by the fact that the recorded brightnesses were the same at all three wavelength bands—a normal distribution if the clouds were of relatively large particles such as might be ejected from the rocket. Further support for this explanation is given by the "cloud" pictures included in the appendix.

An article entitled "Theoretical considerations regarding the dayglow," by Bates and Dalgarno [4], has recently appeared, which would also seem to refute the day sky values reported by Miley, *et al.* Bates and Dalgarno survey various possible sources of high altitude illumination and conclude that "the tenuous air at altitudes greater than 135 km cannot extract enough energy from the incoming solar radiation to supply a source having a photon intensity of some 10^{14} cm^{-2} sec" as inferred by Miley). Their theoretical approach substantiates, in effect, the day sky-brightness values reported in this paper.

SUMMARY

The density of the stereocamera films indicated an upper limit of 0.0075 candle/ft^2 for the brightness of the daytime sky at altitudes ranging from 80 to 220 km. This value is based on 26 exposures made while the cameras were aimed away from the sun and the earth, and is consistent with values based on Rayleigh scattering alone. There were no true clouds in space recorded by the stereoscopic unit.

ACKNOWLEDGMENTS

In conclusion, the author desires to record his grateful thanks to Dr. R. Tousey, Dr. R. J. Havens, and Mr. M. Koomen for their stimulating interest and advice in the preparation of this paper.

PHOTOGRAPHIC EXHIBIT

Whenever a movie-film exposed in a rocket-borne camera is viewed frame by frame, a number of exposures occur which exhibit strange images and effects. Normally, there is no choice but to assign their origin to one of several common phenomena involving either film-processing technique or extraneous optical effects. In a calibrated stereoscopic system as was flown in this rocket, however, it is relatively simple to distinguish positively between images due to real objects in the camera field of view and images due to processing errors or extraneous optical effects—the latter image types being betrayed by either (1) their presence in one film only, (2) their unrelated geometry and dimension, or (3) their unrelated traversal across the field of view in the two films.

Shown below are stereopictures selected as a sample exhibit of objects and effects encountered in this rocket flight.

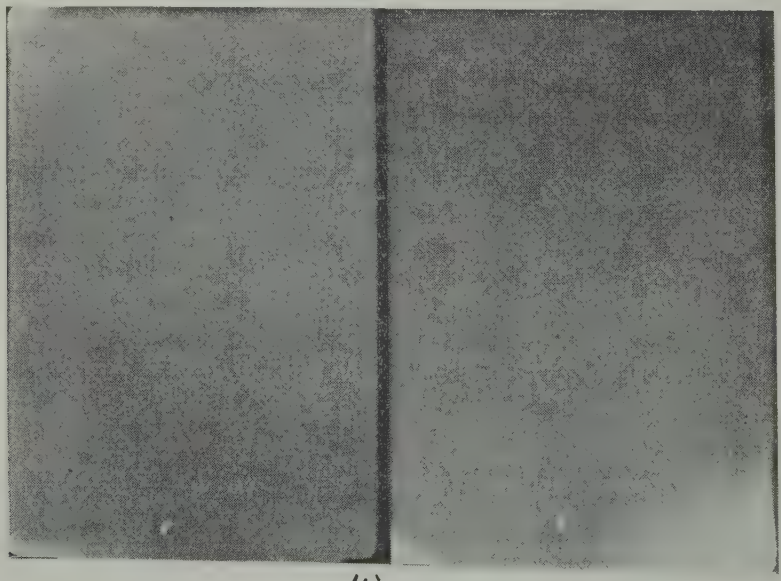

FIG. 4—A set of stereoexposures of the moon

Figure 4—A set of stereoexposures of the moon. These are included to validate the accuracy of the investigation as to image quality or reproduction and to the position of the object with respect to the rocket. The rocket to object distance is given by a comparison of the image within the frame on both stereofilms and reference to a calibration chart. Here, of course, the distance is essentially infinity.

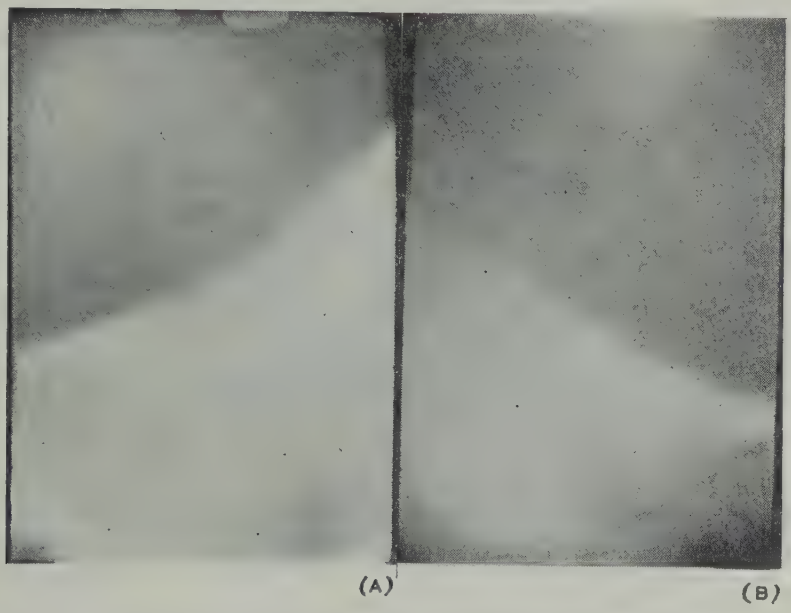

FIG. 5—Images resembling clouds or sunlit aurorae

Figure 5—Images resembling clouds or sunlight auroras, but actually optical scatter as the camera field of view approached the direction of the sun. These are not true stereopictures, since the upper and lower exposures were not taken at the same time by the two cameras, but are separated by one frame or about one-fifth second. The matching exposures from the upper and lower stereocameras that do correspond in time show an over-all, readable density, but no clouds or such effects. These are included in support of a previous suggestion in this paper that the clouds recorded by Miley's single camera may have been produced by a similar effect, or more likely by scattered sunlight in the gaseous envelope of the rocket.

References

[1] H. A. Miley, E. H. Cullington, and J. F. Bedinger, Trans. Amer. Geophys. Union, **34**, 680-694 (1953).

[2] R. P. Teele, Nation. Geog. Soc., Contrib. Tech. Papers, Stratosphere Ser., No. 2, 133-138 (1936).

[3] The Rocket Panel, Phys. Rev., 88, 1027-1032 (1952).

[4] D. R. Bates and A. Dalgarno, J. Atmos. Terr. Phys., 5, 329-344 (1954).

JOURNAL OF GEOPHYSICAL RESEARCH VOLUME 60, NO 3 SEPTEMBER, 1955

ELECTROMAGNETIC INDUCTION IN A TWO-LAYER EARTH

BY BIMAL KRISHNA BHATTACHARYYA

Department of Geology and Geophysics, Indian Institute of Technology, Kharagpur, India

(Received March 18, 1955)

ABSTRACT

The problem of determining the induced field components outside a horizontal two-layer earth has been tackled from theoretical point of view. The expressions obtained have been applied to evaluate the induced magnetic field due to an oscillating magnetic dipole on the surface of the earth. Two separate cases have been considered, for example, (*i*) two layers of nearly equal conductivities, and (*ii*) a conducting layer over an insulating medium, and the formulae have been reduced to a form amenable to numerical integration.

Introduction

A general theory of electromagnetic induction in a semi-infinite homogeneous conducting medium has been developed by Price [see 1 of "References" at end of paper]. A method for calculating the induced field on the surface of the medium for an inducing magnetic field located externally has been described in detail in the excellent paper by Price. It is felt necessary to extend the method so as to apply it to the case of an inhomogeneous medium. With this purpose in view, an attempt is made in this paper to outline the general procedure for determining the induced field on the surface of a medium whose conductivity is a function of depth. For geophysical exploration, this type of treatment may be useful for interpretation of field data.

The case of a two-layer earth is considered in detail. Attention is then focused to determine the field corresponding to the particular inducing field produced by an oscillating magnetic dipole on the surface of the earth. Firstly, the two layers are assumed to be of nearly equal conductivity. The expressions of the induced magnetic field have been deduced in a form which can be numerically integrated. In the second case, the conducting layer is assumed to be placed over an insulating medium. In this case also, the components of the induced field have been expressed in the form of two well-known integrals given by Foster [2] and Sommerfeld [3].

Statement of the problem

Outside a semi-infinite medium, whose conductivity is a function of depth, is located the source of an inducing magnetic field. Cylindrical coordinate system ρ, ϕ, z will be used where the z-axis is assumed to be vertical and positive downward. Let the surface of the ground be the plane $z = 0$, and let the source be placed at $z = -h_0$.

Maxwell's equations when written in mks system of units are

$$\vec{\nabla} \times \vec{E} + \frac{\partial \vec{B}}{\partial t} = 0 \quad \ldots\ldots(1)$$

$$\vec{\nabla} \times \vec{H} = \sigma \vec{E} + \frac{\partial \vec{D}}{\partial t} \quad \ldots\ldots(2)$$

$$\text{div } \vec{B} = 0 \quad \ldots\ldots(3)$$

and

$$\text{div } \vec{D} = \rho \quad \ldots\ldots(4)$$

Due to the rotational symmetry of the electromagnetic field, the components B_ϕ , E_ρ , and E_z are taken to be zero. If the dependence of E and B upon time be sinusoidal, then we can write

$$E = Re\{E_1 \exp(j\omega t)\} \quad \text{and} \quad B = Re\{B_1 \exp(j\omega t)\} \quad \ldots\ldots(5)$$

where E_1 and B_1 are functions of position only and ω is the angular frequency. If the frequency of the alternating inducing potential is not too high, displacement currents may be neglected. Since the decay of any initial volume-charge distribution does not depend upon any other field conditions, we may put

$$\text{div } \vec{E} = 0 \quad \ldots\ldots(6)$$

With the help of equations (1) and (2), we can write for the non-vanishing components of the electric and magnetic vectors, as follows:

$$\frac{\partial}{\partial z}\left(\frac{B_\rho}{\mu}\right) - \frac{\partial}{\partial \rho}\left(\frac{B_z}{\mu}\right) = \sigma E_\phi \quad \ldots\ldots(7)$$

$$\frac{\partial E_\phi}{\partial z} = j\omega B_\rho \quad \ldots\ldots(8)$$

and

$$\frac{\partial E_\phi}{\partial \rho} + \frac{E_\phi}{\rho} = -j\omega B_z \quad \ldots\ldots(9)$$

With the aid of equations (7), (8), and (9), we have

$$\frac{\partial^2 E}{\partial z^2} + \frac{\partial^2 E}{\partial \rho^2} + \frac{1}{\rho}\frac{\partial E}{\partial \rho} - \left[\frac{1}{\rho^2} + j\omega\mu\sigma\right]E = 0 \quad \ldots\ldots(10)$$

where E is written for E_ϕ . Substituting $E = R(\rho)Z(z)$ in (10), we obtain the following two equations:

$$\frac{d^2 R}{d\rho^2} + \frac{1}{\rho}\frac{dR}{d\rho} + \left(\lambda^2 - \frac{1}{\rho^2}\right)R = 0 \quad \ldots\ldots(11)$$

and

$$\frac{d^2 Z}{dz^2} - (\lambda^2 + j\omega\mu\sigma)Z = 0, \qquad (z > 0) \quad \ldots\ldots(12)$$

Above the surface of the earth ($z < 0$), equation (12) yields

$$\frac{d^2 Z}{dz^2} - \lambda^2 Z = 0, \qquad (z < 0) \quad \ldots\ldots(13)$$

Equation (11) is the Bessel equation, the solution of which is

$$R(\rho) = J_1(\lambda\rho)$$

Let $Z(z, \lambda)$ be such a solution of equation (12) that vanishes at infinity. From (13), we easily obtain

$$Z = A_1 e^{\lambda z} + B_1 e^{-\lambda z}, \qquad (\text{for } z < 0) \ldots\ldots\ldots\ldots\ldots\ldots (14)$$

Therefore,

$$\left.\begin{aligned} E_+ &= Z(z, \lambda)\, J_1(\lambda\rho), && z > 0 \\ E_- &= \{A_1 e^{\lambda z} + B_1 e^{-\lambda z}\}\, J_1(\lambda\rho), && z < 0 \end{aligned}\right\} \ldots\ldots\ldots\ldots\ldots\ldots (15)$$

The boundary conditions at the surface of the earth ($z = 0$) demand the continuity of the three electric and magnetic components E_ϕ, B_ρ, and B_z. From equation (15), we note that due to continuity of E_+ and E_- at $z = 0$

$$Z(0, \lambda) = A_1 + B_1 \ldots\ldots\ldots\ldots\ldots\ldots\ldots\ldots (16)$$

It is evident from equation (9) that the condition (16) makes the normal component B_z of the magnetic field continuous at $z = 0$. For the continuity of B_ρ, we must have equation (8):

$$\left.\begin{aligned} &\left(\frac{\partial E_+}{\partial z}\right)_{z=0} - \left(\frac{\partial E_-}{\partial z}\right)_{z=0} = 0, \qquad \text{that is,} \\ &Z'(0, \lambda) = \lambda(A_1 - B_1) \end{aligned}\right\} \ldots\ldots\ldots\ldots\ldots\ldots (17)$$

Now, above the ground's surface ($z < 0$),

$$H_\rho = -\frac{1}{j\omega\mu}\{A_1 e^{\lambda z} - B_1 e^{-\lambda z}\}\frac{\mathrm{d}}{d\rho} J_0(\lambda\rho) \ldots\ldots\ldots\ldots\ldots\ldots (18)$$

and

$$H_z = -\frac{1}{j\omega\mu} J_0(\lambda\rho)\frac{\mathrm{d}}{\mathrm{d}z}\{A_1 e^{\lambda z} - B_1 e^{-\lambda z}\} \ldots\ldots\ldots\ldots\ldots\ldots (19)$$

So the magnetic field intensity may be expressed as the gradient of a scalar potential Φ, which is given by

$$\Phi = -\{A e^{\lambda z} + B e^{-\lambda z}\} J_0(\lambda\rho) \ldots\ldots\ldots\ldots\ldots\ldots\ldots (20)$$

where λ is real and positive, and

$$A = -\frac{A_1}{j\omega\mu} \qquad \text{and} \qquad B = \frac{B_1}{j\omega\mu} \ldots\ldots\ldots\ldots\ldots\ldots (21)$$

It is obvious that Φ is a solution of Laplace's equation $\nabla^2\Phi = 0$ in the region $h_0 < z < 0$.

Now, $Be^{-\lambda z}$ and $Ae^{\lambda z}$ correspond, respectively, to the given inducing field and the induced currents in the semi-infinite medium. So the problem is to express A and $Z(z, \lambda)$ in terms of B, which may be assumed to be known.

Case of a two-layer earth

Let us now consider the case of a two-layer earth (Fig. 1), in which the two

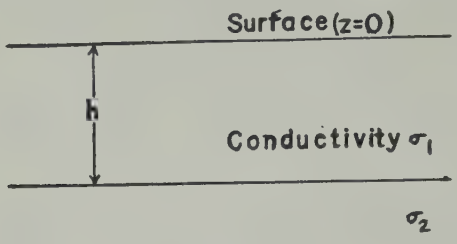

FIG. 1—Two-layer earth

layers are of uniform conductivities σ_1 and σ_2 , respectively. Equation (12) takes the form

$$\frac{d^2Z_1}{dz^2} - \theta_1^2 Z_1 = 0, \qquad (0 < z \leq h) \ldots\ldots\ldots\ldots\ldots\ldots (22)$$

and

$$\frac{d^2Z_2}{dz^2} - \theta_2^2 Z_2 = 0, \qquad (z \geq h) \ldots\ldots\ldots\ldots\ldots\ldots (23)$$

where

$$\left.\begin{aligned} \theta_1^2 &= \lambda^2 + j\omega\sigma_1\mu \\ \theta_2^2 &= \lambda^2 + j\omega\sigma_2\mu \end{aligned}\right\} \ldots\ldots\ldots\ldots\ldots\ldots (24)$$

and z_1 and z_2 correspond, respectively, to the upper and lower medium.

The solutions of equations (22) and (23) may be written as

$$Z_1 = a_1 e^{\theta_1 z} + b_1 e^{-\theta_1 z}, \qquad (0 < z \leq h) \ldots\ldots\ldots\ldots\ldots\ldots (25)$$

and

$$Z_2 = c_1 e^{-\theta_2 z}, \qquad (z \geq h) \ldots\ldots\ldots\ldots\ldots\ldots (26)$$

where the term containing $e^{\theta_2 z}$ has been dropped due to the condition $Z_2\,(z, \lambda) \to 0$ as $z \to \infty$. At the interface between the two boundaries ($z = h$),

$$Z_1(h, \lambda) = Z_2(h, \lambda) \ldots\ldots\ldots\ldots\ldots\ldots (27)$$

and

$$\dot{Z}_1(h, \lambda) = \dot{Z}_2(h, \lambda) \ldots\ldots\ldots\ldots\ldots\ldots (28)$$

When these boundary conditions are applied to equations (25) and (26), we obtain

$$a_1 e^{\theta_1 h} + b_1 e^{-\theta_1 h} = c_1 e^{-\theta_2 h} \ldots\ldots\ldots\ldots\ldots\ldots (29)$$

and.

$$\theta_1[a_1 e^{\theta_1 h} - b_1 e^{-\theta_1 h}] = -\theta_2 c_1 e^{-\theta_2 h} \ldots\ldots\ldots\ldots\ldots\ldots (30)$$

With the help of (29) and (30), we can express a_1 and b_1 in terms of c_1 :

$$a_1 = \frac{c_1}{2} e^{-(\theta_1+\theta_2)h}\left(1 - \frac{\theta_2}{\theta_1}\right) \ldots\ldots\ldots\ldots\ldots\ldots (31)$$

and

$$b_1 = \frac{c_1}{2} e^{-(\theta_2-\theta_1)h}\left(1 + \frac{\theta_2}{\theta_1}\right) \ldots\ldots\ldots\ldots\ldots\ldots (32)$$

So we can write the expression of $Z_1(z, \lambda)$ in the following form:

$$Z_1(z, \lambda) = \frac{c_1}{2} e^{[-(\theta_1+\theta_2)h+\theta_1 z]}\left(1 - \frac{\theta_2}{\theta_1}\right) + \frac{c_1}{2} e^{[-(\theta_2-\theta_1)h-\theta_1 z]}\left(1 + \frac{\theta_2}{\theta_1}\right) \quad \ldots\ldots(33)$$

Substituting the value of $Z_1(0, \lambda)$ into the equations (16) and (17) which satisfy the boundary conditions, we have

$$\begin{aligned} Z_1(0, \lambda) &= \frac{c_1}{2} e^{-(\theta_1+\theta_2)h}\left(1 - \frac{\theta_2}{\theta_1}\right) + \frac{c_1}{2} e^{-(\theta_2-\theta_1)h}\left(1 - \frac{\theta_2}{\theta_1}\right) \\ &= A_1 + B_1 \quad \ldots\ldots(34) \end{aligned}$$

and

$$\begin{aligned} Z_1(0, \lambda) &= \frac{c_1\theta_1}{2}\left[e^{-(\theta_1+\theta_2)h}\left(1 - \frac{\theta_2}{\theta_1}\right) - e^{-(\theta_2-\theta_1)h}\left(1 + \frac{\theta_2}{\theta_1}\right)\right] \\ &= \lambda(A_1 - B_1) \quad \ldots\ldots(35) \end{aligned}$$

Expressing A_1 and B_1 in terms of A and B, we have

$$\left.\begin{aligned} -j\omega\mu(A - B) &= \frac{c_1}{2} D_1 \\ \text{and} \qquad -j\omega\lambda\mu(A + B) &= \frac{c_1\theta_1}{2} D_2 \end{aligned}\right\} \quad \ldots\ldots(36)$$

where

$$D_1 = e^{-(\theta_1+\theta_2)h}\left(1 - \frac{\theta_2}{\theta_1}\right) + e^{-(\theta_2-\theta_1)h}\left(1 + \frac{\theta_2}{\theta_1}\right)$$

and

$$D_2 = e^{-(\theta_1+\theta_2)h}\left(1 - \frac{\theta_2}{\theta_1}\right) - e^{-(\theta_2-\theta_1)h}\left(1 + \frac{\theta_2}{\theta_1}\right)$$

It can now be easily shown from (36) that

$$\left.\begin{aligned} A &= \frac{\theta_1 D_2 + D_1\lambda}{\theta_1 D_2 - D_1\lambda} B \\ \text{and} \qquad c_1 &= j\omega\mu B \frac{4\lambda}{D_1\lambda - \theta_1 D_2} \end{aligned}\right\} \quad \ldots\ldots(37)$$

So with the help of equation (20) we can now express the scalar potential of the induced magnetic field outside the two-layer earth ($h_0 < z < 0$) in the following form:

$$\Phi_1 = -\frac{\theta_1 D_2 + D_1\lambda}{\theta_1 D_2 - D_1\lambda} B e^{\lambda z} J_0(\lambda\rho) \quad \ldots\ldots(38)$$

In the case of a homogeneous earth of conductivity σ_1, we can easily show by putting $\theta_1 = \theta_2$ that

$$\Phi_1 = -\frac{\theta_1 - \lambda}{\theta_1 + \lambda} B e^{\lambda z} J_0(\lambda\rho) \quad \ldots\ldots(39)$$

which is exactly similar to the expression of the scalar potential obtained by Price [1].

With the help of equations (15), (25), (26), (31), (32), and (37), the electric field inside the conductor may be written as

$$\left.\begin{aligned} E_+ &= j\omega\mu B \frac{2\lambda}{(D_1\lambda - \theta_1 D_2)} \left[e^{-(\theta_1+\theta_2)h+\theta_1 z}\left(1 - \frac{\theta_2}{\theta_1}\right) \right. \\ &\qquad \left. + e^{-(\theta_2-\theta_1)h-\theta_1 z}\left(1 + \frac{\theta_2}{\theta_1}\right)\right] J_1(\lambda\rho), \qquad (0 \leq z \leq h) \\ E_+ &= j\omega\mu B \frac{4\lambda}{D_1\lambda - \theta_1 D_2} e^{-\theta_2 z} J_1(\lambda\rho), \qquad (z \geq h) \end{aligned}\right\} \quad \ldots\ldots(40)$$

So the induced current density, $i = \sigma E$, at any point inside the conductor can be easily determined.

Oscillating magnetic dipole at the surface of a two-layer earth

Let us now apply the results of our previous analysis to the case of the induced field produced by an oscillating magnetic dipole whose moment M_1 varies sinusoidally with period $2\pi/\omega$ and which is located at the origin over a semi-infinite two-layer earth of conductivities σ_1 and σ_2, respectively. The inducing potential at a point whose cylindrical coordinates are (ρ, z) is given by

$$\Phi = -\frac{1}{4\pi} M_1 \frac{\partial}{\partial z}\left(\frac{1}{r}\right) \quad \ldots\ldots(41)$$

where

$$r^2 = \rho^2 + z^2$$

Since

$$\frac{1}{r} = \int_0^\infty e^{-\lambda z} J_0(\lambda\rho)\, d\lambda$$

Φ may be expressed as

$$\Phi = M \int_0^\infty e^{-\lambda z} J_0(\lambda\rho)\lambda\, d\lambda \quad \ldots\ldots(42)$$

where $M = M_1/4\pi$. With the help of (38), we now obtain the expression of the induced potential as

$$\Phi_1 = M \int_0^\infty \frac{\theta_1 D_2 + D_1\lambda}{\theta_1 D_2 - D_1\lambda} e^{\lambda z} J_0(\lambda\rho)\lambda\, d\lambda \quad \ldots\ldots(43)$$

Algebraic simplification of (43) leads to

$$\Phi_1 = M \int_0^\infty \frac{(\theta_2 - \theta_1)(\theta_1 + \lambda) + (\theta_1 + \theta_2)(\theta_1 - \lambda)e^{2\theta_1 h}}{(\theta_2 - \theta_1)(\theta_1 - \lambda) + (\theta_1 + \theta_2)(\theta_1 + \lambda)e^{2\theta_1 h}} e^{\lambda z} J_0(\lambda\rho)\lambda\, d\lambda \quad \ldots\ldots(44)$$

This complicated expression has been simplified in the following two examples by assuming (*i*) the difference in conductivities of the two layers to be very small compared to the average conductivity and (*ii*) the lower layer to be an insulating medium.

In the case of a homogeneous earth, we have

$$\theta_1 = \theta_2 = \theta$$

In this case, equation (44) reduces to

$$\Phi_1' = M \int_0^\infty \frac{\theta_1 - \lambda}{\theta_1 + \lambda} e^{\lambda z} J_0(\lambda\rho)\lambda \, d\lambda \quad \ldots\ldots(45)$$

This is the same formula for the induced magnetic field as obtained by Gordon [4]. Gordon has deduced expressions for the radial and vertical components of the induced magnetic field in his paper. So we shall not consider this case here.

Case 1—Two layers of slightly different conductivities

We shall assume that the difference in the two conductivities σ_1 and σ_2 is small compared to the average conductivities, that is,

$$\Delta\sigma = \sigma_1 - \sigma_2 \ll \frac{\sigma_1 + \sigma_2}{2} \quad \ldots\ldots(46)$$

In this case, equation (44) may be reduced to the following simplified expression with sufficient accuracy:

$$\Phi_1 = M \int_0^\infty \left[\frac{(\theta_2 - \theta_1)}{(\theta_2 + \theta_1)} e^{-2\theta_1 h} + \frac{(\theta_1 - \lambda)}{(\theta_1 + \lambda)}\right] e^{\lambda z} J_0(\lambda\rho)\lambda \, d\lambda \quad \ldots\ldots(47)$$

The induced potential may, therefore, be written as

$$\Phi_1 = \Phi_1' + \Phi_1'' \quad \ldots\ldots(48)$$

where Φ_1' is an expression identical with that obtained in the case of a homogeneous earth and Φ_1'' arises from the inhomogeneity in conductivity. Since Φ_1' has already been considered by Gordon [4], let us obtain the induced field due to Φ_1''.

$$\Phi_1'' = M \int_0^\infty \frac{(\theta_2 - \theta_1)}{(\theta_2 + \theta_1)} e^{-2\theta_1 h + \lambda z} J_0(\lambda\rho)\lambda \, d\lambda \quad \ldots\ldots(49)$$

which may be written approximately as (at the surface, that is, $z = 0$)

$$\Phi_1'' = \frac{Mj\omega\mu\Delta\sigma}{4} \int_0^\infty e^{-2\theta h} J_0(\lambda\rho) \frac{\lambda}{\theta^2} \, d\lambda \quad \ldots\ldots(50)$$

where θ is the average conductivity $(\theta_1 + \theta_2)/2$. Similarly, for the components of the magnetic field at the surface, we have

$$H_\rho'' = \frac{Mj\omega\mu\Delta\sigma}{4} \int_0^\infty \frac{e^{-2\theta h}}{\theta^2} J_1(\lambda\rho)\lambda^2 \, d\lambda \quad \ldots\ldots(51)$$

and

$$H_z'' = -\frac{Mj\omega\mu\Delta\sigma}{4} \int_0^\infty \frac{e^{-2\theta h}}{\theta^2} J_0(\lambda\rho)\lambda^2 \, d\lambda \quad \ldots\ldots(52)$$

The integrals in the above expressions can be expressed in terms of the following two integrals given by Sommerfeld [3] and Foster [2], respectively:

$$S = \int_0^\infty J_0(\lambda\rho) \frac{e^{-\theta z}}{\theta} \lambda \, d\lambda = \frac{1}{R} e^{-\sqrt{j\omega\sigma\mu} R} \quad \ldots\ldots(53)$$

where

$$\theta^2 = \lambda^2 + j\omega\sigma\mu \qquad \text{and} \qquad R^2 = \rho^2 + z^2$$

and

$$F = \int_0^\infty e^{-\theta z} J_0(\lambda\rho)\,\frac{d\lambda}{\theta}$$

$$= I_0\left[\sqrt{j\omega\sigma\mu}\,\frac{(R-z)}{2}\right] K_0\left[\sqrt{j\omega\sigma\mu}\,\frac{(R+z)}{2}\right] \quad \ldots\ldots\ldots\ldots (54)$$

where I_0 and K_0 are modified Bessel functions of the first and second kind, respectively. Therefore, it easily follows that

$$\Phi_1'' = \frac{Mj\omega\Delta\sigma\mu}{4} \int_{2h}^\infty \frac{e^{-\sqrt{j\omega\sigma\mu}\,R}}{R}\,dz \quad \ldots\ldots\ldots\ldots\ldots\ldots\ldots\ldots (55)$$

$$H_\rho'' = \frac{Mj\omega\Delta\sigma\mu}{4} \frac{d}{d\rho}\left[\int_{2h}^\infty \frac{e^{-\sqrt{j\omega\sigma\mu}\,R}}{R}\,dz\right] \quad \ldots\ldots\ldots\ldots\ldots\ldots (56)$$

$$H_z'' = -\frac{Mj\omega\Delta\sigma\mu}{4}\left[-\left(\frac{dF}{dz}\right)_{z=2h} - j\omega\sigma\mu \int_{2h}^\infty F\,dz\right] \quad \ldots\ldots\ldots\ldots (57)$$

Case II—Conducting layer above an insulating medium

The formulae for the field intensities and magnetic induced potential will now be determined for the case of a conducting layer above an insulating medium. In this case, $\theta_2 = \lambda$, and so the expression for the induced potential reduces to

$$\Phi_1 = +M \int_0^\infty \frac{(\theta_1^2 - \lambda^2)(1 - e^{2\theta_1 h})}{(\theta_1 - \lambda)^2 - (\theta_1 + \lambda)^2 e^{2\theta_1 h}}\, e^{\lambda z} J_0(\lambda\rho)\lambda\,d\lambda \quad \ldots\ldots\ldots (58)$$

This expression will be simplified by assuming that

$$(\theta_1 + \lambda)^2 e^{2\theta_1 h} \gg (\theta_1 - \lambda)^2$$

so that we can express (58) in the following way:

$$\Phi_1 = +M \int_0^\infty \frac{(\lambda^2 - \theta_1^2)(1 - e^{2\theta_1 h})}{(\lambda + \theta_1)^2 e^{2\theta_1 h}}\, e^{\lambda z} J_0(\lambda\rho)\lambda\,d\lambda$$

$$= +M \int_0^\infty \frac{\lambda - \theta_1}{\lambda + \theta_1}\,(e^{-2\theta_1 h} - 1) e^{\lambda z} J_0(\lambda\rho)\lambda\,d\lambda \quad \ldots\ldots\ldots\ldots (59)$$

So the term Φ_1'' which appears due to inhomogeneity in conductivity is given by

$$\Phi_1'' = +M \int_0^\infty \frac{\lambda - \theta_1}{\lambda + \theta_1}\, e^{\lambda z - 2\theta_1 h} J_0(\lambda\rho)\lambda\,d\lambda \quad \ldots\ldots\ldots\ldots\ldots (60)$$

$$= -\frac{M}{j\omega\sigma_1\mu} \int_0^\infty (\lambda - \theta_1)^2 e^{\lambda z - 2\theta_1 h} J_0(\lambda\rho)\lambda\,d\lambda \quad \ldots\ldots\ldots\ldots\ldots (61)$$

The expressions of the induced potential and the components of the magnetic field at the surface (that is, $z = 0$) are written as

$$\Phi_1'' = -\frac{M}{j\omega\sigma_1\mu}\int_0^\infty (\lambda - \theta_1)^2 e^{-2\theta_1 h} J_0(\lambda\rho)\lambda \, d\lambda \quad \ldots\ldots\ldots\ldots (62)$$

$$H_\rho'' = -\frac{M}{j\omega\sigma_1\mu}\int_0^\infty (\lambda - \theta_1)^2 e^{-2\theta_1 h} J_1(\lambda\rho)\lambda^2 \, d\lambda \quad \ldots\ldots\ldots\ldots (63)$$

and

$$H_z'' = +\frac{M}{j\omega\sigma_1\mu}\int_0^\infty (\lambda - \theta_1)^2 e^{-2\theta_1 h} J_0(\lambda\rho)\lambda^2 \, d\lambda \quad \ldots\ldots\ldots\ldots (64)$$

The integral

$$I = \int_0^\infty (\lambda - \theta_1)^2 e^{-2\theta_1 h} J_0(\lambda\rho)\lambda \, d\lambda \quad \ldots\ldots\ldots\ldots (65)$$

may be broken up into three parts

$$I = I_1 + I_2 - I_3 \quad \ldots\ldots\ldots\ldots (66)$$

where

$$\left.\begin{aligned} I_1 &= 2\int_0^\infty e^{-2\theta_1 h} J_0(\lambda\rho)\lambda^3 \, d\lambda \\ I_2 &= j\omega\sigma_1\mu\int_0^\infty e^{-2\theta_1 h} J_0(\lambda\rho)\lambda \, d\lambda \\ I_3 &= 2\int_0^\infty \lambda^2\theta_1 e^{-2\theta_1 h} J_0(\lambda\rho) \, d\lambda \end{aligned}\right\} \quad \ldots\ldots\ldots\ldots (67)$$

All of these three integrals can be expressed in terms of S and F, which are given in equations (53) and (54).

$$\left.\begin{aligned} I_1 &= 2\left[\frac{d}{dz}\frac{1}{\rho}\frac{d}{d\rho}\left(\rho\frac{dS}{d\rho}\right)\right]_{z=2h} \\ I_2 &= -j\omega\sigma_1\mu\left(\frac{dS}{dz}\right)_{z=2h} \\ I_3 &= -2\frac{d^2}{dz^2}\left[\frac{1}{\rho}\frac{d}{d\rho}\left(\rho\frac{dF}{d\rho}\right)\right]_{z=2h} \end{aligned}\right\} \quad \ldots\ldots\ldots\ldots (68)$$

Thus,

$$\Phi_1'' = -\frac{M}{j\omega\sigma_1\mu}(I_1 + I_2 - I_3)$$

can now be calculated with the help of (68).

Equation (63) may now be expressed in the following way:

$$H_\rho'' = -\frac{M}{j\omega\sigma_1\mu}\frac{d}{d\rho}[I_1(\rho) + I_2(\rho) - I_3(\rho)] \quad \ldots\ldots\ldots\ldots (69)$$

Adopting a similar process, we obtain

$$H_z'' = +\frac{M}{j\omega\sigma_1\mu}[I_1' + I_2' + I_3'] \quad \ldots\ldots(70)$$

where

$$\left.\begin{aligned} I_1' &= 2\int_0^\infty e^{-2\theta_1 h} J_0(\lambda\rho)\lambda^4\,d\lambda \\ I_2' &= j\omega\sigma_1\mu\int_0^\infty e^{-2\theta_1 h} J_0(\lambda\rho)\lambda^2\,d\lambda \\ I_3' &= 2\int_0^\infty \lambda^3\theta_1 e^{-2\theta_1 h} J_0(\lambda\rho)\,d\lambda \end{aligned}\right\} \quad \ldots\ldots(71)$$

These three integrals may be replaced by the following expressions:

$$\left.\begin{aligned} I_1' &= -2\frac{d}{dz}\frac{1}{\rho}\frac{d}{d\rho}\left[\rho\frac{d}{d\rho}\left\{\frac{1}{\rho}\frac{d}{d\rho}\left(\rho\frac{dF}{d\rho}\right)\right\}\right]_{z=2h} \\ I_2' &= j\omega\sigma_1\mu\left[\frac{d}{dz}\left\{\frac{1}{\rho}\frac{d}{d\rho}\left(\rho\frac{dF}{d\rho}\right)\right\}\right]_{z=2h} \\ I_3' &= -2\left[\frac{d^2}{dz^2}\left\{\frac{1}{\rho}\frac{d}{d\rho}\left(\rho\frac{dS}{d\rho}\right)\right\}\right]_{z=2h} \end{aligned}\right\} \quad \ldots\ldots(72)$$

Now, with the help of (72), H_z'' can be computed.

Conclusion

In this paper, expressions have been obtained for the induced electromagnetic field for the case of a two-layer earth. The general expressions have been applied to deduce the induced field when an oscillating magnetic dipole is placed on the surface of the earth. The expressions of the components of the induced magnetic field have been obtained in a form which is suitable for numerical integration. The results of the analysis may prove to be useful for interpretation of field data in electromagnetic exploration. Further work in this line is in progress at this Institute.

Acknowledgments

The author takes this opportunity and pleasure of thanking Prof. P. K. Bhattacharyya for his kind interest and many valuable suggestions.

References

[1] A. T. Price, Q. J. Mech. Appl. Math., **3**, 385 (1950).
[2] R. M. Foster, Bell System Tech. J., **10**, 408 (1931).
[3] A. Sommerfeld, Partial differential equations in physics, Academic Press, Inc., New York (1949).
[4] A. N. Gordon, Q. J. Mech. Appl. Math., **4**, 106 (1951).
[5] J. A. Stratton, Electromagnetic theory, McGraw-Hill Book Co., Inc., New York (1942).

JOURNAL OF GEOPHYSICAL RESEARCH VOLUME 60, No. 3 SEPTEMBER, 1955

AN EXPERIMENTAL ANALYSIS OF THE EFFECT OF AIR POLLUTION ON THE CONDUCTIVITY AND ION BALANCE OF THE ATMOSPHERE

BY B. B. PHILLIPS, P. A. ALLEE, J. C. PALES, AND R. H. WOESSNER

United States Weather Bureau, Washington, D.C.

(Received March 21, 1955)

ABSTRACT

A series of conductivity measurements made in a large sealed sphere has shown that in ordinary outside air the suspended nuclei or pollution normally so modify the ionic combination that the electrical conductivities approach equality. Equal conductivities are normally associated with an excess in the density of the small positive ion. It is found that with decreasing pollution the value of the negative conductivity increases more than does the positive, and the ionic densities approach equality. In clean air, equal densities of the positive and negative light ions are observed, and the conductivities become proportional to the commonly accepted laboratory values for the ionic mobilities. The results are consistent with recently developed expressions for the diffusion of ions and their attachment to atmospheric particles.

1. *Introduction*

During the past few years, aircraft-based measurements have suggested that the positive and negative components of the electrical conductivity of the atmosphere are roughly equal at all accessible levels. Since the variation of potential gradient with altitude is small, the positive space-charge excess is small and can hardly account for the observed conductivity ratios. As the ionizing agencies of the atmosphere invariably generate ion pairs, it has been suggested that the observed equality of the conductivities implies a similar equality in the positive and negative ionic mobilities. The analysis of recent measurements of the positive and negative conductivities and ion densities within the Weather Bureau's 3,000 cubic meter cloud-chamber, at Hitchcock, Texas, indicates that neither the presence of a positive space-charge nor the equality of the ionic mobilities is a necessary condition to describe the observed conductivity values in the lower atmosphere. The results show that suspended nuclei or pollution in the air normally so modify the ionic combination that the electrical conductivities approach equality. However, as these nuclei are withdrawn from the air, the negative and positive conductivities both increase. When most of the nuclei are removed, the ratio of the conductivities approaches the commonly accepted ratio of the respective ionic mobilities.

2. *Experimental Procedure*

Three separate experiments are discussed in this paper. In the first experiment, simultaneous measurements were made of the positive and negative conductivities

of air lying stagnant within the sealed sphere. For the first test, the air was left to free itself of pollution through the natural mechanisms of coagulation, diffusion, and sedimentation. These natural cleansing mechanisms proceeded very slowly within the enclosure. Because of this sluggishness, a second series of measurements was made after installing two simple electrostatic precipitators inside the sphere. These units consisted of a set of four concentric tubes, each of which was mounted on insulated supports. Alternate tubes were connected to a 10,000 volt source and adjusted so that no corona was produced. Air within the sphere was circulated through the inter-electrode region by a small electric blower. This second experiment was terminated after seven days by unfavorable weather conditions. For the last phase of the experiment, the sphere was again sealed with the electrostatic precipitators in operation and a series of measurements made of both the polar conductivities and the positive and negative small-ion densities. Knowledge of the values of the constituent ionic densities and conductivities enables one to calculate the value of the respective ionic mobilities directly by means of the defining conductivity equation. This final set of data included observations made at the rate of one to three times per day over a period of almost three weeks.

3. *Apparatus and Details*

The 3,000 cubic meter cloud-chamber is described in [1] see "References" at end of paper. Briefly, the chamber is a hollow steel-tank, 60 feet in diameter. Since absolute closure of the chamber was not feasible, it was desirable to conduct the experiment at a slight positive pressure to prevent the leakage of fresh outside or "polluted" air into the chamber. To accomplish this result, the sphere was thoroughly ventilated following a cold frontal passage and sealed on the morning of minimum temperature. This procedure established and maintained a small positive-pressure differential. The slight leakage of air was not sufficiently great to appreciably influence the pressure within the sphere. However, it was found that the nuclei in a small amount of outside air profoundly modified the conductivities and ionic densities inside the chamber whenever leakage due to an inward pressure differential existed.

The conductivities were measured by the discharging conductor method, previously adopted for measuring the electrical conductivity of clouds [2]. This method consisted of simultaneously observing the rate of discharge of two oppositely-charged wire-cages. The conductivity, λ, of such a discharge system expressed in electrostatic units is defined in terms of the potential by the equation

$$\lambda = \frac{\ln \frac{V_0}{V_t}}{4\pi t}$$

where V_0 is the potential at time $t = 0$, and V_t is the potential at time $t = t$. The wire-cage conductors were approximately identical cylinders, 50 cm in diameter and 91 cm in length. Individual cages hung from insulated supports at opposite ends of a five meter pole, suspended horizontally near the center of the sphere. A symmetrically-placed grounded screen shielded each discharge system from the

other. The cages were connected by highly insulated conductors to electrometers in a small room immediately beneath the sphere. The voltages of the discharging cages were continually balanced manually at the null-point of the electrometers by elevating the normal ground of these instruments to a potential equal to that of the cages. A multipoint recorder connected across this electrometer bias furnished a time trace of the potential of the cage. Thus, each conductivity measurement represented some 100 points.

The electrostatic precipitators were each constructed from four metal tubes, eight feet long and of diameters 1, 6, 12, and 18 inches. These were mounted concentrically on insulated supports and alternate tubes connected to a 10,000 volt power-supply. Air was drawn through each unit at the rate of 50 cubic feet per minute. The combined flow was such that an amount of air equal to the volume of the sphere was processed in approximately 18 hours. The precipitators were always turned off for 30 minutes prior to all measurements.

A Gerdien conductivity apparatus, so polarized to function as an ion counter, served to measure the densities of the positive and negative ions. The collecting element for this apparatus was mounted two meters above the floor of the sphere. The ion current collected was calculated from the measured potential drop across a calibrated resistance.

The temperature within the sphere was periodically measured by means of a thermocouple, suspended well away from the wall of the chamber. In addition, a hygro-thermograph was installed a few feet above the lower surface of the sphere.

4. *Results*

The first measurements of conductivity in the sealed chamber were exploratory in nature and are summarized in Figure 1. Natural precipitation of the nuclei and

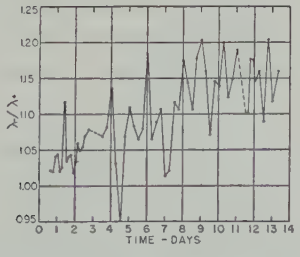

FIG. 1—Time variation of the conductivity ratio corresponding to natural clean-up processes

other air pollution by diffusion and sedimentation accounts in these tests for the observed systematic changes in the conductivity. Both the positive and negative conductivities increased with time, as did their ratio as shown in Figure 1. The large excursions in the ratio are doubtless related to air circulation within the sphere due to diurnal heating effects. The experiment became so prolonged that a second experiment was initiated, in which the nuclei and normal atmospheric pollution were swept out by an electrostatic precipitator.

The variation of the positive and negative conductivities as the air was gradually cleaned by electrostatic precipitation is shown in Figure 2. Under these circumstances, the rate of increase of each of the conductivities is initially quite rapid. The differences existing between simultaneous determinations of the positive

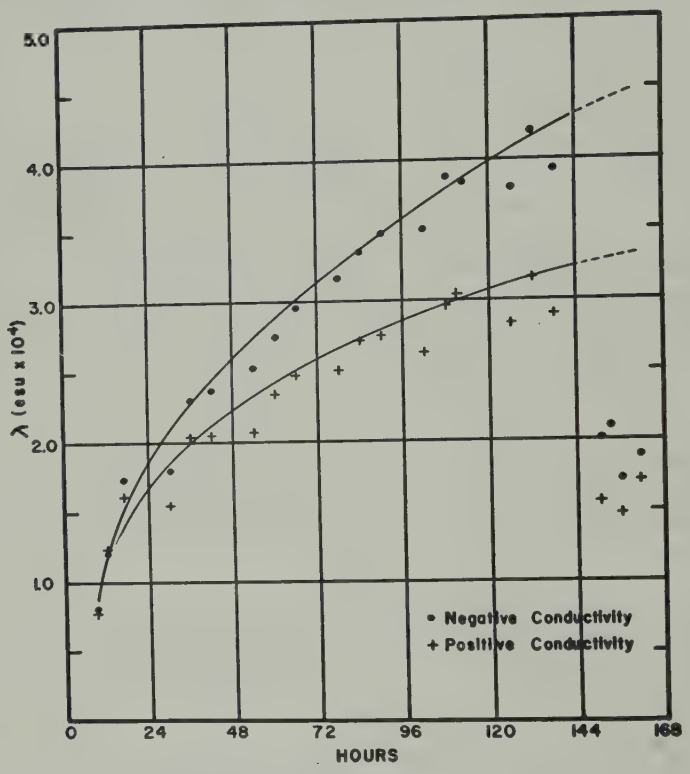

FIG. 2—The variation of conductivity with decreasing air-pollution with electrostatic clean-up

and negative conductivities are seen to increase steadily. At the beginning, in normal surface air, the values of the conductivities were approximately equal. Both conductivities increased with time, but the negative conductivity increased to greater values than did the positive. At the end of five days, the negative conductivity was roughly one-third greater. The daily superimposed variation, which had been observed in the preliminary experiment, is again evident in the data of Figure 2. The two curves superimposed on the plotted points have been drawn to correspond with those conductivities determined during the afternoon temperature maximum. Figure 3 shows the variation with time of the ratio of negative to positive conductivity for the same period. Unfortunately, at the end of 140 hours, a cold frontal passage occurred and the resulting temperature drop caused the pressure within the sphere to fall well below the ambient atmospheric pressure. The resulting leakage of outside air and pollution into the sphere caused the conductivities to drop to half their previous values within 24 hours and interrupted the sequence of data.

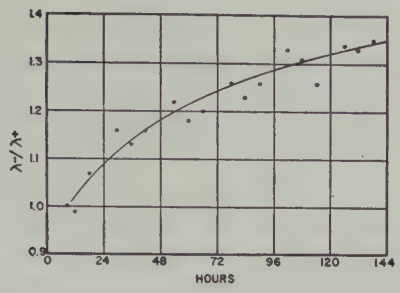

FIG. 3—Time variation of the conductivity ratio with decreasing air-pollution using electrostatic precipitators

Values for the ionic mobilities were calculated from the defining equation of the conductivity and the coordinated measurements of conductivity and ion density. These results are shown in Figures 4 and 5. The calculated mobilities represent measurements made over a wide range of humidity and age of the entrapped air. During the experiment, it was necessary to enter the sphere on two occasions, and negative pressure differentials existed during at least three days. Consequently, the measured values of the conductivities and ion densities fluctuated considerably from day to day.

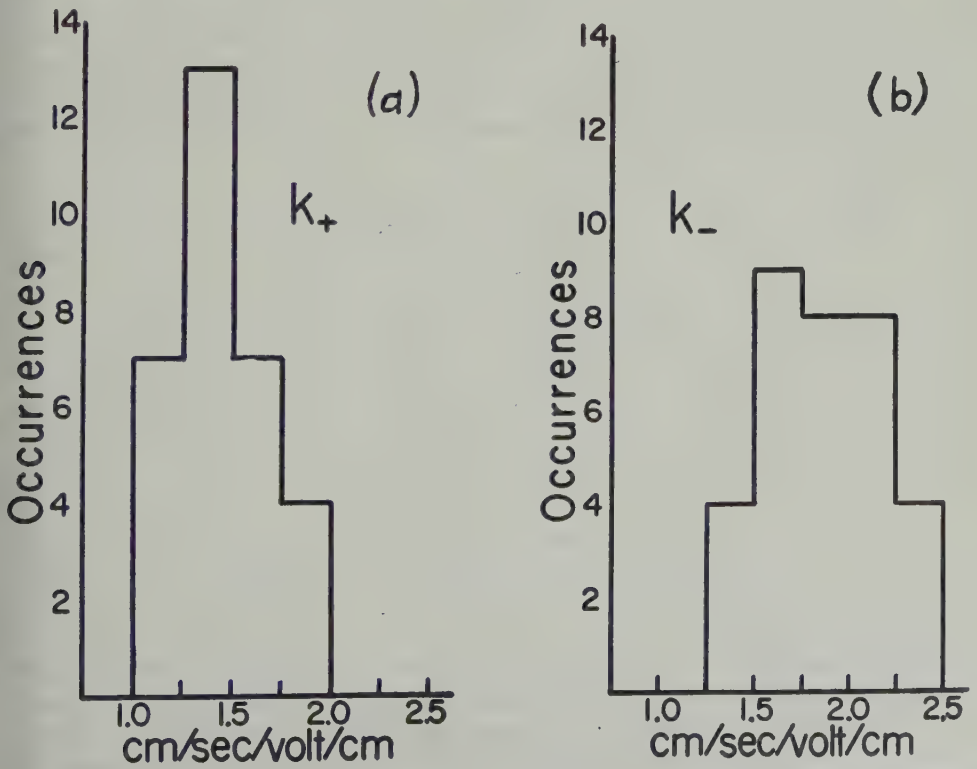

FIG. 4—Distribution of (*a*) positive small-ion mobilities, and (*b*) negative small-ion mobilities

Throughout the experiment, fresh surface air introduced into the sphere was associated with nearly equal conductivities and with a notable excess in the density of the small positive ion. In aged cleaned air, the ionic densities approached equality and the ratio of the conductivities approximated the usual laboratory-determined

Fig. 5—Distribution of small-ion mobility ratios

ratio of the ionic mobilities. No systematic spectrum of mobilities was evident for either the negative or positive ion. The mean value of all determinations for the positive-ion mobility is 1.52 cm/sec/volt/cm and for the negative-ion mobility 2.00 cm/sec/volt/cm. The computed ratios of the negative- to positive-ion mobilities for the separate observations shown in Figure 5 have a mean value of 1.30.

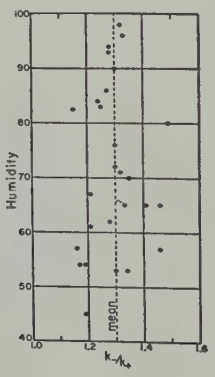

Fig. 6—Plot of small-ion mobility ratios *vs* humidity

Figure 6 is a plot of observed mobility ratio *vs* humidity. Since the humidity record for the three-week period was incomplete, not all mobility data are represented. The relation of these two parameters is of extreme interest in the light of the importance of the relative values of the ion mobilities in the ionic diffusion charging mechanisms.

5. *Discussion*

There can be little doubt that the observed variations of the polar conductivities and ionic densities result from the removal of condensation nuclei and pollution elements from the air. The experiment demonstrates that the concentration of suspended particulate matter profoundly influences the electrical equilibrium. The magnitudes of the positive and negative conductivities and ion densities are dependent on the concentration of pollution particles. The results also show that there is little or no decrease in the mobility of either the negative or positive ion in surface air, throughout wide variations of pollution and humidity.

The explanation of the observed results is clear. Though we know nothing of the actual nature of the particulate matter concerned, it is reasonable to assume that they are identical with the passive particles described in the recent theory of ionic diffusion charging of aerosols developed by Ross Gunn [3]. Gunn has shown that the rate of ionic combination with atmospheric particles or droplets of appreciable size is different for positive and negative ions. In the absence of a marked predominance of one type ion, the negative-ion combination rate is greater as a result of the excessive mobility of the negative ion. Thus, when particulate centers of appreciable size exist, the greater combination rate results in a net deficiency in the density of the negative *small* ion. Even so, the conductivities remain essentially equal because of the lower mobility of the positive ion. On the other hand, if all centers of radii greater than about 10^{-5} cm are swept out, either by gravity or electrostatic processes, the ions undergo random diffusion as the result of molecular bombardment. The rate at which ions combine with oppositely charged centers (or ions) is then governed by the random thermal motions and the probability of recombination, once the charge centers are close enough to actively attract each other. *This process is not selective in regard to sign.* In the absence of electric fields, the positive- and negative-ion densities, therefore, must be identical, and the ratios of the conductivities become proportional to the ionic mobility ratios commonly measured in the laboratory.

It is reasonable to explain the observed conductivities of the lower atmosphere by a similar argument. A close examination of the conductivities reported by Gish and Wait [4] shows the positive conductivity slightly exceeds that of the negative to the level of 25,000 feet. Above this level, the ratio of the negative to positive conductivity grows successively greater than unity. Measurements made during flight aboard the *Explorer II* [5], though incomplete below 35,000 feet, indicate that the negative conductivity is greater than the positive by a factor of approximately 1.3 to a height of 21 km. Callahan, Coroniti, Parziale, and Patten [6] report approximately equal conductivities to 36,000 feet. Disregarding the effect of space charge, the variation in the conductivity ratio can be attributed to the decrease in air pollution with altitude. Such a decrease in air pollution with altitude has been shown by Sagalyn and Faucher [7]. The equality of the conductivities up to the 8-10 km level is a measure of the extreme height reached by suspended particles and possibly defines the upper level of vertical convection in the middle latitudes. The measurements from the *Explorer II* show the absence of pollution at great heights.

The above explanation does not, in itself, imply the production of a negative

or positive space-charge within the atmosphere. Equal ionic conductivities are associated with an unbalance in the small ionic densities, but steady-state conditions decree an equal but opposite charge unbalance on the larger atmospheric elements.

In view of the above, it is doubtful that the ionic mobility ratio aloft differs substantially from surface values. The difference in the positive- and negative-ion mobility is ascribed to the formation of complex ions of a specific electrochemical character. The chemical homogeneity of the atmospheric stratum in question does not suggest a departure from surface ion-formation characteristics. It also is implausible that the results witnessed in the cloud-chamber are attributable to a variation in the chemical nature of the entrapped air.

The observed increase in conductivity with decreasing air pollution confirms the results obtained by Smith and Schilling [8] in their experiments on the variation of the positive-ion conductivity within a sealed room.

6. *Acknowledgment*

Our grateful appreciation is extended to Dr. Ross Gunn of the Division for foreseeing the importance of this experiment and aiding in the interpretation of its results.

References

[1] R. Gunn and P. A. Allee, A three thousand cubic meter cloud chamber, Bull. Amer. Met. Soc., **35**, 180-181 (1954).

[2] R. Gunn, Electrical conductivity of cloud, Baltimore meeting, American Meteorological Society, 1954.

[3] R. Gunn, Diffusion charging of atmospheric droplets by ions, and the resulting combination coefficients, J. Met., **11**, 339-347 (1954).

[4] O. H. Gish and G. R. Wait, Thunderstorms and the earth's general electrification, J. Geophys, Res., **55**, 473-484 (1950).

[5] O. H. Gish and K. L. Sherman, Electrical conductivity of air to an altitude of 22 kilometers, Nation. Geog. Soc., Contrib. Tech. Papers, Stratosphere Ser., No. 2, 94-116 (1936).

[6] R. C. Callahan, S. C. Coroniti, A. J. Parziale, and R. Patten, Electrical conductivity of air in the troposphere, J. Geophys. Res., **56**, 545-551 (1951).

[7] R. C. Sagalyn and G. A. Faucher, Aircraft investigation of the large ion content and conductivity of the atmosphere and their relation to meteorological factors, J. Atmos. Terr. Phys., **5**, 253-272 (1954).

[8] L. G. Smith and G. F. Schilling, The variation of the electrical conductivity of air within sealed rooms, J. Atmos. Terr. Phys., **4**, 314-321 (1954).

MAGNETIC EFFECTS DURING SOLAR ECLIPSES

BY A. M. VAN WIJK

Magnetic Observatory, Hermanus, Union of South Africa

(Received April 13, 1955)

ABSTRACT

To investigate solar eclipse effects of December 25, 1954, a study was made of the day-to-day trend in the hourly values of the magnetic elements at Hermanus during the control period December 23-26, 1954. A cooperative program is suggested.

Dr. J. Egedal has proposed that "future investigations of the effect on geomagnetism and earth currents during solar eclipses should be carried out by international cooperation and conducted by the International Association of Geomagnetism and Aerometry (IAGA) through its Committee No. 10" (Committee on Rapid Magnetic Variations and Earth Currents, Circular No. 1/55).

I would suggest that the proposal be extended to include a review of past work in this field. An authoritative report on the earlier investigations, giving (*a*) the circumstances of each eclipse, (*b*) copies of the relevant magnetic records, and (*c*) a careful assessment of the results in the light of Chapman's theory [see 1 of "References" at end of paper], would greatly facilitate the work of future investigators.

I gather from Dr. Egedal that an investigation carried out by himself and Dr. N. Ambolt in respect to the eclipse of June 30, 1954, revealed geomagnetic effects at ten observatories. This news has encouraged me to publish the rather doubtful effect recorded at Hermanus (34°26′ south, 19°14′ east) during the partial (annular) eclipse of December 25, 1954. Figure 1 is a copy of the Hermanus

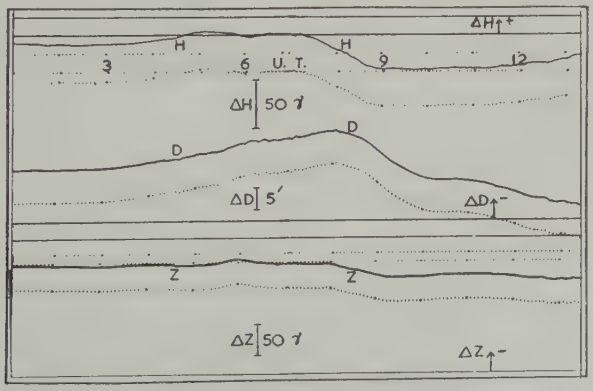

FIG. 1—Hermanus magnetogram, December 25, 1954

magnetogram for that day. Figure 2 shows the same curves against the background of minor magnetic activity prevailing at the time. The broken curves represent the mean diurnal variations for the three days December 23, 24, and 26.

A study of the day-to-day trend in the hourly values of the magnetic elements over an extended period centered round the day of the eclipse [2], and of the daily

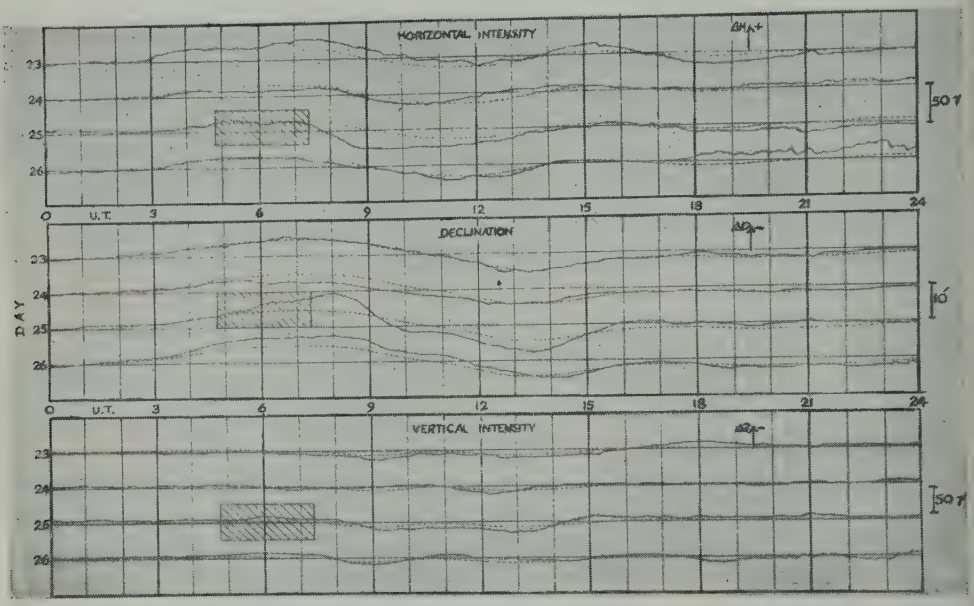

FIG. 2—Diurnal variation of the magnetic elements at Hermanus, December 23-26, 1954

vector diagrams for the period December 23-26, tells us little more than what is already evident from the accompanying diagrams, namely, that conditions were by no means normal on the day of the eclipse. While the decrease in horizontal intensity during the period of the eclipse conforms in type to the effect predicted by Chapman, the corresponding numerical increase in vertical intensity is not so easily accounted for.

At Cape Town (90 km to the northwest of Hermanus), the eclipse began at 04^h48^m UT and ended at 07^h23^m UT, the magnitude at greatest phase (06^h00^m UT) being 0.88.

References

[1] S. Chapman, Terr. Mag., **38**, 175-183 (1933).
[2] L. I. Gama, Terr. Mag., **53**, 405-428 (1948).

JOURNAL OF GEOPHYSICAL RESEARCH VOLUME 60 NO. 3 SEPTEMBER, 1955

DAYTIME ENHANCEMENT OF SIZE OF SUDDEN COMMENCEMENTS AND INITIAL PHASE OF MAGNETIC STORMS AT HUANCAYO

BY S. E. FORBUSH AND E. H. VESTINE

Department of Terrestrial Magnetism, Carnegie Institution of Washington, Washington 15, D.C.

(Received May 19, 1955)

ABSTRACT

Applying statistical tests to 428 SC's, the frequency of occurrence is found to be independent of time of day. Statistical tests indicate that the average sizes of SC's and of IP are both significantly greater during the daylight hours at Huancayo. Also from 102 SC's occurring between 08^h and 14^h 75° WMT at Huancayo, we find that the average size of SC's is greater for those days with the larger diurnal variation (S_q) in H. This result is not only statistically significant but also the average size of SC's was about 50 per cent greater for the group of days with 50 per cent greater diurnal variation in H. The diurnal variation of SC's averaged on 75° WMT for San Juan and Honolulu is practically negligible. The augmentation of SC sizes at Huancayo with S_q in H at Huancayo was found to be the same whether the average size of the same SC's at San Juan and Honolulu was large or small. No significant diurnal variation was found in the frequency of occurrence of SC's observed both at Huancayo and Watheroo. A simple explanation is offered for the diurnal variation in the frequency of SC's found by Newton from Greenwich results.

The relation of daytime enhancement of the size of SC's to S_q in H at Huancayo indicates that the current system responsible is closely associated with the electrojet effect responsible for the large diurnal variation in H at Huancayo. The effects found are not predicted on the basis of the Chapman-Ferraro theory of magnetic storms in its present form. One possibility being examined is that the electric currents in the atmosphere near Huancayo are driven by electrojets of polar regions.

I. *Introduction*—Ever since Birkeland [see 1 of "References" at end of paper] first showed that the geomagnetic disturbance in auroral regions was best explained mainly by concentrated electric currents flowing linearly along the auroral zone, it has been clear that important sources of the field of magnetic storms were located within the atmosphere. He showed that magnetic disturbance near the auroral zone changed very rapidly with distance from the auroral zone, and found that the

local field pattern on the ground was such that it closely resembled that due to an infinite linear current flowing at a height of about 100 km to perhaps 300 km above the ground. More refined estimates made since have shown that the current flow in high latitudes is probably closer to 100 km than to 300 km.

It is the purpose here to bring forward and discuss more critically new evidence for locating another concentration of current definitely within the atmosphere, and along the geomagnetic equator, where the current usually persists for an hour or so at the beginning of a magnetic storm. The effect of these currents is that of the local daytime enhancement of the sudden commencement (SC) and the initial phase (IP) of storms, seen most clearly in the horizontal magnetic component. This effect is shown to depend also upon the amplitude of the solar daily variation (S_q) on the day on which the SC or IP occurs. This suggests that substantial currents associated with the SC or IP flow in or near the E-region. The close association of the enhancements in IP and S_q may then be simply explained by supposing each to depend upon the locally enhanced conductivity in the E-region near the magnetic equator [2]. This result is of considerable interest, since it has long been known that SC's are larger in auroral regions than elsewhere. For instance, Chree [3] found those in the Antarctic to average about 4.5 times the values at Greenwich. Accordingly, in recent years it has been remarked that SC's must in part be due to atmospheric sources, because from potential theory it follows that local field patterns cannot readily arise from sources at a distance greater than the linear cross-section of the pattern [4,5,6]. In fact, it is quite clear that atmospheric sources of SC's and IP's are often dominant in the polar regions, and Nagata [4] has shown that the preliminary reverse impulse (SC*) of SC's also must be due to atmospheric sources. It thus appears likely that the sources of SC's and IP's are dominantly atmospheric, and consist of electric currents flowing in the ionosphere. These currents may be driven by emf's mainly originating in polar regions, as suggested for magnetic bays [7], and the so-called disturbance daily variation (D_S) [8].

The remarkable dependence of SC's and IP's upon the observed amplitude of S_q (as estimated here from the mean of the hour previous to an SC) makes possible the tentative removal of the very large part of SC's associated linearly with S_q amplitude at Huancayo. When this is done, the part remaining, whether due to currents flowing in solar streams or otherwise, is at least difficult to understand in terms of electric currents flowing beyond the atmosphere. It is found that the remainder of SC's (or IP's) at Huancayo is about twice the average for Honolulu and San Juan, which require no important addition of field values since the diurnal variation in SC's averaged on 75° WMT for San Juan and Honolulu is quite small. Hence, even this part is not readily assigned to current sources beyond the atmosphere, but is at least in fair accord with expectations based on atmospheric conductivity, assuming that all major currents actually flow within the atmosphere.

II. *Relation for Huancayo between diurnal variation (DV) in SC sizes*—In order to examine magnetic conditions near the magnetic equator during SC's and IP's, data for the years 1922-1946 were derived for Huancayo, Peru, with geographic

position (ϕ = 12°.0 south, λ = 284°.7 east), nearly directly on the magnetic equator, and the station Watheroo, Australia (ϕ = 30°.3 south, λ = 115°.9 east).

Use was also made of data for the stations Honolulu (ϕ = 21°.3 north, λ = 201°.9 east), San Juan (ϕ = 18°.4 north, λ = 293°.9 east), and Cheltenham (ϕ = 38°.7 north, λ= 283°.2 east). The only other established station near the magnetic equator is Kodaikanal (ϕ = 10°.2 north, λ = 77°.5 east) in southern Asia, but results for this station have not been used here, though a similar investigation to that in this paper would be of particular interest.

The total number of SC's and IP's found at Huancayo and Watheroo was 428 after removing what were considered to be crochets, which often arise during solar flares, and have a field pattern resembling that of the quiet-day daily geomagnetic variation. The scalings of SC's at Huancayo and Watheroo were checked satisfactorily against those of Ferraro and Parkinson, whose earlier scalings of SC's at Honolulu, San Juan, and Cheltenham comprised the data of the latter stations. The convenient distinction by Ferraro, Parkinson, and Unthank of SC's into two classes, SC's and sudden impulses (SI's), depending on whether or not the initial sudden field departure was followed by a magnetic storm or otherwise, was not retained. This distinction may be somewhat artificial, since magnetic disturbance does not appear to change much in general type within wide ranges in the level of disturbances. It is also often found that the greater the intensity of a magnetic storm, the more rapidly does it go through its various phases; hence, very weak magnetic storms, barely distinguishable or indistinguishable from other fluctuations in amplitude during quiet days, may, at least at times, have SC's. Ferraro and Unthank [9] and Sugiura [6] called attention to the similarity of the DV in the average size of SC's in H at Huancayo to the DV of S_q in H there. This is illustrated by a new analysis here. The results are shown in Figure 1(A), in which the average S_q in H (solid curve) for those days on which 428 SC's occurred is compared with the median size (crosses) of SC's which occurred in each bihourly interval of the day. Figure 1(B) exhibits the correlation between the median sizes of SC's and the bihourly mean departures ΔH in S_q from the midnight value. The mean ΔH for each bihourly interval, for which the median size of SC was determined, was obtained in the following way. For the hour just preceding the hour of each SC, the departure of the hourly mean in H from the preceding midnight value was recorded as ΔH_t . For each of the 24 values of t, $(1/n) \sum \Delta H_t$ was computed with n the number of all SC's in the hour $(t + 1)$. These averages are the circled points plotted in Figure 1(A). To obtain the averages of ΔH for the hours (and days) on which the SC's occurred, the amplitude of the 12-year average S_q curve [8] for ΔH at Huancayo was multiplied by 1.24 to fit the plotted points in Figure 1(A) for ΔH_t . From this curve, bihourly means of ΔH were obtained, for the same bihourly intervals for each of which the median size SC was determined. These bihourly means of ΔH are plotted in Figure 1(B) against the median size of SC which occurred in the corresponding bihourly intervals. The excellent fit of the curve to the points in Figure 1(A) indicates that the average ΔH is not noticeably affected by the lunar variation in H. If values of ΔH had been determined during or following the hour of the SC, these would certainly have been affected (and systematically) by the initial or main phase of the storms.

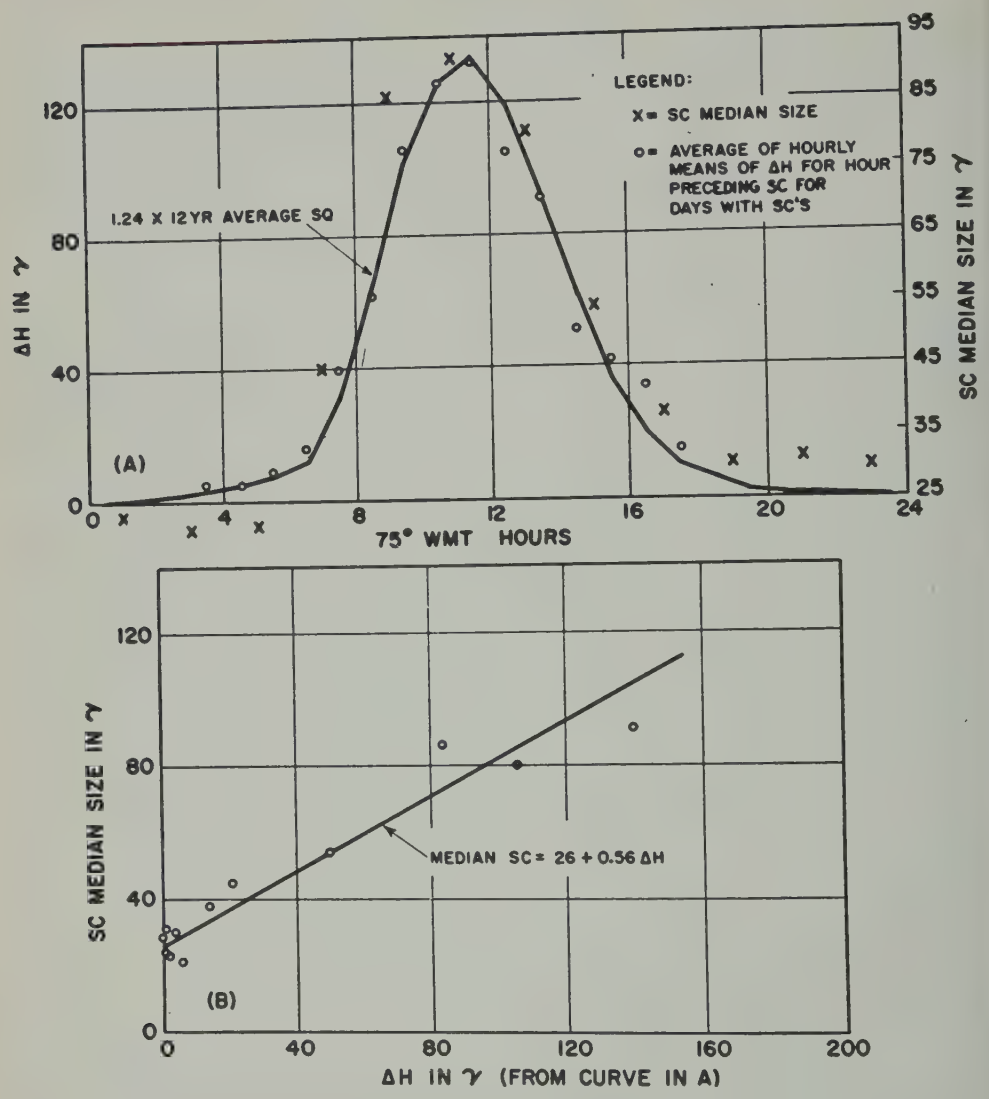

FIG. 1—(*A*) Comparison of diurnal variation in 428 SC's and S_q in H at Huancayo; (*B*) correlation between bihourly median sizes of SC's and mean bihourly departures ΔH in S_q from midnight value

III. *Normal distribution of log size of SC, and its utility for statistical tests*—In Figure 2 are plotted cumulative frequency distributions of SC sizes (*A*) for day and (*B*) for night at Huancayo. Since these cumulative distributions are well approximated by straight lines when plotted on logarithmic normal probability paper, it means the logarithm of the median size is the ordinate for 50 per cent on the abscissae scale. This size corresponds to the median of the frequency distribution of sizes (not their logs). The slope of the line determines the sample standard deviation of the logs of the sizes. Besides providing a simple representation of the

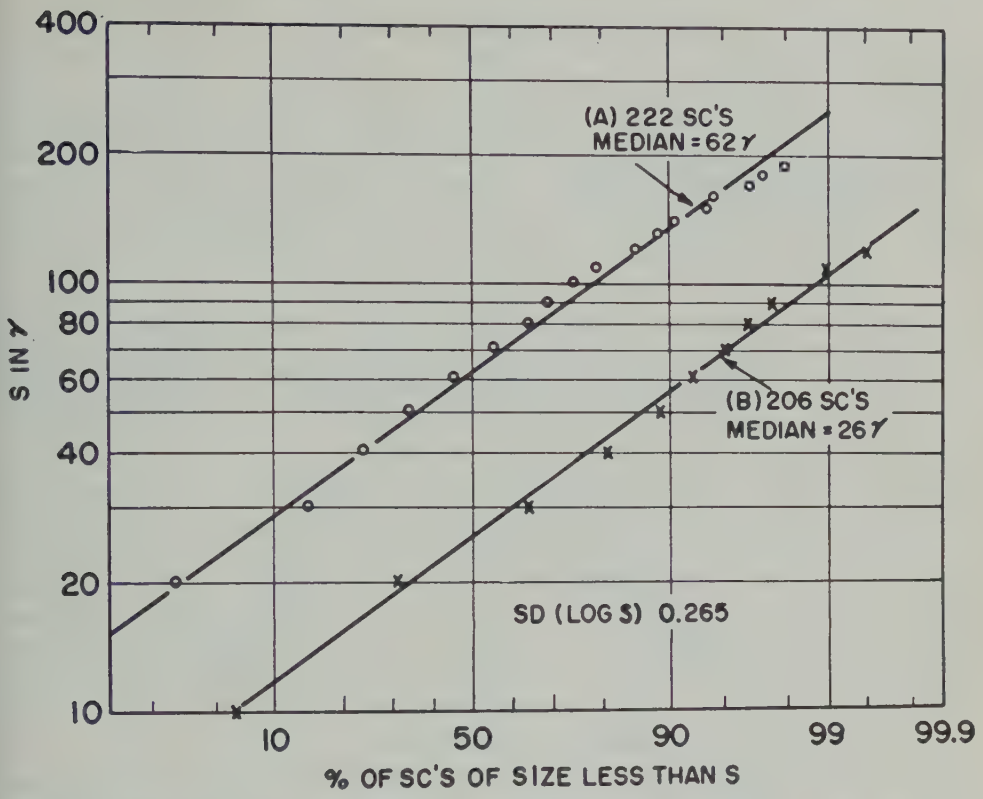

FIG. 2—Cumulative frequency distribution of SC sizes (S) at Huancayo: (A) for day (hours 0600-1800 75° WMT), (B) for night (hours 1800-0600 75° WMT)

frequency distributions, the fact that the distribution of log size is essentially normal makes it convenient for statistical tests of hypotheses concerning the data.

This convenience is illustrated by (A) and (B) of Figure 2. The sample standard deviations (SD) of log size are both approximately 0.265; the two sample means of log size are log 61.5 and log 25.5, and the difference in the two means of the logs is log (61.5/25.5) = 0.384. The SD for the difference between the two means is approximately $0.265\ \sqrt{2}/\sqrt{200} = 0.0265$. Thus, the difference between the two means is about 14.5 times its SD and the difference is thus definitely significant. Hence, there is little doubt that the median sizes of SC's during the daytime at Huancayo are greater than for night.

There was scarcely need to test this point, but the method illustrates how the median size of SC for bihourly intervals was determined. Incidentally[10], if $m\{S\}$ is the mean of the sizes, and $\log \xi$ = mean $\log S$, then

$$\log m\{S\} = \log \xi + 1.1513\ \sigma^2 \quad \ldots\ldots (1)$$

$$m\{S\} = \xi \cdot k \quad \ldots\ldots (2)$$

in which $\log k = 1.1513\ \sigma^2$ and σ^2 is the variance of $\log S$. For example, from Figure 2 the sample estimate of $\sigma = 0.265$, so that $1.1513\ \sigma^2 \doteq 0.0809$ and $m\{S\} \doteq$

1.20 ξ; thus, for $\sigma \doteq 0.265$, the means are about 20 per cent greater than the medians. Consequently, the DV in mean SC at Huancayo is about 20 per cent greater than that shown in Figure 1(*A*).

Similarly, from Figure 6, the sample estimates $\sigma = 0.301$ for Watheroo; hence, the means at Watheroo are about 1.27 times the medians. For Honolulu and San Juan, the sample estimates of σ are, respectively, 0.248 and 0.261, and the factors by which the medians are multiplied to give the means are, respectively, 1.18 and 1.20.

IV. *Dichotomy of DV in size of SC, according to DV in H for Huancayo*—If the large DV in SC sizes is actually due to or connected with the DV in H, then the DV in the SC should be greater on days with large DV in H than on days with small DV in H. To test this point, the n values of ΔH_t corresponding to the n values of SC which occurred (on different days) in the hour $(t + 1)$ were dichotomized. This was done in groups I and II, respectively, according to whether ΔH_t was greater than or less than the median of the n values of ΔH_t . Averages of ΔH_t were formed for each hour and for each group. These averages for group I and II are plotted, as circles and crosses, respectively, in Figure 3(*A*). The points are well fitted by the 12-year average curve for ΔH when its amplitude is multiplied by the indicated factor. Figure 3(*A*) indicates that the average amplitude of the DV in ΔH for days in group I is about 60 per cent greater than for days in group II. From each of these two curves in Figure 3(*A*), means of ΔH were obtained for each two-hour interval of the day. For the same bihourly intervals, the median size SC was obtained for each of the two groups.

In Figure 3(*B*), these median sizes of SC are plotted as ordinate; the abscissae are the means of ΔH for the corresponding bihourly interval. The line in Figure 3(*B*) is the same as that in Figure 1(*B*), and it is is seen to fit both sets of points in Figure 3(*B*). Moreover, the three uppermost points in (*B*) of Figure 2 are from group I, for which the DV in ΔH was greater than for group II. This result indicates that the median size of SC is greater on days (group I) with the larger DV in H, and that the median size SC increases linearly with ΔH.

The basis for a statistical test of whether the median size SC is significantly greater on days in group I (with the larger DV in ΔH) is indicated in Figure 4 by the frequency distributions of SC sizes. Here the difference in the logs of the two medians is log (81/60) = 0.130. Its SD is $\sqrt{2} \times 0.265 / \sqrt{60} = 0.047$. Thus, the ratio (0.130/0.047) of the difference to its SD is about 2.75, which indicates that in samples of size 60 the median for group (*A*) should exceed that in group (*B*) by as much or more than it does in this sample, with probability about 0.003. Thus, the excess of the median size for the group I over that for group II can be regarded as statistically significant.

V. *Comparison of DV in size of SC's for several observatories*—The median size SC for bihourly intervals for Huancayo and Watheroo (from the same 428 SC's) is shown in Figure 5(*A*). Median sizes of SC's are also shown for each four-hour interval of the day for Cheltenham, San Juan, and Honolulu, for which the numbers of SC's available for the samples were, respectively, 221, 225, and 271. All of these SC's occurred at Huancayo also.

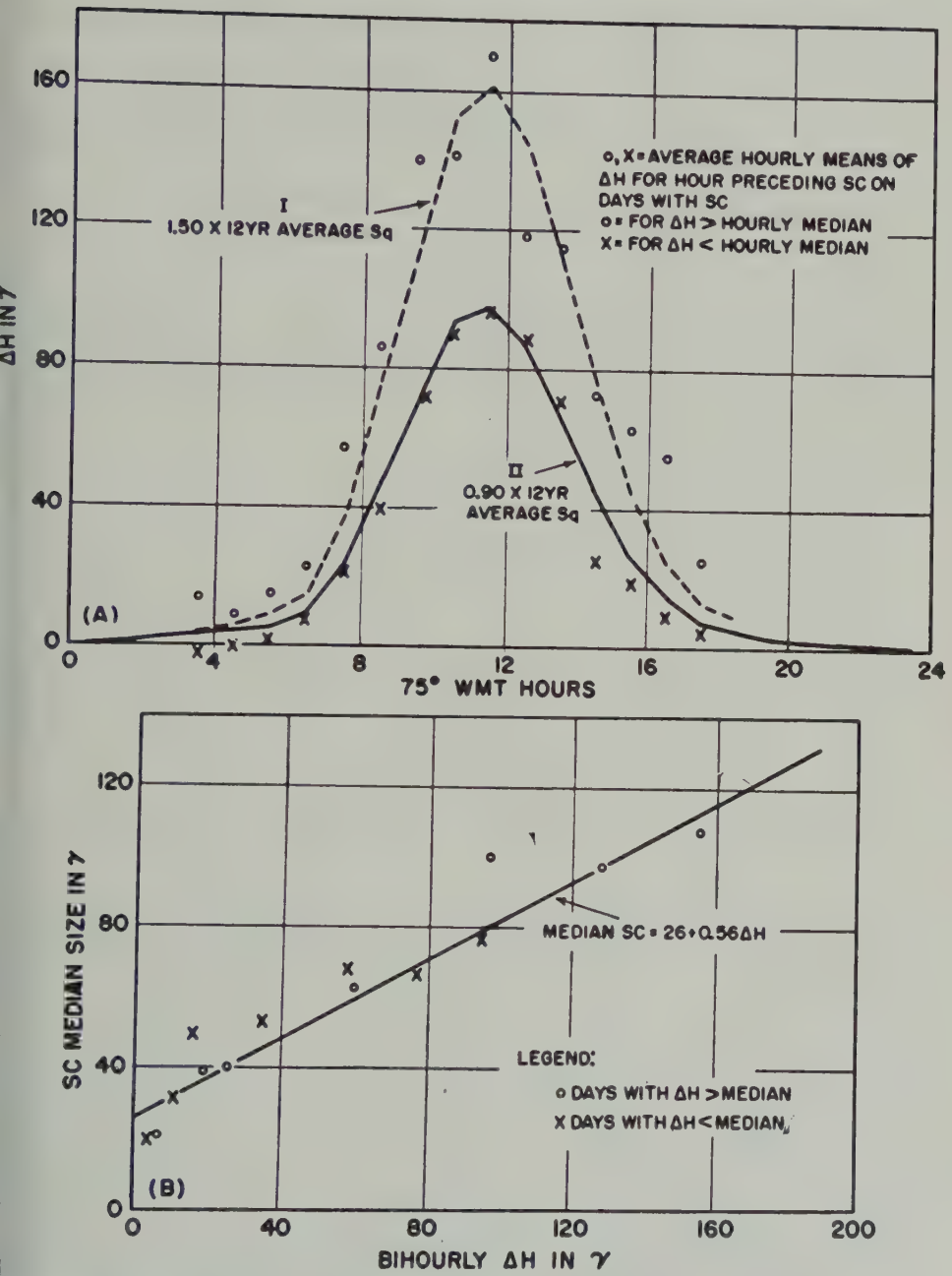

IG. 3—(*A*) Diurnal variation of ΔH in S_q at Huancayo for days of large and small S_q ; (*B*) correlation between ΔH and median size of SC's showing increase in median size of SC on days with larger average diurnal variation S_q in H

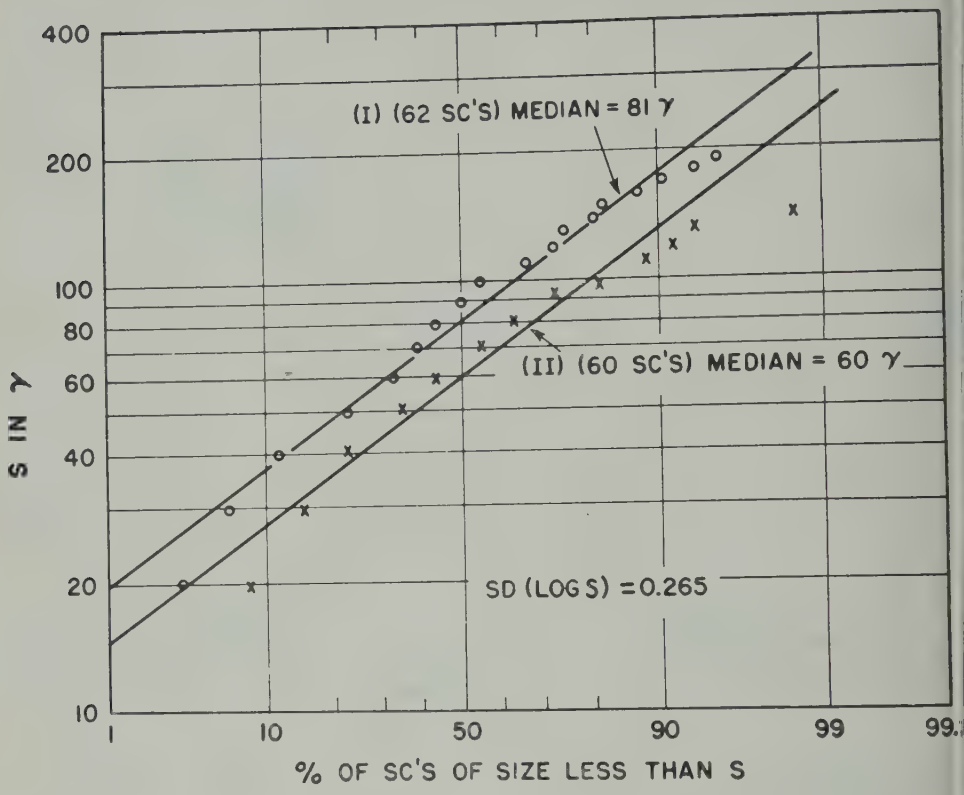

FIG. 4—Cumulative frequency distribution of SC sizes (S) at Huancayo for 75° WMT hour 0800 to 1500: (I) for days with large DV in H, (II) for days with small DV in H

Besides the large DV in median size of SC's at Huancayo (range 20 to 90 γ), considerable DV in median size SC's is also evident for Cheltenham and Watheroo. The small DV in SC's at San Juan and Honolulu is probably not significant. The frequency distributions of SC's at Watheroo for day and night are compared in Figure 6. Testing the hypothesis that the samples (A) and (B) in Figure 6 are from the same population, it is found that differences between two medians, as great or greater than that for these two samples, should occur with probability about 0.002 for samples of the indicated size if these are actually from the same population. Thus, the median size SC at Watheroo is significantly greater during the night than during the day. It may be noted that while the daily average of the median size SC's (for four-hour intervals) is less at Watheroo than at Cheltenham, the ratio of maximum to minimum values is about 2.5 for each. Since the phase of the DV in SC's at Watheroo differs from that for Cheltenham by about 12 hours when both are plotted on 75° WMT, as in Figure 5, the two DV's would have about the same phase on LMT.

It is clear from Figure 5(A) that the DV in the ratio of sizes of SC's at Huancayo to that at Cheltenham, which was used by Sugiura [6], would differ quite considerably from the DV in SC's at Huancayo shown by the top graph in Figure

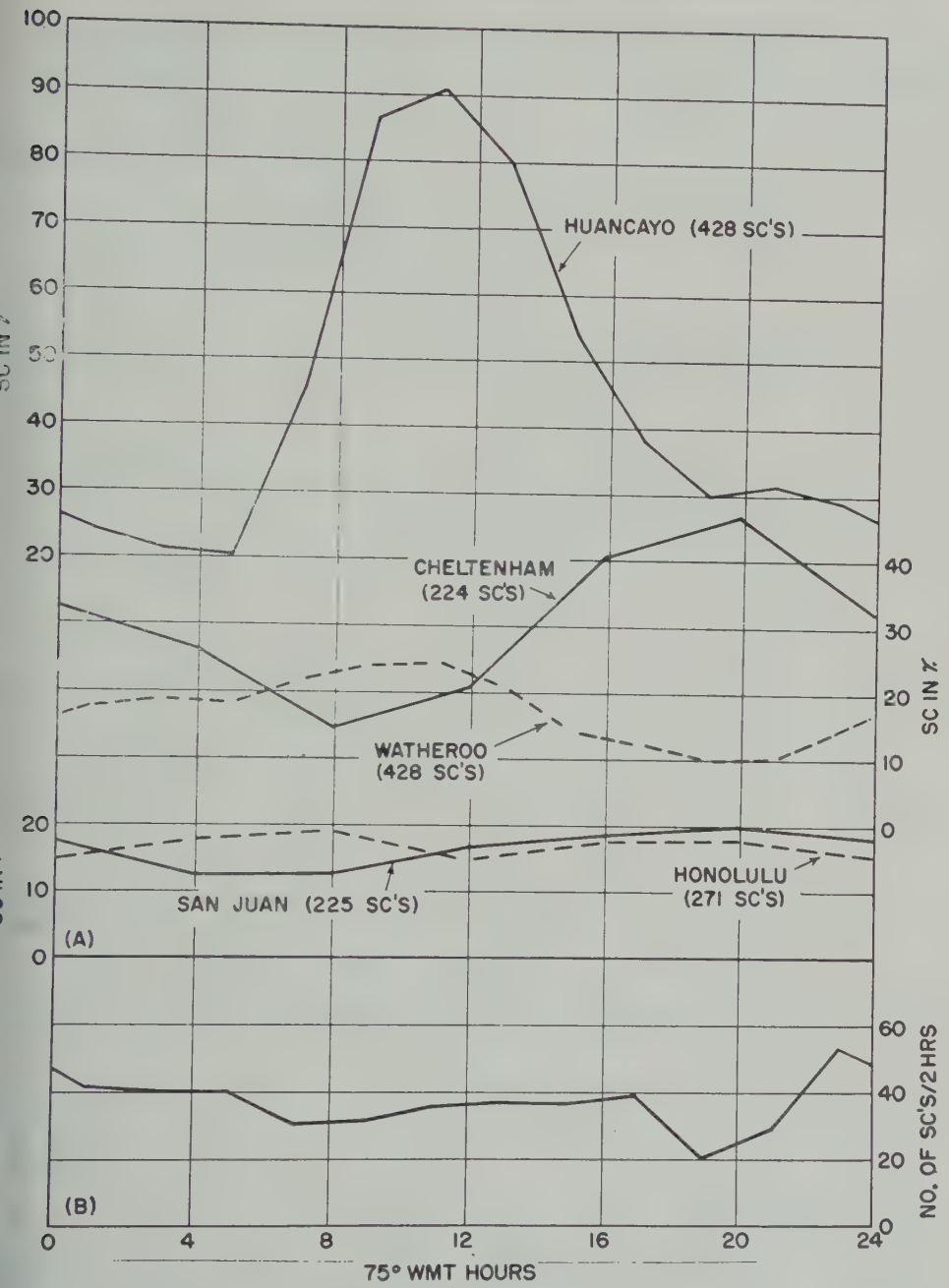

G. 5—(*A*) Diurnal variation in median size of SC's at several stations; (*B*) number of SC's for each two-hour interval of day for 428 SC's occurring both at Huancayo and Watheroo

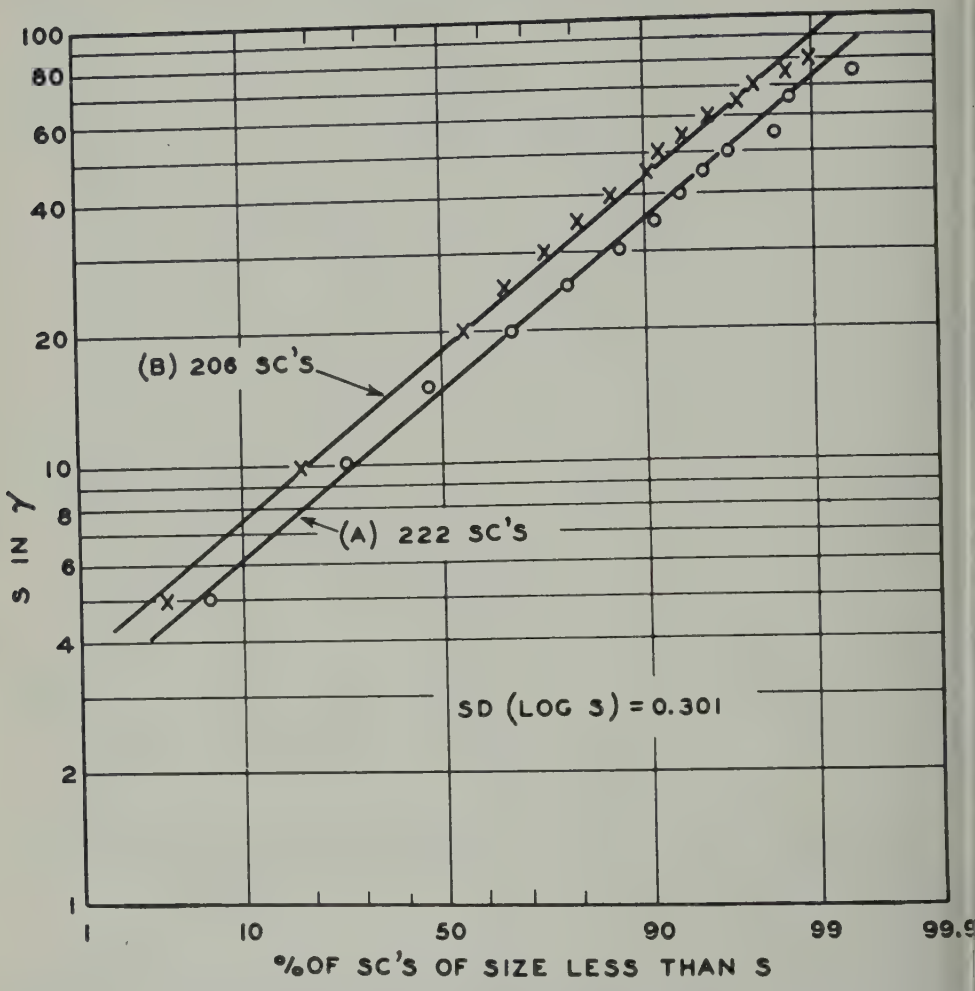

FIG. 6—Cumulative frequency distribution of SC sizes (S) at Watheroo: (A) for day (hours 0700-1900 120° EMT), (B) for night (hours 1900-0700 120° EMT)

The graphs for San Juan and Honolulu in Figure 5(A) indicate that SC sizes averaged for San Juan and Honolulu are nearly constant throughout the 24 hours of the day. This suggests that this average would be useful to normalize the sizes of SC's at other stations.

Since at Cheltenham there were some inverted (negative) SC's in H, the median size SC's were determined directly without the use of cumulated frequency distributions on log normal probability paper. In Figure 7, the DV in the mean size of SC's for four-hour intervals at Cheltenham and that for Newton's results [11] at Greenwich are seen to agree reasonably well.

VI. *Tests for DV in frequency of SC's and comparison with Newton's results*—Figure 5(B) shows for each bihourly interval of the day the number of SC's tha

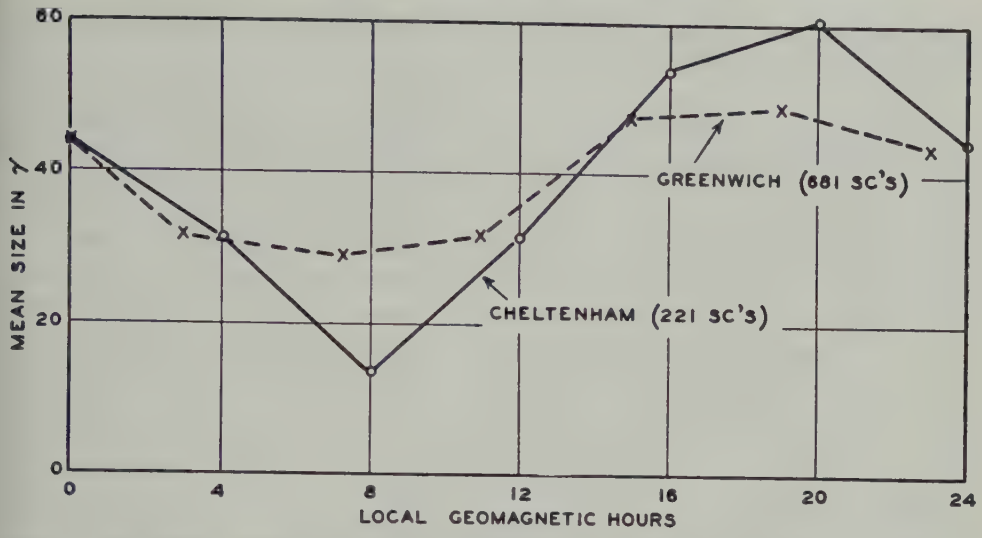

FIG. 7—Comparison of diurnal variation of mean size SC for four-hour intervals for Cheltenham and Greenwich

occurred both at Watheroo and Huancayo. The average number of SC's for each bihourly interval is about 36. A chi square test for homogeneity gives $P = 0.05$, which is scarcely small enough to reject the hypothesis of equal frequency (*viz.*, 36) in each of the 12 two-hour intervals. If the SC's occur randomly throughout the day, then a Poisson distribution is expected, for which the mean and variance are equal. For the sample in Figure 5(*B*), the mean and variance are, respectively, 36 and 66. However, this difference is not statistically significant ($P = 0.05$). The deviations for the hours 18-20 and 22-24 are the largest in the set.

The value in the interval 18-20 hours is undoubtedly somewhat low due to the loss of trace (or incomplete records of the SC's) during the interval when one or the other or both of the records were changed (*viz.*, *circa* 19^h 75° WMT). The largest number of SC's is for the interval 22-24 hours, which deviates by +17 from the mean. Using the normal approximation to the Poisson distribution, it is found (using variance = 36) that deviations greater than 17 in magnitude should occur with probability about 0.004, or once in about 20 sets of data like that in Figure 5(*B*), so that such a deviation is not too improbable in the sample under consideration.

Thus, there appears no evidence for any significant DV in the frequency of occurrence of SC's in the sample of 428 SC's which occurred simultaneously at Watheroo and Huancayo. This is quite different from the results found by Newton [11] from 681 SC's on the Greenwich records. Statistical tests for homogeneity based on the data in his Figure 3 definitely show that the DV indicated is real. Newton also indicated [11] that the SC's which occur near 08^h to 09^h GMT at Greenwich are often inverted (that is, negative in *H*). Effects from current systems which result in "inverting" the SC's during certain hours at one station and not at others, can doubtless also often "wipe out" SC's during those hours, with a resulting apparent decrease in frequency of occurrence during those hours. This

would seem to explain why Newton's data indicate a DV in the frequency of SC's while the result in Figure 5(*B*) does not.

VII. *Dependence of the DV in SC sizes at Huancayo upon the size of SC's at San Juan and Honolulu*—Since the DV in median size SC's at Huancayo is greater on days with larger DV in H, it is of interest to determine whether this augmentation depends on the size of the SC's. For this purpose, data were available only 161 simultaneous SC's at Huancayo, San Juan, and Honolulu. The size for each of the 161 SC's was averaged for San Juan and Honolulu. Let $A_{i,j}$ indicate this average for the jth among the n_i SC's occurring in the ith four-hour interval ($i = 1, 2, \cdots 6; j = 1, 2, \cdots n_i$) and let M_{i,n_i} represent the median of $A_{i,j}$. All $A_{i,j} > M_{i,n_i}$ were put in group I and the $A_{i,j} < M_{i,n_i}$ were put in group II. For each four-hour interval, the mean size SC at Huancayo was determined, and also $(1/n_i) \sum_{j=1}^{n_i} A_{i,j}$. The results are given in (*a*) and (*b*) of Table 1, together with ΔH_i from Figure 1(*A*) averaged for the indicated intervals, i. The results are plotted in Figure 8. The same values of ΔH_i were used in plotting the average size of SC's in groups I and II. It was assumed that the DV in ΔH for groups I and

TABLE 1—*Mean sizes of SC's in H at Huancayo for different intervals of the day, and for groups I and II dichotomized according to whether the size of SC averaged for San Juan and Honolulu was greater or less than the median of these averages for the interval*

75° WMT interval, i	No. of SC's in I	Mean SC in group I		No. of SC's in II	Mean SC in group II		ΔH_i at Huancayo*
		Huancayo	San Juan Honolulu		Huancayo	San Juan Honolulu	
hours		γ	γ		γ	γ	γ
(*a*)							
0000–0400	13	64	40	14	22	14	1
0400–0800	14	35	23	14	34	11	2
0800–1200	7	130	27	7	106	14	107
1200–1600	17	111	31	16	70	13	78
1600–2000	12	82	35	13	31	15	10
2000–2400	17	50	29	17	28	14	0
Mean	..	..	31	..	..	14	..
(*b*)							
0000–0400, 2000–2400	30	57	34	31	25	14	0
0040–0800, 1600–2000	26	58	29	27	32	14	6
0800–1200	7	130	27	7	106	14	107
1200–1600	17	111	35	16	70	13	78
Total	80	..	..	81	..	..	..

*Average for indicated interval from Figure 1(*A*).

II was that shown in Figure 1(*A*). Since this assumption may not be justified and since the number of cases in some intervals is small, the true slopes for groups I and II may differ considerably from those shown in Figure 8. If the augmentation of SC's at Huancayo depends on the electromotive driving force, a smaller slope would be expected for group II than for group I. A statistical test of this expectation is under way utilizing more extensive data.

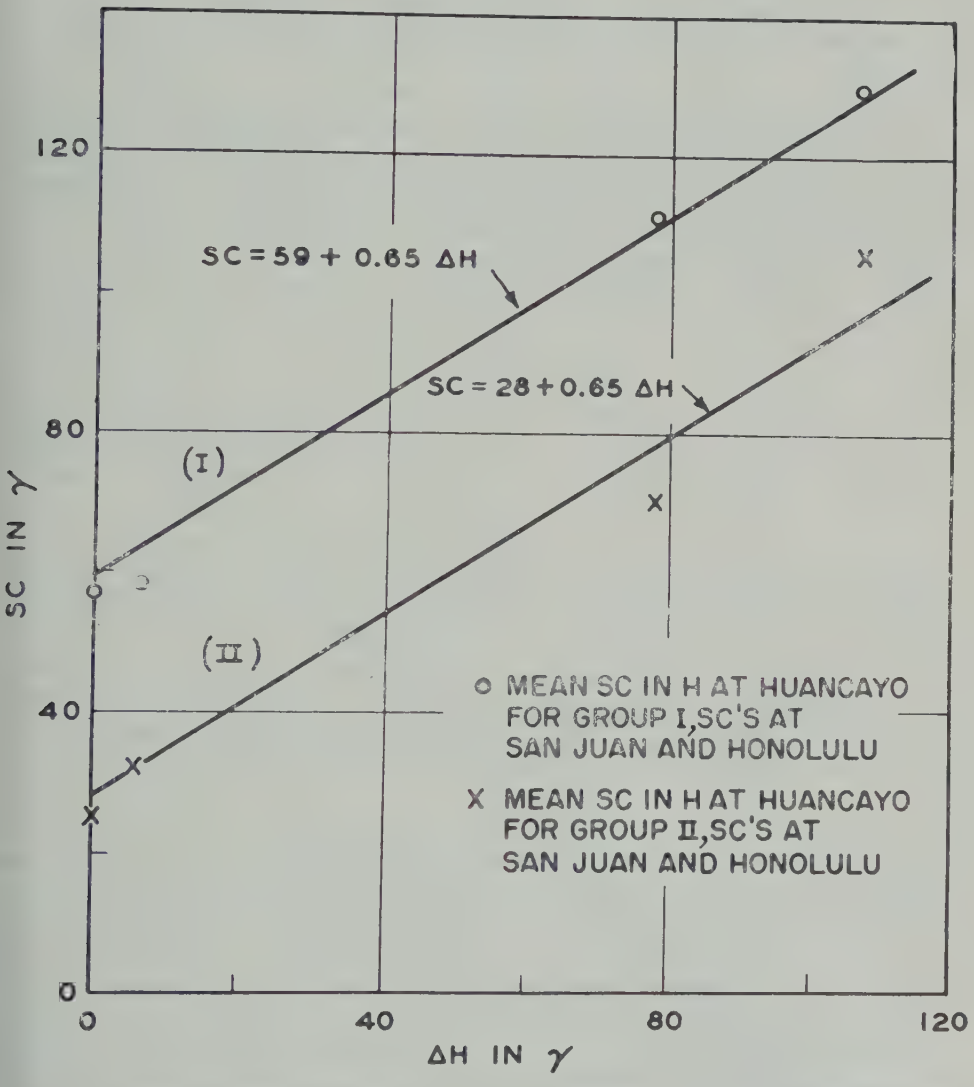

FIG. 8—Correlation between mean size SC in H with departure ΔH in S_q from midnight value: (I) and (II), respectively, for large and small SC averages for San Juan and Honolulu

Figure 8 shows that the mean size, $\overline{SC_i}$, of SC's for a particular interval, i, of the day has the average approximation

$$\overline{SC_i} = A + 0.65\Delta H_i \quad \ldots\ldots\ldots\ldots\ldots\ldots\ldots\ldots\ldots\ldots (3)$$

in which ΔH_i is the departure of H, averaged for the same interval i, from midnight value. Only the value of A is greater for the group of SC's with the larger average for San Juan and Honolulu. The ratios of A to the mean size SC's at San Juan and Honolulu (Table 1) are, respectively, $59/31 = 1.9$ and $28/14 = 2.0$ for groups I and II. It may be noted that the slope of the lines in Figure 8 is somewhat greater than for those in Figures 1(B) and 2(B). However, the former applies to means and the latter to median size SC's. Since (at Huancayo) it was shown that the mean SC = median SC $\times$ 1.205, then a slope = $0.56 \times 1.20 \doteq 0.67$ would be expected for Figure 8.

It was not surprising to find the value of A greater for group I than for group II, but it is surprising to find the value of A about twice the size of SC's averaged for San Juan and Honolulu for the same groups. This suggests a rapid change with latitude of what might be called the world-wide (analogous to D_{st}) component of SC's. Such a rapid latitude variation suggests that the current system for the world-wide component of SC's also flows in the atmosphere.

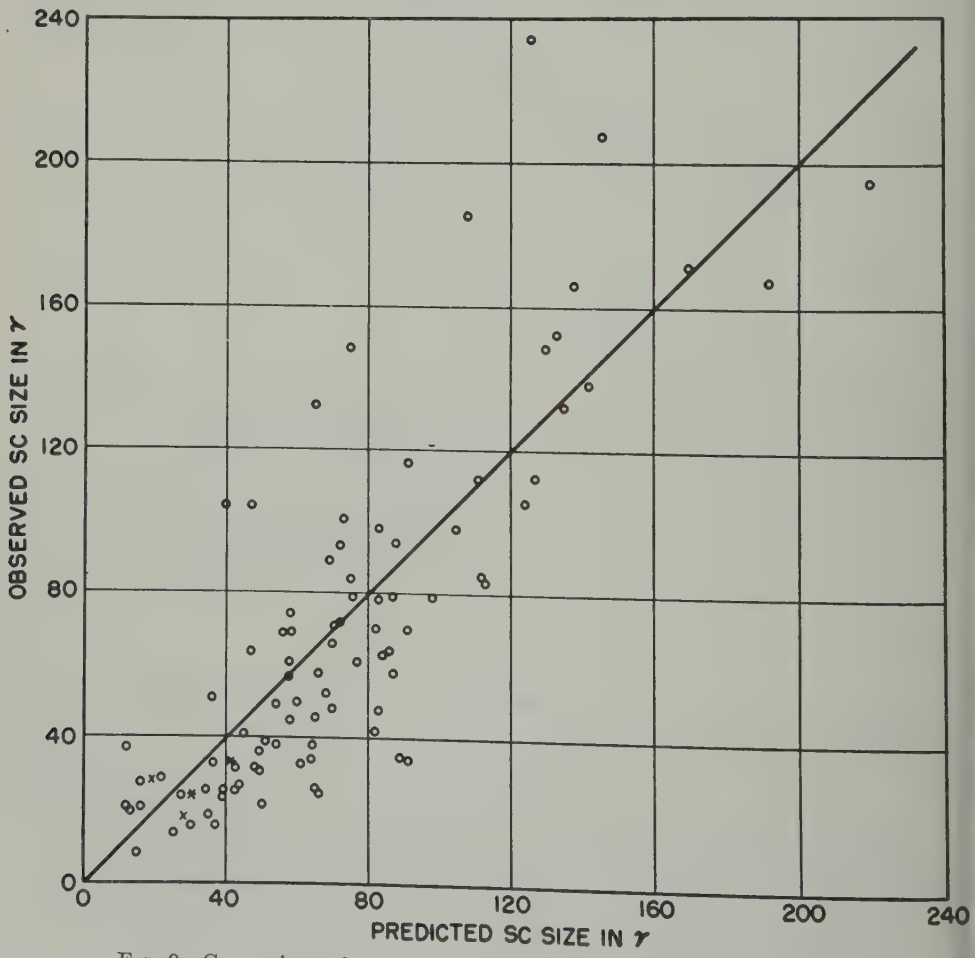

FIG. 9—Comparison of observed SC size at Huancayo with size predicted

In Figure 9, the observed size of 161 individual SC's at Huancayo is compared with the size predicted from the equation: SC (predicted) = 2 × size averaged for San Juan and Honolulu + 0.65 ΔH, in which ΔH is the estimated DV departure in H (from midnight) at the time of the SC. In view of the uncertainties in estimating ΔH (no correction for lunar variation, etc.), the correspondence is reasonably good.

VIII. *DV in magnitude of IP at Huancayo and its dependence on amplitude of the DV in H of* S_q—For each of the 428 SC's which occurred both at Huancayo and Watheroo, the IP averaged for one-half hour [IP_0 (1/2)] and for one hour [$IP_0(1)$] was measured, for Huancayo. $IP_0(1/2)$ is thus simply the difference between the mean value of H measured for the half-hour immediately following the SC and the value of H for the instant preceding the SC. $IP_0(1)$ is the measured mean of H for the whole hour immediately following the SC, less the value of H for the instant preceding the SC. These measured values, $IP_0(1/2)$ and $IP_0(1)$, are each somewhat affected (especially those between the hours 07-11 and 12-16, 75° WMT) by the change in H due to the large DV in H at Huancayo. The values of IP(1/2) and IP(1) are the measured values $IP_0(1/2)$ and $IP_0(1)$ corrected for the change in the mean of H, due to the DV in H, which occurs, respectively, during the half-hour and one-hour intervals following the SC. The individual IP's were dichotomized according to whether the DV in H was large or small, in the same manner as described for SC's in section IV. Since the same days apply for the IP's as for the SC's, the DV in ΔH shown by curves I and II in Figure 3(A) were used as a basis for the corrections in the IP's.

The curve in Figure 10(A) shows the DV in the size of IP(1/2) for all days. The encircled points are the bihourly averages of IP(1/2) for days in group I (larger DV in H) and the crosses the bihourly averages of IP(1) for days in group II (small DV in H). The curve in Figure 9(A) is, except for amplitude, quite like that for SC's for Huancayo in Figure 5(A). Furthermore, the values of IP(1/2), for the hours 08-14 75° WMT, are larger for the group with larger DV in H. This implies that the magnitude of the IP at Huancayo is augmented in the same way as is the size of SC's.

Figure 11 shows the cumulative frequency distribution of the sizes of IP(1/2) for days with large (group I) and small (group II) DV in H. The difference between the mean log IP(1/2) for the two groups is about 3.8 times the SD [log IP(1/2)], which leaves little doubt that the effect is real. This test, it should be observed, does not depend very critically upon whether the distribution of log IP(1/2) is exactly normal. This follows from the central limit theorem of statistics, which states that the distribution of means of samples from non-normal distributions approaches normality. For samples of 30 (as in Fig. 11) the approximation is quite close.

In Figure 10(B), the average size of IP(1/2) is seen to be about 0.87 times the median size SC's for the same bihourly intervals, or since the mean size of SC's at Huancayo is 20 per cent greater than the median, then the mean IP(1/2) is about 0.72 times the mean size of the SC's.

In Figure 10(C), the means of IP(1/2) are plotted against the means of IP(1)

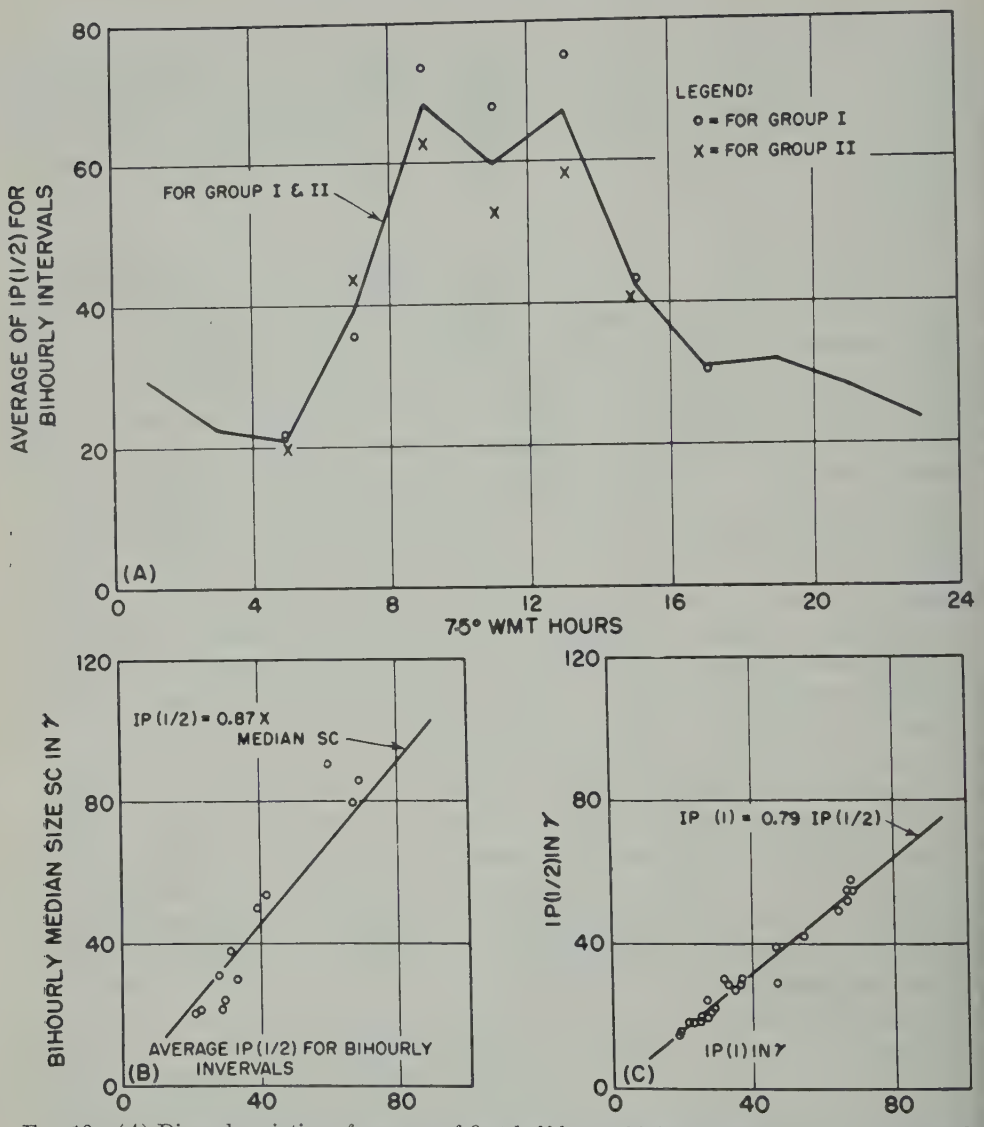

FIG. 10—(*A*) Diurnal variation of average of first half-hour of initial phase, IP(1/2), for bihourly intervals at Huancayo; (*B*) correlation between bihourly median size of SC's and average IP(1/2) for corresponding bihourly intervals; (*C*) correlation between average IP(1/2) and IP(1) for corresponding bihourly intervals

for corresponding bihourly intervals. The line indicates IP(1) = 0.79 IP(1/2), from which it follows that the IP for the interval 0.5 hour to 1.0 hour after the SC is, on the average, about 58 per cent as large as IP(1/2).

IX. *Discussion of results*—The results of the present paper clearly indicate the presence of a major and immediate atmospheric source of field in SC's and IP's. Although this conclusion accords with earlier tentative findings [4,6], the present results benefit by carefully made statistical tests. A new result found was the

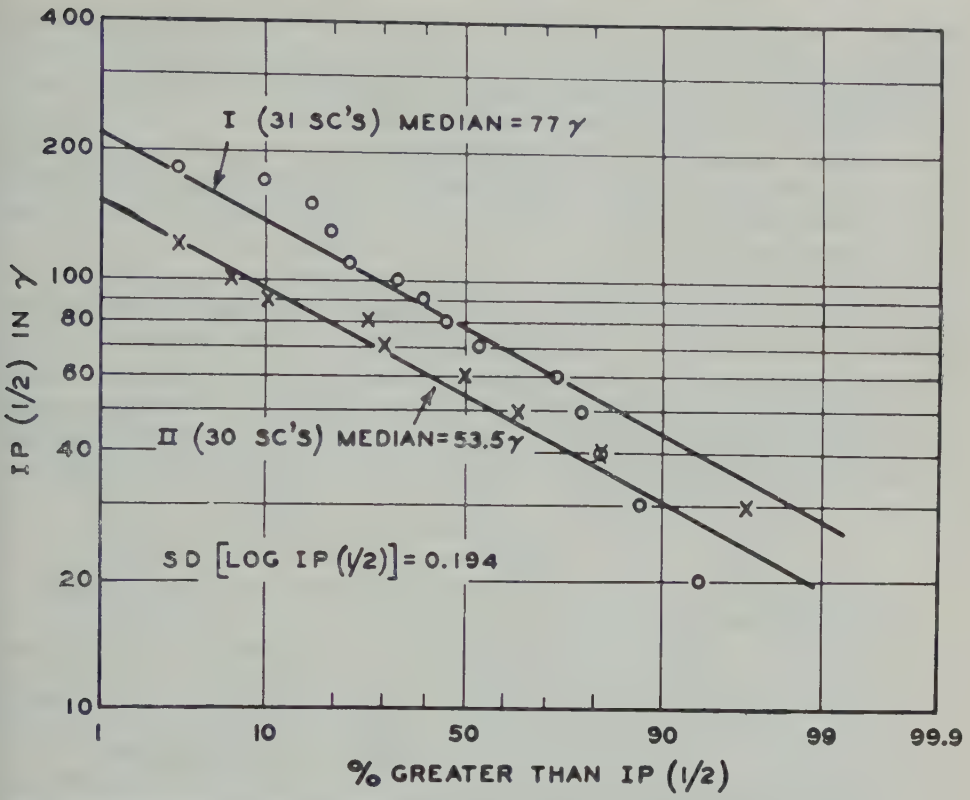

FIG. 11—Cumulative frequency distribution of size of initial phase (half-hour mean) IP(1/2), at Huancayo, hours 1000 to 1300 75° WMT: (I) for days with large diurnal variation in H, (II) for days with smaller diurnal variation in H

surprisingly good correlation between daytime SC and IP amplitude at Huancayo and the amplitude of S_q . This suggests that major currents responsible for SC and IP flow in or near the E-region above Huancayo. However, since the electromotive driving forces for S_q and SC and IP can presumably vary independently of one another, the linear relationship of Figure 9 is not explained in terms of electric conductivity alone. It may be that the charge accumulations which insure continuity of current flow are mutually dependent in some way, as might happen if the electromotive driving forces in middle and higher latitudes show some mutual resemblance in general type. For instance, electric fields originating in high latitudes, as in D_S , may provide the principal electromotive driving forces near Huancayo in the case of SC and IP. The simultaneous ionospheric motions at Huancayo due to possible polar electric doublets at times of SC and IP are in the course of examination and will be reported upon separately.

An interesting experimental program arises naturally from the present work. It was noted that the abnormal augmentation of SC, IP, and S_q at Huancayo is associated with a narrow belt of high electrical conductivity near the magnetic equator. In this event, a concentrated current should flow overhead at Huancayo, the height of which may be estimated using a north-south grouping of magnetic

stations centered at Huancayo, measuring horizontal and vertical components (and space-gradients) of SC, IP, or S_q . In this way, the local currents may be estimated for SC and IP. If large enough, there would be no need to assign major sources of field to regions of space beyond the atmosphere.

For similar reasons, the current systems derived by Vestine [8] for the mean hourly field changes during the IP of magnetic storms should be revised, using instantaneous values, in the hope that this will reveal something of the electrojet at the magnetic equator by day.

It is also clear that it is established beyond reasonable doubt that IP tends to be enhanced by day at Huancayo, as suggested in a recent letter by Vestine [6], so that objections previously raised by Ferraro [12] seem now removed. It would also appear that extensions of existing rudimentary theories of magnetic storms must in future seek to explain the disturbance at ground level in terms of major sources located within the atmosphere, additional to those for D_S . These sources seem to be stronger in polar regions, whence they must ultimately arise from solar influences.

References

[1] Kr. Birkeland, Norwegian Aurora Polaris Expedition, 1902-1903, Christiania, **1**, Pt. 1, 39-315 (1908), and Pt. 2, 319-551 (1913).

[2] M. Hirono, J. Geomag. Geoelectr., **4**, 7-21 (1952); W. G. Baker and D. F. Martyn, Phil. Trans. R. Soc., **246**, 282-320 (1953).

[3] C. Chree, Studies in terrestrial magnetism, Macmillan and Co., Ltd., London (1912).

[4] T. Nagata and N. Fukushima, Indian J. Met. Geophys., **5**, Spl. Geomag. No. 75-88 (1954).

[5] T. Nagata, Nature, **169**, 446 (1952); Rep. Ionosphere Res. Japan, **6**, 13 (1952).

[6] M. Sugiura, J. Geophys. Res., **58**, 558 (1953); E. H. Vestine, *ibid.*, 539, 560 (1953); T. Yumura, Mem., Kakioka Magnetic Observatory, **7**, 27-47 (1954).

[7] N. Fukushima, Polar magnetic storms and geomagnetic bays, J. Fac. Sci., Tokyo Univ., 8, 293-412 (1953).

[8] E. H. Vestine, Terr. Mag., **43**, 261 (1938); E. H. Vestine, L. Laporte, I. Lange, and W. E. Scott, The geomagnetic field, its description and analysis, Carnegie Institution of Washington, Pub. No. 580 (1947).

[9] V. C. A. Ferraro and H. W. Unthank, Geofisica pura e appl., **20**, 3-6 (1951); V. C. A. Ferraro, W. C. Parkinson, and H. W. Unthank, J. Geophys, Res., **56**, 177-195 (1951).

[10] A. Hald, Statistical theory with engineering applications, John Wiley and Sons, New York (1952).

[11] H. W. Newton, Mon. Not. R. Astr. Soc., Geophys. Sup., **5**, 159-185 (1948).

[12] V. C. A. Ferraro, J. Geophys. Res., **59**, 309-311 (1954).

AURORAL ECHOES OBSERVED NORTH OF THE AURORAL ZONE ON 51.9 MC/SEC

BY R. B. DYCE

Geophysical Institute, College, Alaska, and Department of Electrical Engineering, Cornell University, Ithaca, N.Y.

(Received March 23, 1955)

ABSTRACT

During November 1954, a simple radar system, designed for observation of auroral echoes at 51.9 Mc/sec, was operated at Point Barrow, Alaska. Because this location is north of the accepted maximum of the auroral zone, most of the visible aurora is seen to the south of the observing station. The radar used a continuously-rotating antenna to see with equal sensitivity in all directions, but more than 90 per cent of the echoes were obtained from directions north of east and west. Echoes were obtained only from 500 to 1100 km. These effects are explained by the theory of Moore as enlarged by Booker, Gartlein, and Nichols, requiring near-perpendicularity of radio ray paths to the lines of the earth's magnetic field.

During visible aurora, propagation at 51.7 Mc/sec was investigated over an 800-km path from College to Barrow, across the auroral zone. Bursts of signal due to meteor ionization were readily observed. Propagation associated with aurora was almost non-existent, even with visible aurora at the mid-path. If the theory of auroral echoes of Harang and Landmark were true, auroral propagation should have been readily detected.

Introduction

Radio echoes on frequencies higher than 25 Mc/sec from the aurora borealis have been studied by workers in several countries during recent years [see 1, 2, and 3 of "References" at end of paper]. It has been realized that V.H.F. radio waves are not returned by aurora at high angles of elevation [1,2,3,4]. McNamara [5] has measured elevation angles at the observing radar and found them to be about 15° or less.

This apparent aspect sensitivity of the auroral ionization to radar echoes has been explained in three ways. Harang and Landmark [3] have suggested that the echoes are caused by ground-scatter propagated by a smooth-bottomed sporadic ionosphere layer. Lack of high-angle echoes can thus be explained by inability of the sporadic layer sufficiently to bend the radio waves. Currie, Forsyth, and Vawter [1] believe that the echoes are returned directly by the aurora, but, for high elevation angles, the radio waves must pass through a highly absorbing lower region of the aurora. Moore [6] and Booker, Gartlein, and Nichols [7] have suggested

reflection or scattering by columns of ionization, resembling meteor trails along the lines of the earth's magnetic field. Just as meteor ionization is seen best by a radar when looking perpendicular to the trail, so auroral ionization should give the strongest signal when located so that the radio ray paths are approximately normal to the lines of the earth's magnetic field.

It is possible to differentiate between the first two theories and the meteor-trail analogy, by considering echoes to the south of the observing station. For southerly aurora, the ray paths form an acute angle with the lines of the earth's magnetic field instead of being nearly normal. Under this condition, practically no signal should be detectable according to the meteor-trail analogy, whereas the ground-scatter or absorption arguments do not distinguish between northerly or southerly echoes. Currie, Forsyth, and Vawter have obtained a few echoes in the southeast and therefore reject the role of the earth's field. Opening the question again, a decisive experiment would be to determine the ratio of northern to southern echoes at a latitude sufficiently north of the auroral zone that most visible auroras occur to the south. This paper describes such an experiment performed at Point Barrow, Alaska (71°.3 north, 156°.8 west) at a centered-dipole co-latitude of 21°.6 magnetic.

Secondly, observations were made at Point Barrow of transmissions from College, Alaska, 800 km magnetically southeast (see Fig. 1). By observing the

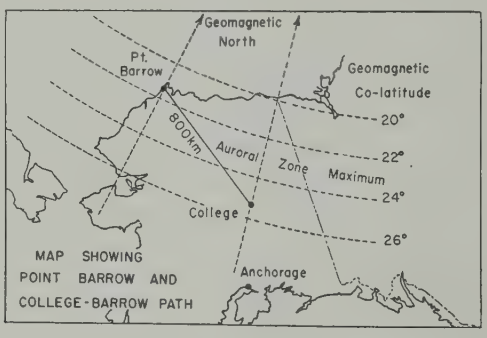

Fig. 1—Point Barrow is located north of the accepted auroral zone maximum

presence or absence, respectively, of a signal propagated over this path, a distinction can be made between the ground-scatter theory and theories favoring direct return from the aurora. The ground-scatter theory would require that there be a potent signal at the point of scatter by the ground, several orders of magnitude stronger than that received back at the originating transmitter (and radar receiver).

Equipment

Low power, simple antennas, and simple circuits were used to facilitate transportation by air and installation. To avoid the use of a TR-switch and to avoid modification of time-constants in an existing receiver, the transmitting and receiving sites were separated by approximately one mile.

The transmitter was crystal-controlled, with a computed peak output power of about one kilowatt at 51.9 Mc/sec (six-meter wavelength). A pulse length of 270

μ sec was used and a pulse rate of 100 per second. The transmitting antenna was a vertical half-wave dipole, with its center 25 feet or $1\frac{1}{4}$ wavelengths above the ground. If the reflection coefficient of the ground was -1, there would be minima in the vertical coverage at 11°.5 and 37°. They are not felt to be important because (1) the pseudo-Brewster angle is on the order of 10°, making the ground-reflected ray almost zero at that angle, and (2) the reflection of snow-cover is not unity at any angle. The most important design feature of this antenna is that it radiates in all azimuths equally.

An electrically quiet receiving site was selected about one mile true east of the transmitter. A low-noise (cascade) R.F. amplifier preceded a crystal-controlled converter, which then fed a communications receiver NC183-D having a bandwidth of about 4 kc. The A-scope sweep circuit was synchronized by the transmitter ground-wave pulse, present at all receiving antenna orientations. Meteor echoes occurred at a rate of one in several minutes.

To obtain azimuth information, twin four-element Yagi antennas, spaced 0.5 wavelength, were used for receiving. This array had a beamwidth of 60° and a front-to-back ratio of 8 db. A slipping coaxial coupling allowed continuous rotation at 35 seconds per revolution. The array was pointed at an elevation angle of about 15° to reduce the effects of the ground on the vertical pattern, in addition to arguments presented for the transmitting antenna. A B-scope display (range *vs* azimuth in linear coordinates) was photographed automatically on 16-mm film each rotation of the antenna. Such records were obtained covering 40 hours on seven days, of which a total of 5.3 hours showed auroral echoes.

Comments on the Visible Aurora

The 12 entirely clear nights that occurred during the course of this experiment showed some aurora each night, despite quiet ionospheric conditions. The aurora usually began as a faint quiet arc overhead or slightly to the north. Usually it then brightened as it moved south toward the "auroral zone," with break-up low in the south. Bright aurora was often north of Point Barrow, especially near the end of the evening. Correlation with the position of radio echoes was generally poor. (Low-angle visibility was usually obscured by ice-crystal precipitation.)

It is interesting to note that the daily sums of K-indices from College, Alaska, were all less than 18 for the 12 nights with aurora mentioned above. On one of these nights, multiple homogeneous bands were seen, although the College magnetogram was so remarkably quiet that a K-sum of 00 was broadcast. Visual aurora notes and Point Barrow magnetogram deviations often showed exact correspondence in time, but there were many cases of non-correlation.

The Positions of the Observed Echoes

The azimuth and range of echoes were later read from the B-scope pictures. An echo was ignored if a previous echo of the same range and azimuth had been read either one sweep or two sweeps earlier. This procedure was intended to reduce the statistical weight of long-lived echoes. Echoes that existed less than the time required for passage through the antenna main lobe were also ignored, to help

exclude meteor possibilities and to improve bearing accuracy. The range determination is accurate to about the nearest 100 km, and the bearing can be in error by about 45° because of the simple equipment and difficulty in interpretation of the film records.

Despite the tendency for visible aurora to be seen in the south, Figure 2 shows

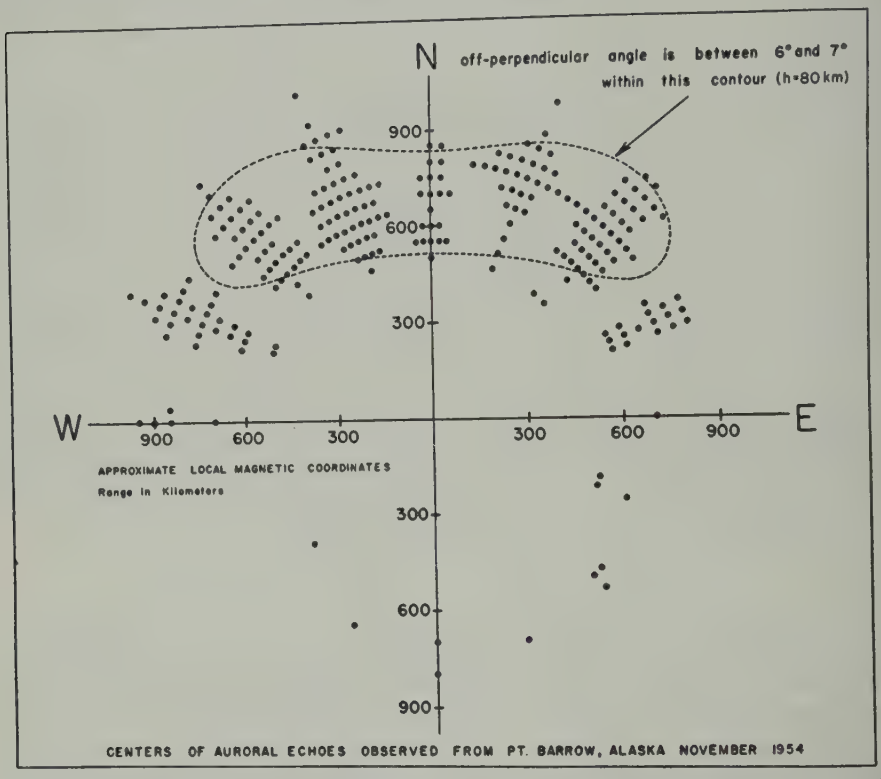

Fig. 2—Each dot represents the occurrence of an echo as a function of slant range and bearing

that the radio echoes were obtained almost entirely in the north. Although the equipment was intended to respond to aurora at all azimuths equally, 93.6 per cent of the echoes were seen north of east and west. Because of film-reading error, there is a deficiency of echoes exactly on the north, west, and east lines. The auroral echoes usually changed from one 35-second sweep to the next. Therefore, during northern activity, some of the southern echoes may be attributable to bursts of auroral echo signal lasting 5 to 10 seconds, entering the back-lobe of the receiving antenna while pointing south. On two occasions, southerly echoes repeated on successive antenna rotations (without echoes at the same range in the north), suggesting that they did, indeed, occur in the south. These unusual exceptions do not detract from the clear tendency for most of the echoes to occur north of Point Barrow.

The maximum range of the radar was limited to 1500 km by the reoccurrence of the transmitted pulse, or to 1100 km by the horizon, for aurora at a height of 100

km. Slow recovery of the receiver reduced the radar response for ranges less than 300 km. Echoes were obtained, as shown in Figure 2, only between 500 and 1100 km, the limit to minimum range not being imposed by antenna vertical patterns.

An explanation of the experimental bearing distribution is suggested by Figure 3. Contours of equal angle between the direct radio path and the plane perpendicular to a line of the earth's magnetic field are plotted for an assumed height of 80 km as a function of slant range and bearing from Point Barrow. It has already been shown by Chapman [8] that exact perpendicularity becomes impossible at high magnetic latitudes for usual auroral heights. Figure 3 bears this out, but shows

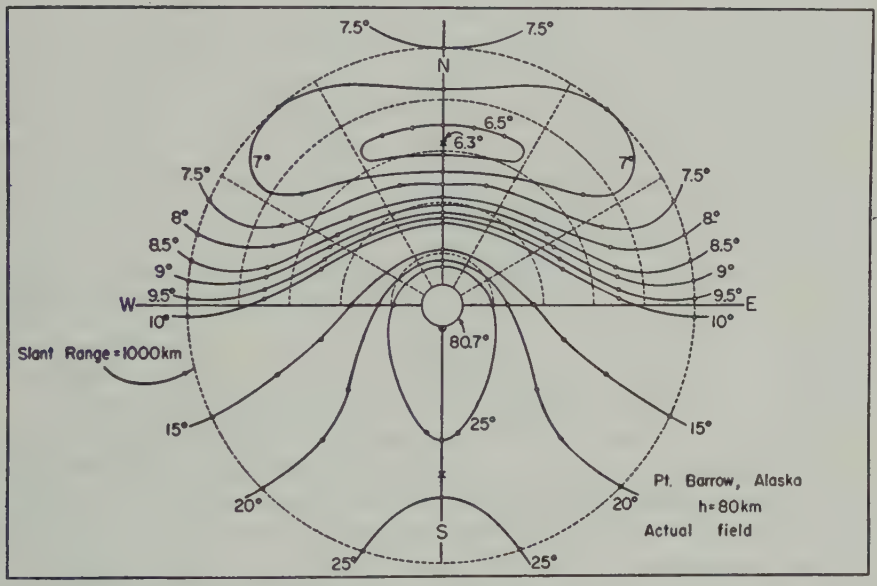

FIG. 3—Contours of equal angle between direct radio path and the perpendicular to the lines of the earth's magnetic field for points located 80 km above the surface of the earth as a function of slant range and bearing from Point Barrow; the actual magnetic inclination angle has been used in the meridian plane and is assumed constant along a geomagnetic latitude

that a range of 630 km, magnetically north, gives the *closest* approach to perpendicularity possible (6°.3) for Point Barrow. With an antenna sharp in azimuth, pointed northward, and with auroral activity distributed over the entire sky, nearness to perpendicularity would predict that most echoes be obtained at a slant range of about 600 or 700 km, with a rapid decrease of echo probability for lesser ranges. For a fixed range of, say, 600 km, echoes will be most probably due north and over a spread of angles near north from northwest to northeast, but will drop off rapidly as east and west are approached. There is a slight improvement in the south, but the angle from perpendicularity is about four times the northerly value, making echoes improbable. The 7° contour from Figure 3 has been redrawn over Figure 2 to demonstrate that the shape of the mass plot of the experimental occurrences fits the theory. It should be recalled that, because the antenna is 60° wide, the experimental points tend to be spread in azimuth.

The rare southerly events not conforming to the above pattern are probably associated with unusually strong aurora or are analogous to mysterious long-duration meteor echoes that can lack aspect sensitivity.

It has now been shown that the statistical location of the echoes are accurately explained simply by considering the nearness to perpendicularity that the radio beam makes with the lines of the earth's field at the point in space where reflection or scattering is occurring. This procedure is especially convincing for the location of Point Barrow, where most visible auroras occur south of the station. Agreement has thus been established with the explanation of auroral aspect sensitivity mentioned by Moore, and enlarged by Booker, Gartlein, and Nichols.

Observations of Auroral Propagation Between College and Point Barrow

At the time of the above observations, a 5-kw radar at 51.7 Mc/sec was being installed at College, Alaska, but the echo recording equipment was malfunctioning. This equipment used a rotatable six-element broadside vertically-polarized array, backed by a screen reflector. During the observations at Point Barrow, the College radar antenna was aimed at Point Barrow (52° west of magnetic north at College) and the transmitter was left on at all times.

By shutting off the Point Barrow transmitter and listening with the Point Barrow receiving antenna pointed at College, meteor ionization could be detected by an audible buzz at the pulse repetition frequency, lasting a fraction of a second. Such bursts occurred about once per minute, verifying that the transmitter and receiver were operating in readiness for detection of auroral propagation.

In lieu of echo records at College, visual aurora was observed on many occasions north, overhead, and south of Point Barrow (including the mid-point of the 800-km College to Point Barrow path). Although the receiving equipment was equal to that successfully used for echo reception at College, no auroral propagation could be detected, even at the above times (except for one case to be described). Assuming that echoes could have been detected at College with a range of 800 km and an azimuth of 52° west (as was frequently done later at College when sweeping PPI), then lack of signal near the earth's surface at Barrow makes the ground-scatter explanation of College auroral echoes improbable.

Total observations of 26.8 hours were made at times when aurora was seen or might have been expected. When particularly bright aurora was visible, the antenna was rotated continuously (a total of 3.3 hours). On the one occasion that an aurorally propagated signal was heard (associated with extremely bright aurora east of Point Barrow), the signal was shown to be arriving at Point Barrow displaced about 20° northward of the direct route.

The fact that this signal was not coming over the most direct path between College and Point Barrow is indication that the ionospheric agent was not a smooth, horizontal layer. This single observation does not bear resemblance to sporadic-*E* layer propagation and is therefore offered as additional evidence against the ground-scatter theory.

Sporadic-*E* propagation was expected occasionally, but was not observed because of the shortness of this path. Bailey [9] reports night sporadic-*E* at 48.9 Mc/sec from Anchorage to Point Barrow (1200 km).

Conclusions

With the exception of the work of Hellgren and Meos [2], and the Tromsö work of Harang and Landmark [3], most V.H.F. research has been done at temperate latitudes where, indeed, the aurora occurs to the north of the observing radar and at low angles. Point Barrow was selected for this experiment to allow study of the auroral ionization at all positions in the sky, so that aspect sensitivity of the auroral ionization itself was the important consideration.

Neither the absorption argument nor the ground-scatter theory can explain why echoes are obtained only from aurora north of the observing station. The lack of signal at the place of supposed ground-scatter is a second reason for rejecting the Harang and Landmark theory. Evidence has thus been presented supporting the meteor-trail analogy of auroral echoes which makes use of the earth's magnetic field for explaining radio aspect sensitivity.

Acknowledgments

This work was sponsored by the Geophysical Institute of the University of Alaska under Signal Corps contract No. DA-36-039-sc-56739. The Arctic Research Laboratory facilities at Point Barrow were indispensable and the generous assistance of the staff was greatly appreciated.

References

[1] B. W. Currie, P. A. Forsyth, and F. E. Vawter, J. Geophys. Res., **58**, 179-200 (1953).
[2] G. Hellgren and J. Meos, Tellus, **4**, 249-261 (1952).
[3] L. Harang and B. Landmark, J. Atmos. Terr. Phys., **4**, 322-338 (1954).
[4] R. Dyce, QST, **34**, 11-15 (1955).
[5] A. G. McNamara and B. W. Currie, J. Geophys. Res., **59**, 279-285 (1954).
[6] R. K. Moore, Trans. Inst. Radio Eng., Prof. Group on Antennas and Propagation, No. 3, 217-230 (1952).
[7] H. G. Booker, C. W. Gartlein, and B. Nichols, J. Geophys. Res., **60**, 1-22 (1955).
[8] S. Chapman, J. Atmos. Terr. Phys., **3**, 1-29 (1952).
[9] D. K. Bailey, Report of Commission III, Eleventh General Assembly of International Scientific Radio Union (URSI), Brussels, August 1954; M. G. Morgan, II, Tech. Rep. No. 6, Thayer School of Electrical Engineering, Dartmouth College, Hanover, N.H. (1954).

A DISCUSSION ON THE VARIATION OF *F*-REGION HEIGHT

BY B. CHATTERJEE

Indian Institute of Technology, Kharagpur, India

(Received April 5, 1955)

ABSTRACT

Variations of *F*2-region height with season and solar activity have been explained in terms of the author's picture of ionization distribution in the *F* region. Different types of behaviours of *F*2-region height at different latitudes are accounted for with the presently accepted model of temperature distribution in the upper atmosphere.

1. INTRODUCTION

It was shown earlier that the apparently anomalous behaviour of *F*2 ionization is due to the particular physical properties of the upper atmosphere at this height, and that the total ionization of the composite *F* region follows the zenith angle of the sun [see 1 of "References" at end of paper]. A tentative picture of the noontime ionization distribution in the *F* region [2] shows that the height of $F2_{max}$ should, in general, increase with increased solar activity and reduced zenith angle of the sun (due to the effects of increased temperature). This fits in well with the experimental data of seasonal and solar-cycle variations of *F*-region height for medium and high latitude stations and also sometimes for the solar-cycle variation of low latitude stations in winter. But the observed data of low latitude stations, in general, show a decrease in *F*2-region height with solar activity. The same results were observed by Ghosh [3] in her studies on the virtual heights of *F* region. Also, the noontime *F*2-region height of low latitude stations is often found to remain constant, or even reduced slightly in some cases, with reduced zenith angle of the sun. All these "anomalous" behaviours occur only when the height of the *F*2 region is already very high (near about 500 km). These have been explained in terms of the presently accepted temperature distribution in the upper atmosphere and are in agreement with the author's picture of ionization distribution in the *F* region.

2. VARIATION OF *F*-REGION HEIGHT WITH SEASON AND SOLAR ACTIVITY

The upper atmospheric temperature (T) may be assumed to increase steadily and more or less linearly with height, in the range 200 to 400 km. Above this region, the temperature falls more or less exponentially with height to merge itself with the interstellar temperature. Assuming the effective mass (m) of the atmospheric particles to remain constant, we may take the variation of scale height H (equals KT/mg) to be proportional to T. Hence,

$$H = H_0 + \beta(h - h_0) \qquad \text{[From 200 to 400 km]}$$

and

$$H = H_m \epsilon^{-\alpha(h-400)} \qquad \text{[Above 400 km]}$$

[The heights are measured in kilometers and the reference level h_0 is at Fl'_{max}, the value of which is taken as 200 km. H_0 is the scale height at h_0 and H_m that at 400 km (that is, $H_m = H_0 + 200\,\beta$)].

With increase in solar activity and reduction in solar zenith angle, both "β" and "α" increase, and as a result the variation of reduced height z (equals $h - h_0/H$) with true height h takes the form as shown in Figure 1. [The value of H_0 also changes,

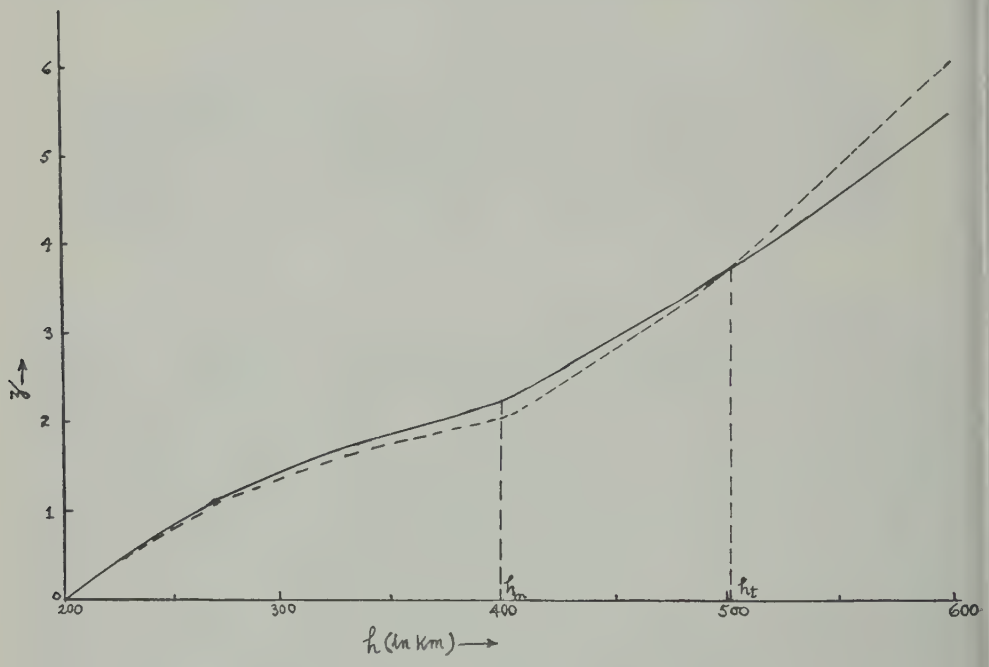

FIG.1

but it does not affect the above variation, except to make the value of h_t a bit higher.] The full line shows the variation for a period of low solar activity and the dotted line that for a high solar activity. They may also be taken as those for higher and lower values of solar zenith angles, respectively. The parameters chosen in plotting the curves are as follows:

$$H_0 = 50\text{ km}, \qquad h_0 = 200\text{ km}, \qquad h_m = 400\text{ km}$$

For low solar activity (or higher zenith angle), $\beta = 0.2$ and $\alpha = 0.001$. For high solar activity (or lower zenith angle), $\beta = 0.25$ and $\alpha = 0.002$.

It may be assumed that the value of z remains constant and the variation of layer height with solar zenith angle or solar activity is due to the fact that with changes in temperature, the same value of z corresponds to different values of h. From Figure 1, it is clearly seen that if the layer height at the low sunspot-activity (or higher solar zenith angle) period is below h_t, then an increase in solar activity (or a reduction in solar zenith angle) increases the layer height. The increase in height is maximum if the original point is just below h_m. But, if the height for

reduced solar activity is above h_t , there is a decrease, instead of increase, of the layer height. For points near h_t , practically no change in height occurs.

Now, as the $F2$ region is situated very high at low latitude stations, it often lies on or above the critical point h_t . [The actual value of h_t depends on the temperature distribution, but in any case lies above 400 km.] Thus, unlike those at medium and high latitude stations, there may be a decrease in layer height with increased solar activity or reduced zenith angle of the sun.

3. ACKNOWLEDGMENT

The author wishes to express his grateful thanks to Dr. S. R. Sen Gupta, the Director, Indian Institute of Technology, and also to Dr. K. K. Bose, the Officer-in-Charge of the Communication Engineering Department.

References

[1] B. Chatterjee, J. Geophys. Res., **58**, 353 (1953); also Nature, **173**, 263 (1954).
[2] B. Chatterjee, Indian J. Phys., **28**, 53 (1954).
[3] M. Ghosh, Indian J. Phys., **27**, 421 (1953).

EVIDENCE OF POLAR SHIFT SINCE TRIASSIC TIME

BY JOHN W. GRAHAM

Department of Terrestrial Magnetism, Carnegie Institution of Washington, Washington 15, D.C.

(Received June 16, 1955)

ABSTRACT

The magnetizations of 343 samples of Permian and Triassic sediments from the United States are compared to magnetizations that have been reported for sediments of approximately the corresponding age in England. It is demonstrated that an impressive number of the observations are in essential agreement simply on the basis of assuming that the rocks were magnetized by a geomagnetic field about like the one today, the essential difference being that this field was in a significantly different orientation. This result is discussed in terms of slip of an outer shell of the earth relative to the axis of revolution.

INTRODUCTION

Since the appearance of the paper by Johnson, Murphy, and Torreson [see 1 of "References" at end of paper] on the magnetizations of Pleistocene varved clays, there has been a basis for hoping that the history of the changes of the earth's magnetic field can be traced far back in time by studies in sedimentary rocks. In the past few years, a number of pertinent findings have been reported. Among the most interesting, given first *in extenso* by Clegg, Almond, and Stubbs [2], and confirmed by Creer, Irving, and Runcorn [3], is the fact that there is a regional consistency in the magnetizations of the late Paleozoic and Triassic sediments of England. These magnetizations were found to be in such a pattern that two obvious interpretations could be advanced, as follows: (1) In Triassic time, England was in its present location but the earth's magnetic field was so oriented that the dipole axis emerged in the vicinity of Kamchatka and southeast of Brazil; or (2) England since Triassic time has experienced a clockwise rotation on a vertical axis of some 34°. Also of interest is the evidence presented to show that the sense of the earth's field reversed during the span of time represented by the sediments.

Earlier studies of Paleozoic sediments in the eastern United States did not reveal as simple a pattern of magnetization [4, 5, 6]. It was established that within the Silurian of the folded Appalachian belt there are zones of sediments which are magnetized as though they had originally been laid down in South Africa [7]. Efforts to confirm this interesting situation by studies of sediments outside the geosyncline were futile [8], and it became obvious that in these rocks there was not the necessary internal consistency to permit an accurate determination of the former orientation of the earth's magnetic field.

The fact noted by Clegg, *et al.*, that the English sediments with the interesting magnetizations had at one time been buried to a depth estimated as 10,000 feet, suggested a parallel with the findings in the Appalachians. There the Silurian sediments, too, had at one time been deeply buried; in addition, however, they had been considerably deformed, and some of the discrepancies in the patterns of magnetization were attributed to deformation. Sediments with magnetizations either parallel to the earth's present field or greatly scattered were found commonly only in sections which had never been deeply buried.

It follows that the deductions made from observations in the once deeply buried sediments of England should be examined by studies elsewhere in contemporaneous beds which also had been subjected to elevated pressures and temperatures. These are abundantly available in the southwestern United States. It was already known that the magnetization directions in a flat-lying section of Permian sediments (in Ohio), which have always been lying at shallow depths, were greatly scattered [6]; see Figure 1. This paper is a first report of studies that are being made to

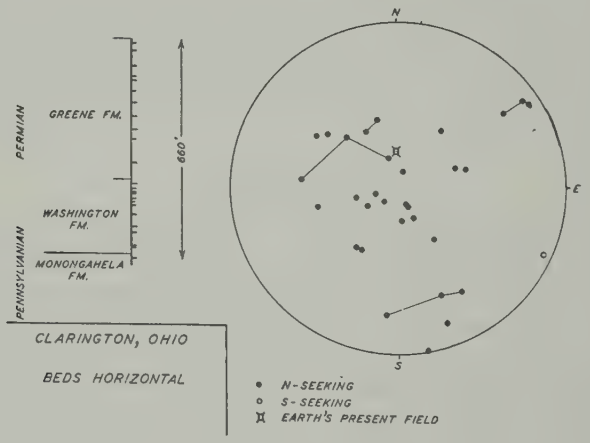

FIG. 1—Magnetizations of Permian sediments, Clarington, Ohio

determine the extent to which the findings in England can be confirmed and generalized by field observations of sediments of the same ages in the United States and elsewhere.

The criteria for selection of sites for sampling were mainly the following: Approximately flat-lying, unmetamorphosed, fine-grained sediments of sufficient coherence to permit preparation of oriented cores; reasonable accessibility; known position in the stratigraphic sequence. All samples which could be measured are reported; no localities were revisited for substantiating "interesting" results. In all, 301 oriented specimens from 12 different sites were collected and measured during the period March 22 to May 20, 1955.

ACKNOWLEDGMENTS

Dr. Charles B. Read, of the Fuels Branch, United States Geological Survey, at Albuquerque, New Mexico, and his colleagues, were most helpful in providing

detailed information on a great many of the sites sampled, and in offering valuable discussion of some of the results as they were obtained in the field. Mr. W. N. Dove, of the Department of Terrestrial Magnetism, assisted during the first two weeks of the trip; his place was then filled by Mr. Kenneth G. Books, of the Geophysics Branch, United States Geological Survey, for two weeks; and he in turn was followed by Mr. William E. Huff, Jr., of the Geophysics Branch, USGS for the remainder of the trip. Coring and measuring oriented samples and driving a truck are arduous tasks, and I am very grateful for the cheerful and able assistance that was given. Finally, I wish to express my appreciation to Dr. E. J. Workman and Prof. Victor Vacquier, of the New Mexico Institute of Mining and Technology, for their cordial hospitality and help.

EXPERIMENTAL PROCEDURE

During the past eight years at the Department of Terrestrial Magnetism, a number of special procedures have been developed and used primarily for studies of the magnetism of sedimentary rocks [6, 9, 10, 11]. Since these have been of great help in the work, a detailed description of the important ones is given below.

Field truck—The truck is a Dodge Power Wagon (9,000 pounds gross weight), having available four-wheel drive and a winch on the front end. It is fitted with an aluminum van, 8 feet long, 6-1 4 feet wide, and 6-1/4 feet high, specially designed to contain all the equipment needed for collecting oriented core samples in the field and completing the measurements of their residual magnetism. The principal components are as follows:

For sampling—A 3.5-kva, 115-volt, ac generator for powering the drilling rig (more than adequate); a drilling rig which can cut cores at the outcrop to a depth of 3 inches; 55-gallon drum of water for cooling the drill-bit; water-pump, hoses, and extension cables which allow the drill-rig to be operated up to 100 feet from the truck; a standard drill-press which can be used when the drill-rig is impracticable; saws for end-cutting the cores to length.

For measuring—Spinner magnetometer (see below); devices for orienting cores and plotting final results.

Miscellaneous hand-tools, spare parts, camping equipment, bedding, etc. The design layout is successful in that it is possible to shift rapidly from one type of operation to another with a minimum of effort.

For the assistance of anyone contemplating constructing a similar field laboratory, the following criticisms of the systems now in use may prove valuable.

The drilling rig was fabricated from a small standard drill-press, a six-foot aluminum ladder, a 1/3-hp, 1725-rpm, ac motor, a flexible cable, and minor parts. It has proved exceedingly effective for sampling some exposures, and completely worthless in others. Its chief drawback is that it is too unwieldy for two men to handle on rough terrain. Occasionally some rocks are too tough to core effectively with the bit pressures that can be exerted on the standard bits which cut a one-inch core standing in a 1-1/8 inch hole. The self-centering behavior of a coring cutter minimizes the problem of accurate spindle alignment. The chief problem in using the drilling-rig is to assure at the start that the legs of the rig will remain

stationary during the coring operation. Once the core has been started, care must be taken to maintain constant pressure on the bit so that its angle of attack is not changed as the frame of the rig is sprung by the applied pressure. This is an arduous requirement when cutting hard rocks in an uncomfortable position.

A greatly improved rig is contemplated, and may include the following features: A lightweight aluminum base (of I-beam?) which by expansion-bolts in small holes can be strapped firmly to the outcrop, carrying a cutter-head mounted on universal swivels in such a way that forces are balanced so as to minimize clamping requirements, a compressed-air or gasoline-driven motor translating with the bit and in-line feed by compressed air operating on a piston. Such a rig could be quickly reduced to lightweight components and could probably be so designed that one man could operate it effectively.

The orientation of the core is accurately established by a device which slips around the core while it is still standing in the outcrop. It consists of a three-inch length of 1″ (I.D.) brass tubing, with a 1/16″ wide slot along its length. At one end of it is a flat surface, normal to the tube axis, adapted to support a standard Brunton-type geologist's pocket transit. When the proper edge of the flat plate has been leveled, the slot of the tube is running along the top element of the cylindrical core surface, and then a thin brass wire is run up and down the slot so as to leave a streak of brass on the side of the core. The inclination of the core axis and its azimuth are determined by measurements on the flat plate. The core is then broken away from its base (frequently completely, merely by sideways force at the exposed end), and the outer end is marked. The measurements of the magnetization are made relative to the brass scribe line and the mark indicating the exposed end of the core.

With this device, hundreds of cores have been oriented, but its practical design could be greatly improved. An immediate improvement would be the elimination of the requirement for the many operations with the pocket transit. Instead, the device should be equipped with level bubbles, a liquid-damped compass, and an inclinometer. Also, a system using spring members to grip the core rather than a rigid tube could be made somewhat more accurate and convenient.

When the drilling-rig cannot be used, samples are oriented by selecting a flat surface on which orientation measurements can be made. The strike is indicated by an arrow and its azimuth determined relative to magnetic north. The dip of the surface is indicated by another mark. Cores are cut from the block on the drill-press, the direction of coring being normal to the orientation plane. The orientation of the cores is established in the same manner as when they are cut *in situ*. The accuracy of this method of sampling is less than with the drill-rig, owing chiefly to the difficulties of finding a completely flat surface and then cutting cores perpendicular to it.

SPINNER MAGNETOMETER

This magnetometer is a further development of the type first pioneered by Johnson [12]. Dr. H. E. Tatel and Mr. P. F. Michelsen were responsible, in a large measure, for the success of this instrument. In it, the sample, a core one inch in diameter by an inch long, is held in a plastic (Lucite) air-driven centrifuge

(Beams type) and spun within a pick-up coil at 282 cps. A phase reference voltage, against which the signal induced in the coil is compared, is obtained by incorporating the revolving sample holder in an optical system consisting of a line filament, a cylindrical lens, the air turbine, and a photocell. A sanded portion of the otherwise transparent plastic rotor interrupts the light. The output of the photocell passes through suitable amplifiers and filters and a variable phase shifter to the phase detector. The pick-up coil, of balanced "pancake" design, is matched by a special transformer to the input grid of the signal amplifiers. The signal is suitably amplified and passed through narrow band-pass filters to the phase detector. The photocell and signal channels are nearly identical as far as phase shift *vs* frequency characteristics are concerned, so that speed control of the rotor is not critical. Speed of rotation, determined by a discriminator circuit connected to the photocell channel, is controlled by a manual valve on the air supply. A vacuum-tube voltmeter is used to measure the voltage output of the signal channel. The gain of the signal channel can be adjusted over a range of 100 db by a variable attenuator near the beginning of the signal amplifier; another 40-db gain control is available in the unit amplifiers which follow.

The limit of sensitivity of the magnetometer, determined by extrapolation of measurements on magnets which were calibrated by the United States Coast and Geodetic Survey, is about 10^{-8} cgs/cc when working with the one-inch cylinders. This figure represents a practical limit imposed by the magnetic moment of the available plastics, and by problems of coil microphonics; it probably could be improved somewhat. The equipment has been repeatedly used in the truck for measuring directions of magnetization at this sensitivity level in such adverse locations as below power-lines and adjacent to busy highways. In some cases, it has been found necessary to null the earth's field at the sample in order to overcome the influence of a magnetically soft component which was causing discrepancies in the measurements. Normally this precaution is not required. Difficulties of measurements on inhomogeneous samples have not been recognized. Anisotropy of susceptibility of samples does not usually effect the measurement accuracy.

The direction of magnetization of the sample is determined by six measurements treated in three pairs. The angular departure of the half plane containing the N-seeking end of the magnetization direction from a reference axis that is normal to the spinning axis, is measured; the sample is then rotated 180° about the reference axis, and the angular departure of the N-seeking half plane in this new position is determined. By symmetry, the sum of the two angles must be 360°, and, if necessary, arithmetical corrections are applied to make them so. This procedure effectively calibrates the whole system for phase fidelity under operating conditions without recourse to a reference standard. Two other pairs of angles are determined in the same way by spinning the sample on other coordinate axes, and the three essential angles corresponding to the three positions are plotted as planes on an equal-area projection net [10, p. 162]. Any discrepancy in closure of the three angles on the net is recognized as a measurement error and its size is gauged by the radius of the circle that can be inscribed in the error triangle. The error radii on samples whose moments are greater than 10^{-7} cgs/cc rarely exceed one degree. The measuring and plotting require about ten minutes per sample.

OBSERVATIONS

In Table 1, the locations where data were obtained during this special expedition to southwest United States have been indicated. A great number of excellent

TABLE 1—*Information on localities sampled*

Site No.	Locality	Latitude (north)	Longitude (west)	Age and formation	Stratigraphic thickness sampled	Lateral extent sampled	Number of oriented samples	Number of measured specimens	Literature reference
		° ′	° ′		*feet*				
				Jurassic					
1	Montoya, N.M.	35 02	104 05	Redonda Fm.	~150	1/2 mile	17	20	13
				U. Triassic					
2	Shyrocks Mill, Md.	39 33	77 23	New Oxford	20	300 ft	14	14	14
3	Las Vegas, N.M. (25 miles southeast)	35 23	104 47	Chinle	5	100 ft	6	8	15
4	Romeroville, N.M.	35 31	105 15	Chinle	15	100 ft	16	16	15
				M. Triassic					
5	Cameron, Ariz.	35 53	111 25	Shinerump	5	20 ft	17	20	16
				Permian					
6	Goulding's Trad. Post, Monument Valley, Utah	37 01	109 58	Cutler Fm., Organ Rock Tongue	200	1/4 mile	12	12	17
7	Tecolote, N.M.	35 26	105 17	Sangre de Cristo	10	100 ft	19	19	15
8	Tecolote, N.M.	35 28	105 16	Yeso	36	200 ft	26	26	15
9	Zuni Mountains, N.M.	35 21	108 26	Abo	25	150 ft	13	25	18
10	Abo Canyon, N.M.	34 27	106 23	Abo	50	400 ft	11	20	19
11	Oak Creek Canyon, Ariz.	34 56	111 41	Supai	100	1.4 miles	17	52	20
12	Carrizo Creek, Ariz.	33 57	110 18	Supai	~1,000	10 miles	30	59	20
13	Clarington, Ohio (1950 data)	39 46	80 54	Green and Washington	660	2 miles	25	32	21
14	Glenwood Spgs., Colo. (1948 data)	39 34	107 25	Cutler	1	50 ft	2	10	10, 22

exposures of various ages and lithologies had to be ignored because of time limitations and the desire to make an extensive rather than intensive study. Many exposures, particularly of the Triassic Chinle formation, were not sampled because of their large grain size and, frequently, their lack of coherence. The Permian beds, in contrast, are generally finer grained, and contain numerous coherent beds from which good cores can be removed. In addition, during the early sampling, the Permian results appeared more interesting, and it thus seemed important to emphasize rocks of this age. The studies of Triassic rocks are being continued.

The procedure in studying an exposure usually was as follows: A day would be devoted to collecting as many samples as possible, either as blocks or with the drilling-rig; the necessary time would then be spent in completing the sample preparation, measurement, and data plotting. The outcrop would then be revisited for study with the magnetic data in hand, but no further specimens would be taken.

Information on the localities sampled is given in Table 1. According to C. B. Read [22], it has been found possible to make some broad generalizations about the genesis of these red beds in New Mexico and Arizona. The Chinle, Abo, and Sangre de Cristo formations are considered to have been derived from pre-Cambrian igneous and metamorphic rocks. They were deposited at grade on broad alluvial plains substantially at water level. Significant and extensive oxidation is believed to have resulted from fluctuations of the level of the ground water in the sediments, and hence it is inferred that much of the ferric iron was formed shortly after sedimentation. In contrast, the Yeso and Supai formations are believed to have been derived from the weathering and reworking of preexisting red sediments. The deposition was in restricted marine basins, where the precipitation of gypsum and other evaporites was favored. A reducing environment is inferred. Baker [17] has discussed the regional development of the Cutler formation.

FIG. 2—Magnetizations of Triassic and Jurassic sediments

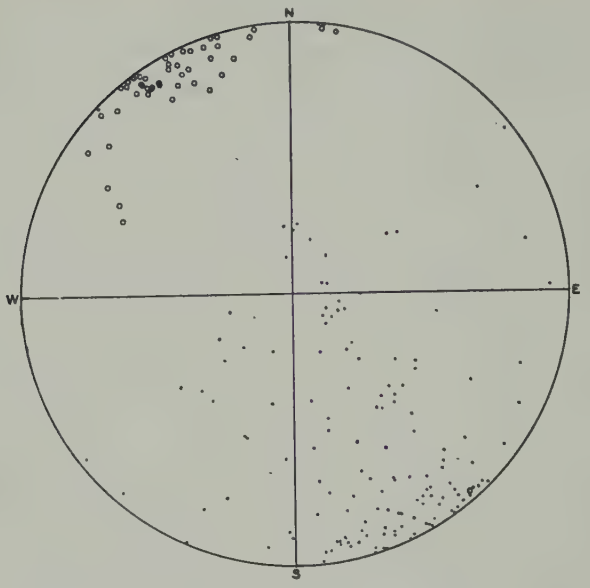

FIG. 3—Magnetizations of Permian sediments

Magnetizations observed—In Figures 2 and 3, all the directions of magnetization measured in Permian, and Triassic and Jurassic sediments, are shown in the lower hemisphere of the equal-area projection.* It is at once obvious that the two groups present a grossly different picture: In the Permian beds there is a concentration of the N-seeking direction of magnetization toward the SSE (S-seeking towards the NNW) and about horizontal; the Triassic and Jurassic beds give results not greatly different from the direction of the earth's present field, and resemble many of the results we have obtained from many different Paleozoic and Tertiary sites. There is only slight evidence of reversals of the sense of magnetization. In order to permit a rapid comparison with the results from England, the directions of the field (dipole formula—see later section) in late Paleozoic and Triassic time as reported by Clegg, *et al.*, as averages at their various sampling sites and as seen from New Mexico and Arizona, have been indicated in Figure 4. Remembering the adopted convention of plotting always in the lower hemisphere, it is seen that, although the polarizations of many samples depart greatly from Clegg's averaged directions, the majority of the Permian samples lie within the limits found in England.

THE STABILITY OF MAGNETIZATIONS

It has long been recognized that the future development of the subject of rock magnetism hinges on the question of the stability of magnetizations in time. In early work, the stability was assumed, or was inferred from simple considerations. Quantitative procedures for testing stability in special selected settings were

*This convention of plotting exclusively in the lower hemisphere differs from the convention recently adopted by some other workers of plotting the N-seeking end of the magnetization vector and indicating whether the point falls in the upper or lower hemisphere. There is obvious need for general agreement on the best procedure.

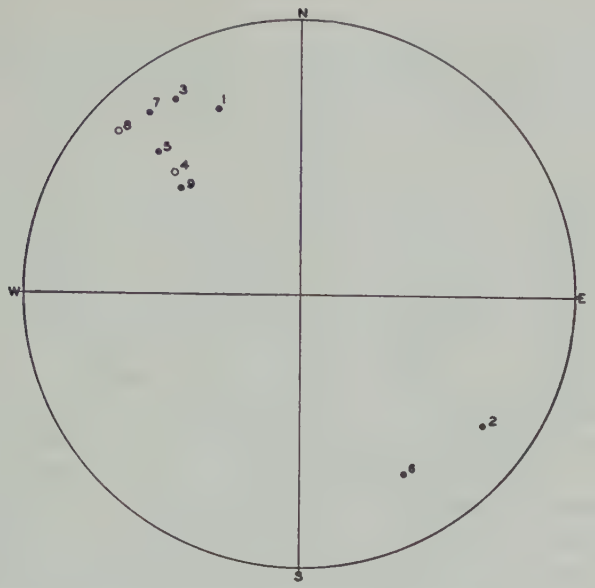

FIG. 4—Magnetizations which should be observed in Arizona for agreement with Clegg's various sites; • = N-seeking, ○ = S-seeking

formulated and first demonstrated in 1949 [10]. These procedures have found extensive use at suitable sites; they have been augmented by theoretical treatments of the properties of dispersed assemblages of tiny magnetic particles [23]. When suitable sites for stability determination are not available, indirect tests of a reassuring, though not positive nature, must be resorted to [24]. Enough observations have been made so that there is no longer any question that a useful fraction of old rocks are retaining to this day the magnetizations they received at remote times.

It seems now that still another approach to the stability question is available, and, though the work involved is tremendous, the results will be unequivocal. The approach will be illustrated by the treatment in this paper. Magnetic instability is known to result from many causes—some more effective than others—and to be certain that in a given sequence of rocks there has been *no* change of magnetization is a rigid requirement. But it seems that this requirement is met by any group of rocks that has a coherent and simple pattern of magnetization differing from the present earth's field, provided the samples come from many different places of the world. We know that many rocks can retain primary magnetizations faithfully for long times; we know also that the magnetizations of many rocks change rapidly. The geophysical problem now is to find in rocks of various ages, on a world-wide basis, the persistent and simple patterns of magnetization that have withstood all remagnetizing influences.

A simple relationship between the magnetizations of the Triassic in England and a majority of the observed magnetizations in the Permian of the southwest United States is indicated by Figure 3 and 4. This leads to the tentative conclusion that the magnetizations in question are stable. The proof of the conclusion

will have to depend on observations made in other parts of the world. Studies in the Karoo series of Africa and its correlatives in South America and Australia should be most interesting. The relatively limited number of Triassic samples from the United States appear, for the most part, to be unstable.

THE PROBLEM OF SCATTERED POLARIZATIONS

The subject of rock magnetism has not yet developed to the point where it is possible to predict whether a given series of specimens, about which a great deal is already known geologically, will be magnetically of geophysical importance. The problem is made complicated by the great number of factors that have to do with magnetization; we are dealing with many unknowns and are groping for generalizations that will unify for us the behavior of nature.

The observations in Oak Creek Canyon, Arizona, are of interest in the problem of the scatter of magnetizations. In Figure 7 (at end of paper), sites 11*A* and 11*B*, the results from flat-lying beds and from overlying conglomerates of essentially the same material have been plotted separately. The non-random grouping indicates that the conglomerates have been magnetized following deposition, and it is thus necessary to believe that the flat beds also may have received some magnetization following the one they presumably received at the time of deposition. It is significant to note two particular features in these two plots: (1) The magnetizations found in the flat beds make a streak on the plot up into the zone where most of the conglomerate polarizations fall; and (2) the streak is roughly along a great circle between a direction close to the earth's present field and the field postulated for Permo-Triassic time. A reasonable interpretation of these observations is that initially the beds were magnetized by the field indicated by most of the other Permian samples and then later were "overprinted," in part, by new directions of magnetization in a changed earth's field. The tendency to a similar streaking in the conglomerates suggests that they, too, were magnetized, in part, in the direction of the postulated field, following their redeposition. The scatter of a couple of the points outside of the conglomerate group suggests that these samples have retained some magnetization acquired before redeposition.

A similar streaking of magnetizations is seen in the samples from Monument Valley, Figure 7, site 6, and the same interpretation of an initial magnetization plus a later overprinting in a changed earth's field seems reasonable. That the overprinting is not a simple matter of a soft magnetization produced by the earth's present field is suggested by the observation that a ± 50-gauss field applied for one minute did not alter any of the magnetizations which are in equilibrium with the present field. The very limited data available (sampling difficulties) from the Chinle southeast of Las Vegas, New Mexico (Fig. 7, site 3), also have an appearance of "streaking," but the initial and secondary fields are not known.

Some magnetization following deformation is suspected in the samples which came from an unusual group of sediments enclosed by typical M. Triassic Shinerump conglomerate (Fig. 7, site 5). Here the specimens were obtained from two settings: Exceedingly fine-grained alternating thin layers of yellow and purple material (volcanic ash?) in the flat-lying condition, and the same material in a completely disorganized jumble. The general appearance implies that the deformation took

place when the beds were soft. Since the magnetizations fall into a far more coherent pattern than the shapes of the folds would suggest, it follows that magnetization was after deformation. Unfortunately, the magnetic susceptibility of the samples was so low (5×10^{-6} cgs/cc) that the measurement of susceptibility anisotropy could not be used as an index of deformation [25].

The concept of an initial stable magnetization plus a later overprinting does not apply to the problem of explaining the observations in the Abo formation in the Zuni Mountains (Fig. 7, site 9). Here two contrasting types of sedimentation mechanics are represented by samples from wind-laid deposits with complex cross-bedding and water-laid deposits with fine laminations having considerable horizontal extent. The color, grain size, and composition to the naked eye of the two types are identical and their magnetization patterns are indistinguishable. This material is soft and it is easy to crumble it down to individual grains. The fraction that could be extracted with a saturated Alnico V bar magnet is found to have a grain size comparable to that of the clastic quartz grains, that is, about 0.1 mm. It seems reasonable that owing to the coarse grain size of the magnetic fraction the conditions were never proper for achieving uniform magnetization at deposition. The Sangre de Cristo formation (Fig. 7, site 7) is very similar and the same situation may have applied to it. In the beds in Abo Canyon (Fig. 7, site 10), it appears that there were several layers of sufficiently fine grain to acquire a magnetization parallel to the applied field.

THE PROBLEM OF THE UNIFORM MAGNETIZATIONS

There seems to be no lack of mechanisms by which it is possible to explain away the polarizations that fail to fall in with a group. The problem of deducing the magnetization mechanism that produces a grouping of polarizations is far more subtle, and is also far more important because it involves the concept of time and dating. It is not known whether these groupings of magnetizations date mainly to the time the beds were originally deposited, or whether they date to some time after deposition. Many samples from Carrizo Creek (site 12) favor the latter possibility. Several samples have conspicuous cross-bedding, and yet their polarizations are the same in intensity and direction as those from some evenly bedded finer and coarser sediments. A couple of samples came from a very fine-grained bed, which seems to have suffered some heterogeneous distortion by being forced down into yielding underlying shale; the polarizations of this bed, however, fit in with the rest of the group.

In other rock magnetism studies, it has been demonstrated repeatedly that it is not possible to generalize about the properties of many different rocks from the properties observed in a few selected individuals. The same caution should be used in efforts to deduce the date and mechanism of magnetization of these rocks. Even though in a number of cases it is clear that magnetization followed deposition, it does not necessarily follow that this generalization applies to all samples. Until more information is available, it is not possible to say whether the magnetizations of these beds date to the time of deposition or to some later time. Many studies in younger sediments will be needed to establish the most recent date when the earth's field was in the orientation deduced from these samples.

THE INFLUENCE OF COMPACTION

If the magnetizations observed in these strata are regarded as resulting originally by processes taking place at the time of sedimentation, then the effects of compaction must be considered. By and large, the samples from the United States are moderately fine-grained silts, in which the constituent clastic grains are in contact with one another. Material of this kind is not subject to the appreciable compaction demonstrated by finer grained sediments containing abundant clay and flocculated aggregates that incorporate quantities of water [26]. No field evidence of compaction of the beds sampled was found; therefore, it is suspected that compaction had no significant influence on primary magnetizations. Furthermore, the present magnetizations are essentially parallel to the bedding, and in this favorable orientation the effects of compaction should be minimal.

In the case of the English sediments, the polarizations are oblique to the bedding and, as pointed out by Clegg, *et al.*, compaction would act so as to decrease the original inclinations. However, the consistency of the two sets of observations implies either that compaction had no effect, or that magnetization took place after compaction.

ROTATION

One possible error that is difficult to evaluate can arise from the rotation of the outcrop about a vertical axis. This possibility is especially real in a province that has suffered from deformation, and only when the outcrops are frequent and the structures simple and known in detail can the possibility of rotation be intelligently dismissed. There is no geological basis for believing that the rocks sampled in north central New Mexico (Yeso Fm.) have been rotated 17° clockwise relative to those of central Arizona (Supai Fm.) as might be concluded from the magnetic data, but this possibility must be borne in mind.

THE PROBLEM OF THE SENSE OF THE PERMO-TRIASSIC FIELD

There are now available for consideration a great number of studies on the question of whether the sense of magnetization of a sample indicates the sense of the earth's magnetic field present when the sample was formed, or the opposite sense (for the latest discussions, see *Advances in Physics*, April 1955, for review articles by Nicholls, Néel, and Runcorn). The problem is one of mineralogy and solid state physics and chemistry, and so far has not been amenable to solution solely by field studies and geophysical considerations. Whereas recent field studies in Iceland are convincingly in favor of reversals of the earth's magnetic field [27], other observations in Japanese Pleistocene lavas are equally impressive from the standpoint of the self-reversal of the remanent moment [28]. It seems that there are subtle factors involved that have not yet been recognized; it may be that both types of reversal occur.

The data presented here on the magnetizations of the Permian sediments, when taken at their face value, imply that the north magnetic pole was formerly in the South Atlantic Ocean. This sense is indicated almost without exception by the samples from many localities and environments of deposition, and without regard to the color of the sediment, that is, whether orange, ruby red, purple, brown, pale grey-green, mottled or white. It follows, therefore, that the varied circumstances

giving rise to the different colors of these beds (that is, different iron compounds in various states of subdivision) had no control over the sense of magnetization. Remembering this, we must attempt to visualize the behavior of the ferromagnetic minerals under the conditions governing the color of the beds. We must postulate either that the moments always undergo self-reversal, in spite of the varied environment giving rise to the different iron colors, or that they never reverse but reflect accurately the sense of the applied earth's field.

If we knew that the only magnetization events in the lives of the rocks dated to the time and conditions creating the iron colors, then we should reasonably conclude that these magnetizations reflect the sense of the applied field, for as shown by Néel [29] the conditions required for self-reversal of the moment are rather special and can be dependent on the environment.

But suppose that there were two events in the magnetization history of these rocks: first, a primary magnetization at deposition, which in the next stage dictated the sense of magnetization of secondary ferromagnetic minerals that developed under the influence of a changed environment, when, possibly, the iron colors were developed (deeper burial, higher temperatures, percolating solutions, etc.). Then we might—even though it seems unreasonable—find suitable conditions for reversing the sense of all primary magnetizations of these samples.

This argument certainly will bear no weight with those who prefer to reverse the sense of the earth's field rather than the sense of magnetization of a sample. It is advanced solely to emphasize that we do not know in detail how these rocks were magnetized or what minerals are responsible for the magnetic moment or precisely when or how the beds received their iron content, or what their thermal history has been. Even though it is easy and even reasonable to assume that these rocks reflect the sense of the old applied field, this simple assumption may not do the problem justice in the present state of ignorance of all investigators. Certainly this problem merits further study [30].

THE LOCATION OF THE MAGNETIC AXIS FROM DECLINATION AND INCLINATION MEASUREMENTS

On a sphere which either is uniformly magnetized or which contains at its center a magnetic dipole, the angle I made by the magnetic lines of force with the surface is related to the angular distance θ of the point of observation from the point where the lines of force are vertical (magnetic pole) by the expression $\tan I = 2 \cot \theta$. The magnetic field of the earth is not precisely described by this expression, for in addition to a simple main dipole component which is not exactly centered there are other more complex components. Nevertheless, this expression establishes reasonably well the great-circle distance of the magnetic pole from the point of observation. The direction to the pole is taken as the direction of the horizontal component (declination) at the point of observation. This again is an approximation when dealing with a magnetized sphere having a non-uniform magnetization. An example of the applicability of these approximations is given in Figure 5, where there are plotted the positions of the present magnetic N pole determined from several places along the equator using observed declination and inclination values and the dipole formula. The poorest determination places the

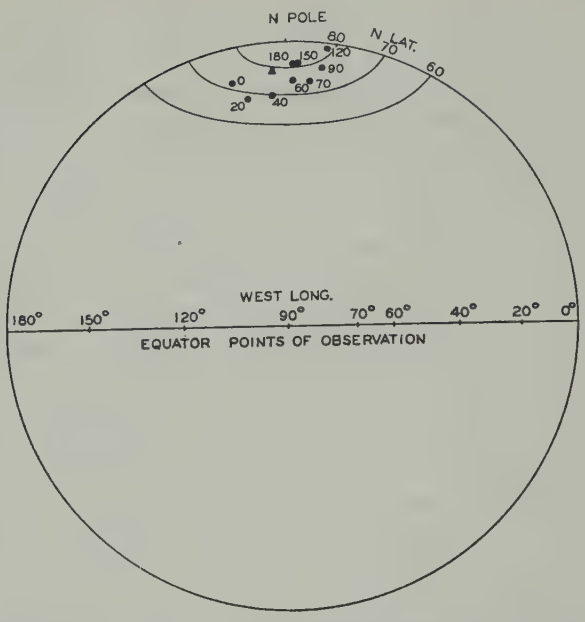

FIG. 5—Fixes on magnetic pole by dipole formula using declination and inclination values at the equator (western hemisphere, equal-area map)

pole 15° from its correct location; the average of several determinations will be close to the actual pole.

In spite of these demonstrated inadequacies, the dipole formula is the best and only one which can be used for pole determinations by rock-magnetism declination and inclination measurements; it will be possible to eliminate errors resulting from the approximation only by many observations. Inasmuch as we have no information yet on the complexity of the earth's field at remote times, we must anticipate that pole determinations made from a limited number of observations will be somewhat uncertain.

GRAPHICAL SOLUTION OF POLE LOCATION PROBLEM

The problem of locating the magnetic pole on the earth by declination and inclination measurements and the dipole formula is conveniently solved graphically by means of the equal-area (or stereographic) projection net. The net is considered to represent a global hemisphere, the small circles indicating latitude and the great circles the meridians of longitude. The site of observation is plotted at its correct latitude and longitude. The declination gives the angle that the great circle joining the magnetic pole and the site must make with the meridian through the site. This great circle is constructed as follows: A great circle 90° from the site is drawn. Along it, an angle equal to the declination is measured (in the right direction) from the meridian that passes through the site. Here a point is plotted. The magnetic pole lies on the great circle joining this point with the observation site at an angular great-circle distance from the site determined from the observed inclination and the dipole formula. The geographical coordinates of the plotted pole can then be read directly.

POLE LOCATIONS FROM PERMO-TRIASSIC SEDIMENTS

Using the foregoing procedures, the data of Clegg, *et al.*, for nine sites in the Triassic of England have been plotted to give the pole positions indicated in Figure 6 by open circles. Notice that this Figure is a map projection, not an

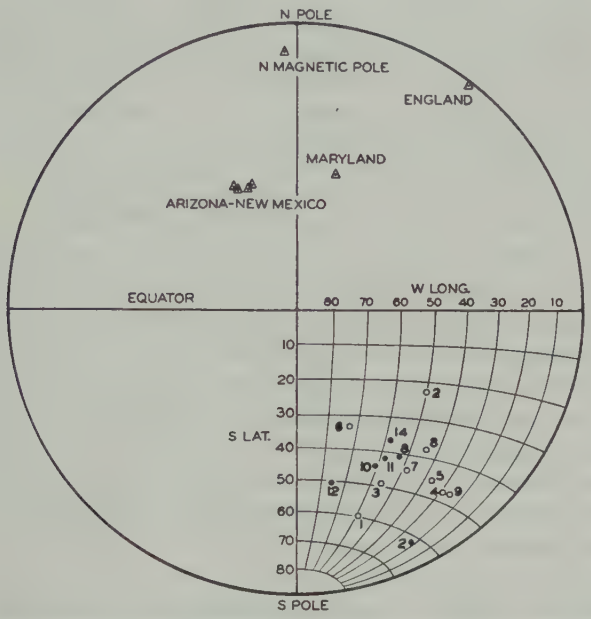

FIG. 6—Map of western hemisphere; ○ = magnetic poles located from England; • = magnetic poles located from United States

equal-area scalar projection. The numbers correspond to those used by Clegg for his sites. The black dots indicate poles determined from Permian and Triassic rocks in the United States; the numbers refer to the sites listed in Table 1. The following procedures, numbered according to the outcrop to which they apply, were used in selecting the values of declination and inclination which give the indicated magnetic poles. All beds are assumed to have been horizontal when magnetized.

Site 2. Maryland Triassic—The average was chosen as the center of the consistent group of polarizations in fine-grained red silts; the scattered directions from coarse greywackes were ignored.

Site 12. The observed polarizations were rotated 90° on a horizontal axis (see Fig. 7, site 12*B*) in order to eliminate the projection distortion by bringing the group into the center of the net; the best average was then selected by eye. This point was then rotated back 90° to give the actual declination and inclination of the average. This procedure, though less accurate than the method provided by Fisher [31], is faster, and for the present purposes is considered sufficiently reliable.

Site 8. Yeso formation—Essentially the same procedure, the four conspicuously divergent points being ignored.

Site 11. Oak Creek Canyon—Here the selection of an average had to be

subjective because of the streaking of the polarizations. The average was chosen as the center of the 22 points making a group centering about on the horizon.

Site 10. Abo Canyon—As in the previous case, the average was chosen as being in the center of eight points forming a group.

Site 14. Glenwood Springs, Colorado (1948 data, ref. 10, p. 148)—The necessary small corrections for the flexure fold were carried out as follows: First the fold axis was made horizontal by rotating it (and the bedding poles) on a horizontal axis at right-angles to it; the beds were then rotated on this new fold axis to make them horizontal. The polarizations were given the same rotations and their final position for flat-lying beds is shown in Figure 7, site 14. Each point represents the average of five other points which were within 4° of one another.

THE SCATTER AMONG THE DIFFERENT DETERMINATIONS

Figure 6 gives evidence that the magnetic pole in Permo-Triassic time was significantly removed from its present location. It is now important to inquire into the reasons for the lack of precise agreement among the various determinations of the pole location. Errors from experimental procedures can probably be dismissed. In those cases where large numbers of samples were individually oriented and measured, the chances of being misled by occasional mistakes (in reading the compass, for example) are minimized. The moments of all samples are sufficiently large that errors in measuring directions of magnetization are small, and errors in plotting, computation, etc., are likewise considerably smaller than the differences that appear from outcrop to outcrop.

An error still to be considered can arise from the geologists' inability to determine initial dips. When magnetizations are found parallel to the bed (horizontal field), the magnetic pole is determined as being 90° away on the sphere. If these beds had had an initial dip of 5°, the pole location would be in error by only 2.5°. In contrast, if magnetizations are inclined 70° to the bed, an uncertainty of $\pm$ 5° in the initial dip introduces an uncertainty of $\pm$ 7.5° in the location of the pole. For this reason, in addition to those cited in the discussion of compaction, it is best to determine former locations of the poles from deposits that were formed near the (then) magnetic equator. The present data fulfill these requirements well, and the discrepancies in locating the pole cannot be ascribed to uncertainties about compaction or initial dips.

It appears that the scatter among the different determinations is real; it is reasonable to assume that it represents a measure of the variability of the earth's field during the period of magnetization of these beds.

THE AGREEMENT AMONG THE DIFFERENT DETERMINATIONS

Even though the positions of the pole as determined from observations in Permo-Triassic rocks are somewhat scattered, some limits can be set on the amount that England or the United States could have rotated since these rocks were magnetized. A rotation of either land mass of 20° would cause obvious discord of the two sets of determinations. There is no way by which both England and the United States could have rotated and preserved the agreement of the observations. Likewise, a simple translation of either land mass in any direction of 20° great-circle distance would eliminate the agreement. Any amount of combined translation

nd rotation about the determined pole position as a center would preserve the greement; this unlikely possibility can be examined by determinations in rocks of nother age when the magnetic pole was in some other position.

Thus, it follows that the Wegener hypothesis of continental drift finds no upport in these observations. If it should turn out that measurements from other ontinents confirm the pole location determined from these measurements, then the Vegener hypothesis will have ceased to be a concept worth serious consideration.

THE RELATIONSHIP OF THE MAGNETIC AND GEOGRAPHIC AXES

From two distinct lines of argument, there is justification for believing that he present-day near-coincidence of the geographic and magnetic axes is not ortuitous. Experimental evidence covering a significant span of time is found n other rock magnetism studies. The declination of Pleistocene varved clays of Jew England over an interval of 5,000 years shows east and west departures of bout 30° from geographic north; the average of the departures centers about on rue north [1]. Magnetic poles, located by a great number of magnetization observa- ons of Tertiary rocks, scatter about the present geographic poles [9, 32, 33, 34]. hese observations establish that over the past 50 million years the average of the agnetic axis positions is coincident with the present geographic axis.

Runcorn [35] has discussed the theoretical aspects of the relationships of the agnetic and geographic axes; he emphasizes that owing to Coriolis forces the most kely form that the core fluid motions would take would be in cylindrical vortices ith their axes parallel to the axis of revolution of the earth. Inasmuch as modern eories on the origin of the earth's magnetic field invoke fluid motions as essential arts of the field generators, it would seem that long period symmetry of the eld about the geographic axis is to be expected.

It follows, even though our understanding of the origin of the earth's magnetic eld is incomplete [36], that observations over a long period of the positions of e magnetic poles will give a fix on the geographic axis.

Therefore, it is believed that, taken together, the observations reported earlier om England and those reported here provide a basis for believing that the e geographic axis in Permo-Triassic time, or possibly somewhat after, appeared about longitude 50° west and latitude 45° south (130° east and 45° north).*

SIGNIFICANCE OF THE IMPLIED POLAR SHIFT

If the inference that there has been a shift of the geographic axis should bear e test of further observations and studies, then there is a basis for expecting at as a result important progress can be made in several other geological and ophysical problems.

The question of how the polar shift might be produced immediately directs tention to the interrelationship of the core, mantle, and crust. Inasmuch as

**Footnote added in proof:* Dr. S. K. Runcorn visited the Department of Terrestrial Magnetism June 27, 1955, and informed us of his unpublished results of measurements on samples he had lected in the same general area in the summer of 1954 in Permian and Triassic sediments. hough he and the author do not necessarily agree fully on the interpretation, they do agree t the two sets of data are strikingly similar and show a highly non-statistical behavior of the th's magnetic field during the ancient epoch when these rocks were magnetized.

evidence has never been found suggesting that since Paleozoic time the earth has been acted on by extra-terrestrial forces of sufficient magnitude to produce a polar shift, the forces causing the shift must be looked for within the earth itself. In such an isolated system, there must be conservation of the earth's total angular momentum. This demands that when a shift of a reference point on the surface of the earth takes place, there is a compensating shift of material within the earth. This reduces the problem to one of considering how much of the outer part of the earth behaves as a coherent unit and how much of the inner part reacts so as to conserve angular momentum. Without further information, an infinity of solutions is possible.

Intimately connected with the problem of determining the relative motions is the problem of finding the driving force that produced them. From the observed shift it is seen that the force was directed obliquely to the geographic axis; to get such a biased force requires axial asymmetry in some feature of the crust, or of the core, or of the mantle between. Treatments of this problem already appear in the literature. For examples, Vestine [37] has discussed the interrelations of the variations of the geomagnetic field, fluid motions of the core, and the rate of the earth's rotation; Vening Meinesz [38] for some time has championed the rôle of convection currents in the mantle; and most recently Gold [39] has considered the problem from the standpoint of asymmetrical changes taking place mainly in the outer 100 km of the earth.

The impact of establishing a significant shift of the geographic axis on our thinking in the subjects of paleontology, stratigraphy, oceanography, climatology, etc., is obvious.

It would thus seem that important problems dealing with the earth's long-time behavior will be made more accessible to quantitative treatment when the promising possibilities of rock magnetism studies are realized.

References

[1] E. A. Johnson, T. Murphy, and O. W. Torreson, Pre-history of the earth's magnetic field, Terr. Mag., **53**, 349-372 (1948).

[2] J. A. Clegg, M. Almond, and P. H. S. Stubbs, The remanent magnetism of some sedimentary rocks in Britain, Phil. Mag., **45**, 583-598 (1954).

[3] K. M. Creer, E. Irving, and S. K. Runcorn, The direction of the earth's magnetic field in remote epochs, Tenth Assembly of the International Union of Geodesy and Geophysics, Association of Terrestrial Magnetism and Electricity, held at Rome, September 14-25, 1954.

[4] J. W. Graham, O. W. Torreson, and E. Bowles, Magnetic polarizations of Silurian sediments of the eastern United States, Abstract, Trans. Amer. Geophys. Union, **31** 328 (1950).

[5] J. W. Graham and O. W. Torreson, Contrasting magnetizations of flat-lying and folded Paleozoic sediments, Abstract, Trans. Amer. Geophys. Union, **32**, 336 (1951).

[6] J. W. Graham, Rock magnetism and the earth's magnetic field during Paleozoic time J. Geophys. Res., **59**, 215-222 (1954).

[7] Carnegie Institution of Washington, Year Book No. 48, 1948-49, Report of the President p. 8.

[8] Carnegie Institution of Washington, Year Book No. 49, 1949-50, pp. 62-63.

[9] O. W. Torreson, T. Murphy, and J. W. Graham, Magnetic polarization of sedimentary rocks and the earth's magnetic history, J. Geophys. Res., **54**, 111-129 (1949).

[10] J. W. Graham, The stability and significance of magnetism in sedimentary rocks, J. Geophys. Res., **54**, 131-167 (1949).

[11] J. W. Graham, Changes of ferromagnetic minerals and their bearing on magnetic properties of rocks, J. Geophys. Res., **58**, 243-260 (1953).
[12] E. A. Johnson, T. Murphy, and P. F. Michelsen, A new high sensitivity remanent magnetometer, Rev. Sci. Instr., **20**, 429-434 (1949).
[13] E. Dobrovolny and C. H. Summerson, Geology of northwestern Quay County, New Mexico, Oil and Gas Investigations Preliminary Map No. 62 (sheet No. 1 of 2), U. S. Geological Survey, 1946.
[14] A. I. Jonas and G. W. Stose, Geologic map of Frederick County, Md., Maryland Geological Survey, 1938.
[15] S. A. Northrop, H. H. Sullwold, Jr., A. J. MacAlpin, and C. P. Rogers, Jr., Parts of San Miguel and Mora Counties, New Mexico, Oil and Gas Investigations Preliminary Map No. 54, U. S. Geological Survey, 1946.
[16] Geologic map of United States, U. S. Geological Survey, 1932.
[17] A. A. Baker, Geology of the Monument Valley-Navajo Mountain region, San Juan County, Utah, Bull. No. 865, U. S. Geological Survey, 1936.
[18] N. H. Darton, "Red beds" and associated formations of New Mexico, Bull. No. 794, U. S. Geological Survey, 1928.
[19] R. H. Wilpolt, A. J. MacAlpin, R. L. Bates, and G. Vorbe, Parts of Valencia, Torrance, and Socorro Counties, New Mexico, Oil and Gas Investigations Preliminary Map No. 61, U. S. Geological Survey, 1946.
[20] J. W. Huddle and E. Dobrovolny, Late Paleozoic stratigraphy and oil and gas possibilities of central and northeastern Arizona, Oil and Gas Investigations Chart No. 10, U. S. Geological Survey, 1945.
[21] G. W. White, Upper Pennsylvanian and lower Permian rock section at Blaine Hill, Belmont County, Ohio, Ohio J. Science, **45**, 173-179 (1945).
[22] C. B. Read, personal communication, 1955.
[23] L. Néel, Théorie du trainage magnétique des ferromagnétiques en grains fins avec applications aux terres cuites, Ann. Géophys., **5**, 99-136 (1949).
[24] J. W. Graham, Tracing the earth's magnetic field in geologic time, Abstract, Tenth Assembly of the International Union of Geodesy and Geophysics, Association of Terrestrial Magnetism and Electricity, held at Rome, September 14-25, 1954.
[25] J. W. Graham, Magnetic susceptibility anisotropy—an unexploited petrofabric element, Abstract, Bull. Geol. Soc. Amer., **65**, 1257-1258 (1954).
[26] I. Sherman, Flocculent structure of sediment suspended in Lake Mead, Trans. Amer. Geophys, Union, **34**, 394-406 (1953).
[27] T. Einarsson and T. Sigurgeirsson, Rock magnetism in Iceland, Nature, **175**, 892 (1955). [Letter to Editor.]
[28] E. Asami, Reverse and normal magnetism of the basaltic lavas at Kawajiri-misaki, Japan, J. Geomag. Geoelectr., **6**, 145-152 (1954).
[29] L. Néel, L'inversion de l'aimantation permanente des roches, Ann. Géophys., **7**, 90-102 (1951).
[30] J. W. Graham, Note on the significance of inverse magnetizations of rocks, J. Geophys. Res., **57**, 429-431 (1952).
[31] R. A. Fisher, Dispersion on a sphere, Proc. R. Soc., A, **217**, 295-305 (1953).
[32] J. Hospers, Rock magnetism and polar wandering, J. Geol., **63**, 59-74 (1955).
[33] N. Kawai, Magnetic polarization of Tertiary rocks in Japan, J. Geophys. Res., **56**, 73-79 (1951).
[34] T. Nagata, Rock-magnetism, Maruzen Co., Ltd., Tokyo (1953), p. 193.
[35] S. K. Runcorn, The earth's core, Symposium on the Interior of the Earth, Trans. Amer. Geophys. Union, **35**, 47-63 (1954).
[36] D. R. Inglis, Theories of the earth's magnetism, Rev. Modern Phys., **27**, 212-248 (1955).
[37] E. H. Vestine, On variations of the geomagnetic field, fluid motions, and the rate of the earth's rotation, J. Geophys. Res., **58**, 127-145 (1953).
[38] F. A. Vening Meinesz, Gravity expeditions at sea, Vol. 4, Technische Boekhandel en Drukkerij J. Waltman, Jr. (1948). [Pub. of the Netherlands Geodetic Commission.]
[39] T. Gold, Instability of the earth's axis of rotation, Nature, **175**, 526-529 (1955).

FIG. 7—Directions of magnetization obtained at sites indicated in Table 1 (p. 334)

FINAL RELATIVE SUNSPOT-NUMBERS FOR 1954

Table 1 contains the final sunspot-numbers for 1954 for the whole disk of the sun, based on observations made at the Zurich Observatory, supplemented by series furnished by other cooperating observatories. Table 2 gives the number of sunspot-groups on each day for the year 1954. The yearly mean of the group-numbers is 0.4 against 1.3 in 1953. The yearly mean of the relative numbers is 4.4 against 13.9 in 1953. Two hundred and forty-one (241) spotless days have occurred in 1954 against 131 in 1953. Therefore, sunspot-activity in 1954 was at a still

TABLE 1—*Final relative sunspot-numbers for the whole disk of the sun for 1954*

Day	Jan.	Feb.	Mar.	Apr.	May	June	July	Aug.	Sep.	Oct.	Nov.	Dec.
1	0	0	9	0	0	0	0	8	0	0	0	0
2	0	0	12	0	0	7	0	9	0	7	0	0
3	0	0	11	0	0	0	8	16	0	14	0	0
4	0	0	7	0	0	0	0	9	7	8	0	0
5	0	0	0	0	8	0	0	12	7	7	7	0
6	0	0	0	0	0	0	0	19	0	0	7	0
7	0	0	0	8	0	0	0	14	0	0	8	7
8	0	7	0	8	0	0	7	10	0	0	7	0
9	0	7	0	15	0	0	0	13	0	0	24	0
10	0	0	0	0	0	0	0	23	0	0	38	0
11	7	0	0	0	0	0	0	14	0	0	41	0
12	0	0	8	0	0	0	7	14	0	7	40	0
13	0	0	17	0	0	0	10	8	0	7	39	0
14	0	0	22	0	9	0	15	7	0	15	26	0
15	0	0	36	7	7	0	8	0	7	17	11	11
16	0	0	40	7	0	0	15	0	9	24	7	18
17	0	0	42	0	0	0	7	0	0	22	7	17
18	0	0	39	0	0	0	7	0	0	7	7	16
19	0	0	29	0	0	0	0	0	0	14	7	20
20	0	0	23	8	0	0	0	0	7	14	0	19
21	0	0	17	0	0	0	0	9	0	8	0	12
22	0	0	12	0	0	0	0	15	0	8	0	7
23	0	0	7	0	0	0	0	18	0	14	0	7
24	0	0	7	0	0	0	8	16	0	8	0	14
25	0	0	0	0	0	0	10	11	0	8	0	14
26	0	0	0	0	0	0	7	9	0	7	0	7
27	0	0	0	0	0	0	7	7	0	0	0	0
28	0	0	0	0	0	0	10	0	0	0	0	0
29	0		0	0	0	0	8	0	0	0	0	13
30	0		0	0	0	0	7	0	7	0	0	29
31	0		0		0		7	0		0		25
Mean	0.2	0.5	10.9	1.8	0.8	0.2	4.8	8.4	1.5	7.0	9.2	7.6

lower level than in 1953. In the second half of the year, solar activity was increasing again. Sunspot-minimum was reached in June. As the epochs of maxima and minima of solar activity are determined from the smoothed sunspot-numbers, this epoch will be 1954.3 for the last minimum. That minimum was both a short and a low one. Figure 1 gives a graphical representation of the daily relative sunspot-numbers for 1954, the times being plotted as abscissas and the relative numbers as ordinates. The limits of the successive solar rotations are indicated by vertical arrows in the upper edge of Figure 1.

More details about the solar activity and the distribution and development

TABLE 2—*Daily numbers of sunspot-groups for 1954*

Day	Jan.	Feb.	Mar.	Apr.	May	June	July	Aug.	Sep.	Oct.	Nov.	Dec.
1	0	0	1	0	0	0	0	1	0	0	0	0
2	0	0	1	0	0	1	0	1	0	1	0	0
3	0	0	1	0	0	0	1	2	0	2	0	0
4	0	0	1	0	0	0	0	1	1	1	0	0
5	0	0	0	0	1	0	0	1	1	1	1	0
6	0	0	0	0	0	0	0	1	0	0	1	0
7	0	0	0	1	0	0	0	1	0	0	1	1
8	0	1	0	1	0	0	1	1	0	0	1	0
9	0	1	0	2	0	0	0	1	0	0	3	0
10	0	0	0	0	0	0	0	2	0	0	4	0
11	1	0	0	0	0	0	0	1	0	0	4	0
12	0	0	1	0	0	0	1	1	0	1	4	0
13	0	0	1	0	0	0	1	1	0	1	4	0
14	0	0	1	0	1	0	2	1	0	2	3	0
15	0	0	1	1	1	0	1	0	1	2	1	1
16	0	0	1	1	0	0	2	0	1	3	1	1
17	0	0	2	0	0	0	1	0	0	3	1	1
18	0	0	2	0	0	0	1	0	0	1	1	2
19	0	0	1	0	0	0	0	0	0	2	1	2
20	0	0	1	1	0	0	0	0	1	2	0	2
21	0	0	1	0	0	0	0	1	0	1	0	1
22	0	0	1	0	0	0	0	1	0	1	0	1
23	0	0	1	0	0	0	0	1	0	2	0	1
24	0	0	1	0	0	0	1	1	0	1	0	2
25	0	0	0	0	0	0	1	1	0	1	0	2
26	0	0	0	0	0	0	1	1	0	1	0	1
27	0	0	0	0	0	0	1	1	0	0	0	0
28	0	0	0	0	0	0	1	0	0	0	0	0
29	0		0	0	0	0	1	0	0	0	0	1
30	0		0	0	0	0	1	0	1	0	0	1
31	0		0		0		1	0		0		1
Mean	0.0	0.1	0.6	0.2	0.1	0.0	0.6	0.7	0.2	0.9	1.0	0.7

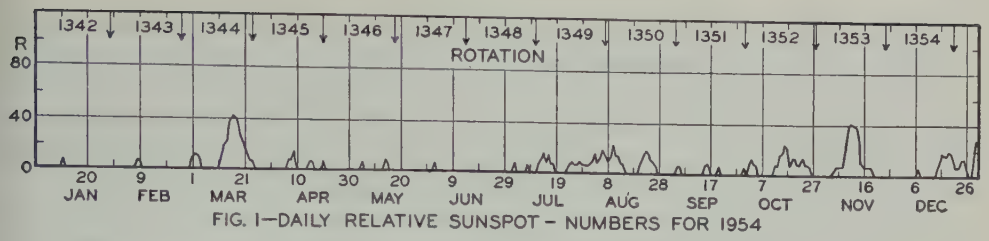

FIG. 1—DAILY RELATIVE SUNSPOT – NUMBERS FOR 1954

of the individual spot-groups will be given in "Die Sonnenaktivität im Jahre 1954" (Astron. Mitt. der Eidgen. Sternwarte, Zürich, Nr. 193) and in "Heliographische Karten der Photosphäre für das Jahr 1954" (Publ. Eidgen. Sternwarte, Zürich, **10**, Fasc. 4).

M. Waldmeier

Swiss Federal Observatory
Zurich, Switzerland, April 13, 1955

INTERNATIONAL DATA ON MAGNETIC DISTURBANCES, FIRST QUARTER, 1955

For explanations, please refer to the last report in this Journal (Vol. 60, No. 2, June, 1955, p. 219).

Preliminary Report on Sudden Commencements

S.c.'s given by five or more stations are in italics. Times given are mean values, with special weight on data from quick-run records.

Sudden commencements followed by a magnetic storm or a period of storminess (s.s.c.)

1955 January 09d 04h 02m: El Am.—*11d 12h 19*: thirty-three.—*17d 03h 22*: sixteen.—*17d 09h 30*: eleven.—27d 08h 52: Gi Ap Va Hr.

1955 February *23d 06h 23m*: five.—28d 00h 52m: Ka Hu Ap Am.

1955 March *30d 10h 39m*: eleven.—*30d 11h 43m*: seven.

Sudden commencements of polar or pulsational disturbances (p.s.c.)

1955 January 01d 18h 59m: Tr Eb Bi Hr.—01d 19h 18: Fu Bi.—*01d 19h 43*: six.—03d 23h 38: Tl Bi Hr.—*04d 00h 26*: eleven.—*05d 20h 58*: nineteen.—06d 03h 13: Ta El.—*06d 18h 50*: five.—06d 19h 35: Ma Db.—08d 23h 49: Fu El Tn Hr.—09d 10h 12: Do Wn Ci.—09d 18h 28: Do SM.—*11d 21h 38*: fifteen.—12d 01h 02: MB El Tn Hr.—*13d 00h 29*: seven.—13d 21h 39: Do Wn IK Eb.—*14d 18h 03*: five.—16d 00h 17: CF MB.—16d 00h 51: Eb SF El.—17d 13h 46: Do Ci.—17d 21h 28: Ci Ta.—18d 01h 03: Wn Ci Ta MB.—18d 17h 28: Fu Ci Ta Bi.—19d 00h 10: Ta Bi.—*19d 19h 06*: seven.—19d 21h 20: SM Ta MB Bi.—*20d 19h 25*: eighteen.—20d 21h 26: Ta Bi.—*20d 23h 43*: six.—21d 19h 21: Wn Fu.—21d 20h 12: Ta Bi.—23d 00h 27: Fu CF Eb.—*23d 19h 57*: six.—*23d 20h 20*: six.—29d 00h 45: El Hr.—*29d 20h 31*: eight.—30d 20h 50: CF Eb Tl.—*31d 21h 48*: seventeen.

1955 February *01d 20h 18m*: five.—*01d 22h 46*: five.—01d 23h 55: Ma Fu Bi El.—02d 06h 28: Ta El Ap.—02d 10h 23: Ta Ap Hr.—02d 23h 55: Ma CF.—*03d 00h 27*: seven.—*03d 21h 51*: fifteen.—*04d 08h 32*: six.—*04d 19h 50*: seven.—04d 20h 35: Ma Db.—*04d 21h 36*: eight.—05d 18h 11: Do Qu.—05d 21h 49: SM El.—*06d 23h 13*: five.—07d 23h 56: CF Eb Ta.—08d 15h 45: Do Fu Ta Qu.—*08d 20h 41*: six.—08d 21h 38: Tr Ta.—*10d 19h 31*: ten.—*10d 21h 14*: thirteen.—*10d 21h 47*: seven.—11d 20h 44: CF Eb.—*12d 21h 23*: seventeen.—*13d 01h 00*: nine.—14d 20h 40: Tr Do.—14d 21h 00: Tr SM.—14d 21h 43: CF Tl SF Ta.—*16d 18h 25*: five.—*16d 23h 44*: five.—17d 21h 42: Tl Gi.—17d 22h 46: Fu SM Ta.—*18d 22h 53*: eight.—18d 23h 25: IK Ci Gi.—*19d 21h 43*: five.—*20d 02h 05*: seven.—20d 02h 56: CF Ta.—*20d 18h 17*: six.—*20d 23h 59*: nineteen.—21d 04h 32: SM Ta.—22d 03h 45: CF Ta.—22d 14h 55: Ka To.—*23d 01h 43*: seven.—23d 13h 17: Ka Ap Am.—*23d 16h 56*: nine (si?).—*23d 20h 41*: ten.—24d 00h 20: Ma Db.—24d 01h 02: Ka Ap.—*24d 20h 39*: seven.—*25d 00h 04*: twenty-one.—*26d 03h 45*: six.—27d 23h 38: Wn Hr.—28d 00h 00: CF SM.

1955 March 01d 00h 34m: Tl Bi.—02d 00h 48: Eb Tl SM SF.—*03d 21h 00*: six.—04d 03h 24: SM Bi.—04d 19h 59: CF IK.—*04d 23h 17*: eleven.—*05d 20m 41*: thirteen.—05d 21h 12: Ma Db.—*06d 01h 55*: twelve.—06d 19h 53: Tr Do Le Bi.—*07d 00h 48*: nine.—*07d 17h 26*: sixteen.—*07d 19h 59*: twenty-one.—*08d 17h 20:* five.—*08d 22h 13*: six.—09d 05h 45: Ch SM SJ Hu.—09d 17h 57: Ma IK Ta Hr.—10d 19h 12: Tr Wn Tn Hr.—*11d 00h 09*: seven.—11d 02h 48: Do Db IK.—11d 11h 45: Ap To Am.—*12d 02h 48*: nineteen.—*12d 20h 46*: seven.—13d 17h 18: Ma Gi.—*13d 20h 13*: twelve.—14d 00h 00: Ta Hr.—14d 17h 36: Ma Fu Tl Hr.—*14d 17h 54*: six.—15d 02h 55; SJ Hr.—15d 22h 18: Ta El.—16d 16h 44: So Do Cm.—*16d 20h 22*: eight.—17d 00h 17: Le SM SJ.—17d 16h 46: MB Ba.—17d 20h 58: Ma Ta Hr.—18d 16h 45: Db IK Gi.—*18d 20h 10*: fourteen.—19d 00h 28: Do CF Tl Ta.—19d 20h 18: Ma Ta.—*20d 01h 13*: five.—*20d 22h 40*: five.—*20d 23h 00*: seven.—*21d 20h 39*: fourteen.—21d 21h 25: Ma SM El.—*23d 20h 45*: seven.—25d 19h 12: Do CF.—26d 05h 33: SM SJ.—28d 21h 51: Eb El.—29d 21h 36: Tr So Tl El.—30d 01h 05: CF Eb El.—30d 21h 00: Cm SM Ta.—31d 01h 35: SM Ta Hr.—*31d 18h 40*: five.—31d 21h 25: Ta El.

Sudden impulses found in the magnetograms (s.i.)

1955 January *12d 19h 44m*: six.—13d 04h 39: Ka Qu El Hr.—13d 04h 50: Ka MB El Tn.—16d 10h 21: Cm MB.—17d 17h 40: Ta MB.—17d 17h 54: El Tn.—*17d 18h 52*: seven.—18d 07h 22: Wn IK.—18d 19h 43: Ap Tn.—19d 03h 27: Ta El Tn.

1955 February *01d 13h 30m*: twelve.—04d 14h 05: Ma Db.—*21d 03h 52*: twenty-four (p.s.c.?).—23d 15h 55: MB Ba Hu.—26d 00h 58: MB Ba.—26d 12h 52: MB Ba.—26d 22h 10: MB Ba.—27d 22h 13: Ma Ci.—*28d 07h 23*: five.—28d 13h 51: Gi SM Hr.—28d 14h 12: Ka Qu Bi El.

1955 March *10d 14h 01m*: six.—15d 20h 02: MB Ba.—22d 03h 20: MB El.—24d 09h 35: Es MB.—27d 08h 43: Cm SM.

TABLE 1—*Geomagnetic planetary three-hour-range indices Kp, preliminary magnetic character-figures C, average amplitudes Ap (unit 2_γ), and final selected days, January to March, 1955*

January 1955									
E	1	2	3	4	5	6	7	8	Sum
1	1+	1+	1+	2o	1o	1+	2o	2+	13−
2	3−	1+	2+	2−	1o	2−	1−	2−	13o
3	1−	1−	2−	2−	2−	1+	0+	1+	9+
4	4−	2+	1+	2+	3−	2o	2+	2o	19−
5	1+	1−	1o	0+	1o	1+	2+	3o	11o
6	3−	3+	2−	1+	2−	2−	2+	1+	16o
7	2o	2o	2o	2−	2+	2o	2+	2−	16o
8	1+	0+	2−	1−	0+	1−	2o	3−	10−
9	4o	3−	4o	3o	4−	5−	3+	1o	26+
10	1o	1−	1o	1o	1−	1+	2+	0o	8o
11	2+	2−	1−	1o	5−	1+	3−	5o	19+
12	5o	2+	2−	1−	0o	0+	1+	0+	12−
13	3o	4o	3+	4−	3o	2+	2o	2−	23o
14	1o	1+	1+	2−	3−	2o	3+	0+	14−
15	0+	0+	0+	0+	0o	0o	0o	0+	2−
16	1+	1o	1o	2+	2+	2o	2+	2o	14+
17	1+	3o	3o	4o	7−	6−	5o	5+	34o
18	8−	7o	6−	2−	2+	4+	4o	4−	36+
19	5o	6+	6+	5+	5−	4o	4o	5−	40+
20	4+	4−	2+	1o	2+	2+	3+	4−	23o
21	4o	3−	2o	1−	1−	1o	2o	2+	15+
22	3−	2o	2o	1−	1o	1−	1−	1o	11−
23	3−	2+	2+	2+	3o	3−	3+	3−	21+
24	2−	2−	1o	0+	1−	2−	1−	1o	9−
25	1o	1+	1o	0+	1o	1o	1o	1−	7+
26	1−	1−	1o	1−	0+	1−	0o	0o	4o
27	0o	0o	1+	2+	1+	3+	4−	4o	16o
28	3o	3−	2+	2−	0+	1+	1o	2+	15−
29	1+	1o	1−	1+	1−	1+	3−	4−	13−
30	2−	2+	1−	2−	3−	2o	2+	2o	15+
31	2−	1+	1+	1−	0+	1−	1o	2+	9+

February 1955									
1	2	3	4	5	6	7	8	Sum
0o	0o	0+	1−	1+	1o	1o	1+	6−
1o	0+	1+	1o	1+	2−	2−	2−	10o
4−	3+	2+	1+	1o	2−	1o	2+	17−
1o	2+	3−	5−	3o	3o	4o	4o	25−
4−	2+	3−	3−	3o	2+	3+	4o	24o
2−	3+	3−	2+	3o	3+	3−	4−	23−
4−	4o	3−	2o	4o	3o	2o	1o	22+
2o	2−	2−	2o	2−	4−	4−	4−	20o
2+	3−	4−	3+	2o	2+	3−	1o	20o
1+	1+	3−	2−	1+	1o	2−	2−	13−
1−	1o	1o	1+	2o	4−	5−	5−	19o
3+	3+	2+	2o	2+	2o	3−	4−	22−
4o	3o	2−	3+	2−	3o	2+	0o	19o
1+	3−	3−	2o	2+	3o	2+	4−	20o
3+	3o	3+	2o	1−	0o	0o	0o	12+
0o	0+	1o	2+	3−	2−	2+	2o	12+
3o	2o	1o	2o	2o	0+	0+	2−	12+
1+	3+	2o	1+	0+	0o	3−	3+	14+
2o	2+	2+	1−	2−	1o	1o	1+	12+
1o	3−	2o	2o	3−	2o	3−	1o	16o
3o	5−	3o	2o	3−	2+	2o	2−	21+
3o	4+	3−	4−	3o	2o	3−	3−	24o
3+	3o	3o	4+	4+	4o	4o	2+	28+
3−	3o	3−	2o	3+	1+	3−	2−	19+
4−	4−	2−	3+	2+	3−	1+	3−	21+
3+	4o	1+	2o	1+	1−	2−	1o	15+
0o	0+	2−	1o	1+	1+	2o	2+	10o
5+	6o	4o	4−	5o	3+	1−	2−	30−

March 1955									
E	1	2	3	4	5	6	7	8	Sum
1	1−	1o	0+	1−	1o	1o	1+	1o	7o
2	2−	1+	1+	1+	1−	1−	1−	0+	8o
3	0o	2o	2o	1+	1o	0+	0o	0o	7−
4	0+	1o	1−	1+	0+	0o	2o	2+	8o
5	2+	3−	2−	2−	2−	2+	2+	3+	18o
6	4o	2+	2o	3−	2+	1+	3o	2+	20o
7	5−	4−	3+	3+	1+	4+	6o	4o	31−
8	4−	3−	3+	2o	2o	4+	4o	3o	25o
9	4−	3+	4−	3−	3o	4o	5o	3+	29−
10	3−	3o	4+	4o	4+	3−	4o	4−	29−
11	3+	3+	4o	4−	4o	4−	2o	1+	25+
12	4o	4+	4−	3−	3o	4−	4−	3+	28+
13	3−	3o	3−	2o	2+	3−	4o	3−	22o
14	4o	2+	1o	2+	2+	4−	3+	3o	22o
15	3+	4o	4+	3+	3−	2−	3o	3o	25+
16	3o	4−	2−	1+	1−	2o	3−	3−	18−
17	3+	2o	3+	3+	3−	3o	1+	2o	21o
18	2+	1+	3−	3o	3−	5−	4−	2o	22+
19	3−	1o	2−	1−	1−	1+	2o	1o	11o
20	2−	1+	2o	1+	1+	1−	1−	3+	12+
21	3+	1o	2−	2−	2−	1o	2+	3−	15+
22	2−	2o	3o	5o	6o	6+	4−	2+	30o
23	2o	1o	2o	1o	3+	4o	5o	5+	24−
24	4−	4o	3o	3o	2o	1o	1o	1−	18+
25	0+	0+	2o	2o	1−	2+	3−	2−	12o
26	1−	2+	4o	3+	3+	2+	1−	2+	19o
27	1o	2−	2−	4+	3−	2+	2−	2−	17o
28	2o	1o	2+	2−	1o	0+	0+	2o	11−
29	2−	1o	1+	1+	1o	0o	0+	0+	7o
30	1+	0+	1o	3o	3−	2o	4+	6−	30+
31	6o	6o	6+	5o	3+	4+	5−	4+	40o

	Preliminary *C*, 1955			Average amplitude *Ap*		
	Jan.	Feb.	Mar.	Jan.	Feb.	Mar.
	0.4	0.1	0.1	6	3	4
	0.3	0.3	0.1	6	5	4
	0.2	0.6	0.1	4	10	3
	0.7	1.2	0.2	10	18	4
	0.5	0.9	0.7	6	16	9
	0.6	0.9	0.7	8	14	12
	0.5	0.8	1.3	7	15	30
	0.4	1.0	1.1	5	12	18
	1.2	0.6	1.4	20	12	23
	0.2	0.2	1.1	4	6	22
	1.2	1.1	1.0	16	15	18
	0.7	0.8	1.0	9	13	21
	0.8	0.7	0.8	15	12	13
	0.7	0.8	0.9	7	11	14
	0.0	0.4	1.0	1	8	18
	0.5	0.5	0.8	7	6	10
	1.7	0.3	0.9	43	6	12
	1.7	0.5	1.1	59	8	15
	1.7	0.1	0.3	53	6	6
	1.0	0.6	0.3	16	8	6
	0.6	0.8	0.5	9	14	8
	0.2	0.8	1.6	5	16	35
	1.0	1.2	1.2	12	22	21
	0.1	0.8	0.5	4	11	12
	0.1	0.8	0.4	4	13	6
	0.0	0.5	0.8	2	9	12
	0.9	0.2	0.6	11	5	10
	0.4	1.4	0.2	8	32	5
	0.6		0.0	7		4
	0.6		1.1	7		18
	0.2		1.6	5		53

TABLE 1—(Concluded)—*Final selected days, January to March, 1955*

Month	Five quiet days	Ten quiet days	Five disturbed days
1955			
January	10 15 24 25 26	3 5 8 10 15 22 24 25 26 31	9 17 18 19 20
February	1 2 10 19 27	1 2 10 15 16 17 18 19 20 27	4 5 22 23 28
March	1 2 3 4 29	1 2 3 4 19 20 21 25 28 29	7 9 22 30 31

Preliminary Report on Solar-flare Effects

Effects confirmed by ionospheric or solar observations are in italics.

1955 March 03d 12h 28m–12h 40m: Ch.—*05d 09h 00m* (?): CF.—*06h 09h 46m*(?): CF.—*06d 10h 03m* (?): CF.—06d 14h 42–14h 47: Ch.—*07d 10h 23m* (?): CF.—07d 11h 38m (?): CF.—*10d 11h 58m*: CF.—*11d 10h 15m* (?): CF.—12d 07h 15m: El.—12d 16h 07m: Hu.—15d 14h 45m: Hr.—16d 10h 21–10h 28 (?): Eb.—*19d 13h 10m* (?): CF.

1955 February 01d 13h 31m: Hu.—04d 08h 30m–08h 32m: Bi.—*10d 10h 46m* (?): CF.—24d 01h 03m: Ap.—24d 11h 50m: Db Ma.—28d 07h 23-07h 25: El.—28d 08h 00–08h 30: El.

1955 March 03d 07h 38m: El.—20d 12h 45m (?): Ma Db.—20d 13h 15m (?): Ma Db.—20d 13h 40m (?): Ma Db.—24d 09h 34m–09h 40m (?): Hr.—27d 08h 42m: El.

Ionospheric or solar disturbances without clear geomagnetic effect

None.

Minor disturbances reported by one station only are listed in the De Bilt quarterly circular, but omitted here.

Committee on Rapid Variations and Earth Currents
A. Romañá, Chairman, Observatorio del Ebro, Tortosa, Spain

TABLE 2—*Monthly mean values of Ci, Cp, and Ap*

Index	Jan. 1955	Feb. 1955	Mar. 1955
Mean *Ci*	0.63	0.67	0.75
Mean *Cp*	0.52	0.70	0.70
Mean *Ap*	12	12	15

COMMITTEE ON CHARACTERIZATION OF MAGNETIC DISTURBANCES
J. BARTELS, *Chairman*
University
Göttingen, Germany

J. VELDKAMP
Kon. Nederlandsch Meteorologisch Instituut
De Bilt, Holland

PROVISIONAL SUNSPOT-NUMBERS FOR APRIL TO JUNE, 1955

(Dependent on observations at Zurich Observatory and its stations at Locarno and Arosa)

Day	April	May	June
1	9	23	26
2	14	21	17
3	8	32	13
4	21	45	22
5	36	44	25
6	30	28	33
7	32	20	26
8	31	17	23
9	19	0	24
10	10	0	27
11	0	9	48
12	0	7	46
13	0	0	40
14	0	0	63
15	7	7	56
16	9	16	69
17	13	29	74
18	0	32	71
19	0	34	67
20	0	45	74
21	8	60	55
22	0	51	38
23	0	55	15
24	8	50	0
25	0	46	0
26	0	47	0
27	10	47	0
28	22	47	8
29	23	45	11
30	29	36	23
31		24	
Means.....	11.3	29.6	33.1
No. days.....	30	31	30

Mean for quarter: 24.7 (91 days)

M. Waldmeier

Swiss Federal Observatory
Zurich, Switzerland

CHELTENHAM THREE-HOUR-RANGE INDICES *K* FOR APRIL TO JUNE, 1955

[$K9 = 500\gamma$; scale-values of variometers in γ/mm: $D = 5.4$; $H = 2.4$; $Z = 4.3$]

Gr. day	April 1955		May 1955		June 1955	
	Values *K*	Sum	Values *K*	Sum	Values *K*	Sum
1	4332 1134	21	3311 0111	11	2222 2222	16
2	3433 3233	24	0121 1222	11	2233 2223	19
3	3323 2222	19	3121 1132	14	2222 2233	18
4	2223 2334	21	2100 1122	9	2232 2122	16
5	4342 4231	23	2232 2423	20	1122 2231	14
6	4423 2213	21	4344 5145	30	1221 1344	18
7	5443 2223	25	4444 2234	27	4323 3224	23
8	2231 1122	14	4543 4334	30	3432 4333	25
9	2321 0013	12	2331 2223	18	0133 3233	18
10	1003 3213	13	3323 1223	19	3122 2121	14
11	2332 1222	17	2221 0122	12	1123 2133	16
12	4323 2123	20	2221 0123	13	3422 3223	21
13	4333 1234	23	3133 2222	18	1032 3333	18
14	2332 1111	14	2333 2223	20	2333 4332	23
15	2221 2222	15	3320 1122	14	4444 3244	29
16	2111 1033	12	4523 0112	18	3333 3323	23
17	1232 2122	15	2321 1112	13	2333 2233	21
18	0001 1111	5	2210 1222	12	2433 1132	19
19	2210 1022	10	1111 1111	8	4433 1112	19
20	2351 1222	18	2322 2123	17	2222 1322	16
21	1222 2222	15	0111 2112	9	2111 1112	10
22	3322 1122	16	2211 0232	13	1114 3324	19
23	0112 1101	7	1001 1101	5	4322 2254	24
24	2322 4434	24	2121 1122	12	4443 3333	27
25	2411 2223	17	2100 4356	21	4243 3131	21
26	3433 2135	24	6655 2222	30	2300 1013	10
27	4431 1366	28	2221 3454	23	2222 1122	14
28	6353 2345	31	5554 3234	31	2312 1123	15
29	5434 2344	29	3332 1223	19	2122 1232	15
30	5433 2234	26	1121 1322	13	2101 1122	10
31			2221 1122	13		

J. B. Campbell
Observer-in-Charge

Cheltenham Magnetic Observatory
Cheltenham, Maryland, U.S.A.

PRINCIPAL MAGNETIC STORMS

(Advance knowledge of the character of the records at some observatories as regards disturbances)

Observatory (Observer-in-Charge)	Greenwich date	Storm-time: GMT of begin.	Storm-time: GMT of ending[1]	Sudden commencement: Type[2]	Sudden commencement: Amplitudes[3] D	H	Z	C-figure, degree of activity[4]	Maximal activity on K-scale 0 to 9: Gr. day	Gr. 3-hr. period	K-index	Ranges: D	H	Z
(1)	(2)	(3)	(4)	(5)	(6)	(7)	(8)	(9)	(10)	(11)	(12)	(13)	(14)	(15)
	1955	*h m*	*d h*		′	γ	γ					′	γ	γ
College	Apr. 27	16 23	30 13	s.c.*	+3	+37	+7	ms	28	3	7	170	1270	640
(C.J.Beers)	May 25	15 33	26 11	.....	....	....	....	ms	26	3	7	220	1610	690
	June	None												
Sitka	Apr. 27	16 24	30 13	s.c.	5	14	6	ms	27	7,8	6	90	510	59
(T.L.Skillman)									28	1,3	6			
									29	4	6			
	May 5	22 ..	8 20	.....	....	....	....	ms	6	5	7	84	1017	640
									8	5				
	May 25	14 33	26 12	s.c.	5	28	5	ms	26	1,2,3	7	97	806	60
	June	None												
Witteveen	Apr. 24	12 00	24 24	.....	....	....	....	m	24	5,8	5	25	120	6
(D.van Sabben)	Apr. 27	16 24	30 07	s.c.*	−4	+87	−3	ms	27	7	7	45	240	13
	May 6	08 00	8 24	.....	....	....	....	ms	6	8	6	30	160	7
	May 25	14 33	26 19	s.c.*	−3	+87	−6	ms	25	7	6	35	300	12
									26	1	6			
	May 27	12 00	28 14	.....	....	....	....	m	27	6,7	5	25	165	5
									28	2	5			
	June 6	17 28	8 24	s.c.	−2	+34	0	m	8	5,6,8	5	25	135	7
Cheltenham	Apr. 27	16 23	30 06	s.c.	−1	+8	0	ms	27	7,8	6	43	183	23
(J.B.Campbell)									28	1	6			
	May 5	21 ..	8 24	.....	....	....	....	m	6	5,8	5	20	113	9
									8	2	5			
	May 25	14 33	26 11	s.c.	+1	+31	+3	ms	25	8	6	39	167	16
									26	1,2	6			
	May 27	12 ..	29 01	.....	....	....	....	m	27	7	5	18	92	7
									28	1,2,3	5			
	June 22	10 40	25 13	s.c.	+2	+20	0	m	23	7	5	20	101	5
Tucson	Apr. 27	16 23	30 13	s.c.	3	6	−1	ms	27	7	7	16	170	4
(M.L.Cleven)	May 5	14 31	9 09	.....	....	....	....	m	8	2	5	14	109	4
	May 25	14 33	26 18	s.c.	1	20	1	ms	26	2	6	16	178	6
	May 27	13 00	28 13	.....	....	....	....	m	28	2	5	13	83	4
	June 6	17 27	9 00	s.c.*	1	3	0	..	8	2	4	14	101	2
	June 22	10 38	25 12	s.c.	−1	35	2	m	22	4,6	5	15	124	5
San Juan	Apr. 27	16 23	28 02	s.c.	0	+16	−5	ms	27	7	7	13	128	6
(P.G.Ledig)	May 25	14 32	26 12	s.c.	0	+10	−4	ms	25	7,8	6	10	212	4
	June	None												
Honolulu	Apr. 27	16 27	30 12	s.c.	+2	+16	−11	ms	27	7	7	11	170	5
(R.F.White)	May 5	15 00	7 11	.....	....	....	....	m	6	5	5	9	121	4
									7	3	5			
	May 25	14 36	26 11	s.c.	+1	+27	−14	ms	25	8	6	12	210	4
	June	None												
	1954													
Alibag	Feb. 15	03 ..	16 00	.....	....	....	....	ms	15	4	6	4	131	2
(A.S.Chaubal)	Feb. 21	10 33	24 00	s.c.	0	+6	0	m	21	5,6,7	5	3	99	6
	Feb. 26	04 ..	27 18	.....	....	....	....	ms	26	4	6	3	126	2
	Mar. 22	17 17	25 15	s.c.	0	+14	−2	ms	23	7	6	5	113	4

[1]Approximate time of ending of storm construed as the time of cessation of reasonably marked disturbance movements in th traces; more specifically, when the *K*-index measure diminished to 2 or less for a reasonable period.

[2]s.c. = sudden commencement; s.c.* = small initial impulse followed by main impulse (the amplitude in this case is that of th *main impulse only*, neglecting the initial brief pulse); .... = gradual commencement.

[3]Signs of amplitudes of *D* and *Z* taken algebraically; *D* reckoned positive if towards the east and *Z* reckoned positive if vert cally downwards.

[4]Storm described by three degrees of activity: *m* for moderate (when *K*-index as great as 5); *ms* for moderately severe (whe *K* = 6 or 7); *s* for severe (when *K* = 8 or 9).

PRINCIPAL MAGNETIC STORMS—Continued

Observatory (Observer-in-Charge)	Greenwich date	Storm-time GMT of begin.	Storm-time GMT of ending[1]	Sudden commencement Type[2]	Amplitudes[3] D	H	Z	C-figure, degree of activity[4]	Maximal activity on K-scale 0 to 9 Gr. day	Gr. 3-hr. period	K-index	Ranges D	H	Z
(1)	(2)	(3)	(4)	(5)	(6)	(7)	(8)	(9)	(10)	(11)	(12)	(13)	(14)	(15)
	1954	*h m*	*d h*		′	γ	γ					′	γ	γ
ag	Mar. 30	08 ..	31 03	.....	....	....	....	m	30	5,8	5	5	112	23
(Continued	Apr. 11	05 ..	13 00	.....	....	....	....	ms	12	1	6	4	148	41
.Chaubal)	Sep. 6	10 ..	8 00	.....	....	....	....	m	6	7	5	5	71	51
	Sep. 13	21 ..	15 18	.....	....	....	....	m	14	4,6	5	5	102	49
	Sep. 19	03 30	21 21	.....	....	....	....	m	20	6	5	5	132	49
	Oct. 23	07 23	25 21	s.c.	0	+14	−2	m	23	4	5	4	133	41
									24	6	5			
									25	5	5			
	Oct. 27	07 47	28 00	s.c.*	0	+14	−2	m	27	4	5	3	95	29
	Nov. 23	11 44	23 23	s.c.	0	+11	−3	m	23	6	5	2	95	16
	Dec. 17	03 ..	18 03	.....	....	....	....	m	17	3,6	5	3	125	33
	1955													
	Jan. 8	06 ..	10 00	.....	....	....	....	m	9	6	5	4	67	52
	Jan. 11	12 18	12 15	s.c.	0	+14	−3	m	11	5,8	5	3	78	35
	Jan. 17	03 22	20 03	s.c.	−1	+25	....	ms	17	5,6,7	6	6	192	81
	Jan. 27	08 51	28 09	s.c.	0	+13	−3	m	27	6	5	3	81	40
	Feb. 4	06 ..	6 00	.....	....	....	....	m	4	4	5	3	106	41
	Feb. 21	03 52	23 04	s.c.	0	+23	−10	m	21	5	4	4	92	28
	Feb. 23	06 ..	24 00	.....	....	....	....	m	23	4	5	3	106	30
	Feb. 27	22 ..	28 18	.....	....	....	....	m	28	1,2,3,5,6	4	5	108	32
	Mar. 22	02 ..	24 00	.....	....	....	....	ms	22	4,5	6	7	215	47
	Mar. 30	10 36	1 00	.....	....	....	....	m	31	3	5	4	112	39
ı	May 5	15 42	7 10	.....	....	....	....	m	6	5	5	4	134	28
L.Burrows)	May 25	14 32	26 10	s.c.	0	+18	−7	ms	25	8	6	3	197	34
	June 6	17 29	7 12	s.c.	0	+5	−2	m	6	8	4	3	50	13
									7	2	4			
manus	Apr. 24	12 ..	24 24	.....	....	....	....	m	24	6,8	5	14	95	96
M.van Wijk)	(*Note* Sharp deflection at 12h 12m; inverted s.c.?)													
	Apr. 27	16 23	30 12	s.c.	+1	+16	+4	ms	27	8	7	27	136	135
	May 5	14 ..	8 24	.....	....	....	....	m	6	8	5	19	106	76
									7	1	5			
	May 25	14 33	26 19	s.c.	+1	+11	+7	ms	25	7	6	26	150	131
	June 6	17 28	7 13	s.c.	0	+3	+3	m	7	1	5	16	72	70
heroo	Apr. 27	16 24	30 13	s.c.	+1	+29	+10	ms	27	8	6	16	148	122
F.Tillott)	May 25	14 33	26 10	s.c.	+1	+20	+6	m	25	8	5	12	126	....
	(*Note*: No record of *Z* from 02h to 13h, May 26, 1955)													
	June	None												
langi	Jan. 8	18 00	9 21	.....	....	....	....	m	9	6	5	12	87	31
.	Jan. 13	02 00	.. ..	.....	....	....	....	m	....	..	..	....	....	....
veringham)	(*Note*: Record incomplete from 11h 00m on January 13)													
	Jan. 17	03 00	21 06	.....	....	....	....	ms	17	5	7	38	308	112
	Feb. 4	04 00	5 14	.....	....	....	....	m	4	4	5	13	100	31
	Feb. 11	10 00	12 11	.....	....	....	....	m	11	7,8	5	16	62	27
	(*Note*: Record incomplete from 11h 30m on February 13)													
	Feb. 23	08 30	26 16	.....	....	....	....	m	23	5	5	19	129	44
	Feb. 28	00 50	28 18	s.c.	....	19	....	m	28	5	5	21	106	31
	Mar. 30	10 35	.. ..	.....	....	....	....	..	....	....	..	....	....	....
	(*Note*: Record off from 09h 20m to 23h 59m on March 31)													
	Apr. 27	16 23	30 13	s.c.	2	28	4	ms	27	7,8	6	27	215	42
	May 5	14 45	9 14	.....	....	....	....	ms	6	5	6	24	196	59
									8	5	6			
	May 25	14 33	26 20	s.c.	2	35	6	m	25	8	5	19	95	25
									26	3,4	5			
	May 27	12 36	28 16	.....	....	....	....	m	28	3,4	5	11	120	34
	June	None												

PRINCIPAL MAGNETIC STORMS—Concluded

Observatory (Observer-in-Charge)	Greenwich date	Storm-time		Sudden commencement				C-figure, degree of activity[4]	Maximal activity on K-scale 0 to 9			Ranges		
		GMT of begin.	GMT of ending[1]	Type[2]	Amplitudes[3]				Gr. day	Gr. 3-hr. period	K-index	D	H	
					D	H	Z							
(1)	(2)	(3)	(4)	(5)	(6)	(7)	(8)	(9)	(10)	(11)	(12)	(13)	(14)	
	1955	*h m*	*d h*		′	γ	γ					′	γ	
Amberley	Mar. 30	11 ..	8 09	.....	....	....	....	m	31	1,3,4	5	17	240	
(A.L.	Apr. 10	09 32	11 16	.....	....	....	....	m	10	5	5	15	51	
Cullington)	Apr. 24	00 ..	27 09	.....	....	....	....	m	26	4	5	20	144	
	Apr. 27	16 24	30 15	s.c.*	+2	+22	−9	ms	27	7	6	37	242	
	May 5	15 ..	10 13	.....	....	....	....	ms	6	5	6	25	151	
									8	2	6			
	May 25	14 34	29 17	s.c.	+1	+25	−4	ms	26	2	6	25	167	
	June	No *K*-index greater than 4 in June.												
	1955	*Reports added in galley-proof:*												
Instituto	Apr. 24	00 45	25 05	.....	....	....	....	m	24	6	5	4	205	
Geofísico de	Apr. 27	16 24	29 06	s.c.	+2	+92	−7	ms	27	7	7	6	411	
Huancayo	May 5	02 33	7 06	.....	....	....	....	ms	6	5	6	4	222	
(A.A. Giesecke,	May 25	14 32	26 20	s.c.*	+2	+91	−5	ms	25	8	6	5	419	
Jr.)	June 22	10 39	24 18	s.c.	+1	+34	−5	m	24	6	5	6	229	
Vassouras	Apr. 27	16 24	29 03	s.c.	+2	14	+10	ms	27	7	7	12	253	
(Lelio I. Gama)	May 25	14 34	26 06	s.c.	+2	40	+13	ms	25	8	6	9	282	
	June 6	17 27	7 03	s.c.	0	14	+5	m	6	7	3	12	63	
	June 22	10 39	23 06	s.c.	+2	28	+9	m	22	4	3	7	86	

HENRY FAUL (Editor): *Nuclear geology*—"A symposium on nuclear phenomena in the earth's sciences." John Wiley and Sons, Inc., New York, and Chapman and Hall, Ltd., London, 414 pp. (1954). 23 cm. (Price $7.00)

The application of the principles of nuclear and atomic physics to geologic problems has aroused great interest in recent years and as a consequence several text-books have appeared which deal with different phases of the subject. The authors of these works have usually placed more emphasis on the geochemistry of the stable isotopes than on problems relating to the radioactive nuclei, and as a result a text covering this latter topic was badly needed.

"Nuclear Geology" fills this role.

Presented in symposium form, it describes how nuclear theory has been applied to clarify various geologic problems.

As the very nature of symposium presentation imposes constantly varying style and differing treatment of subject matter on the reader, there are some chapters which must suffer by comparison, and to try and avoid this situation a brief summary chapter by chapter follows.

The introductory chapter, outlining the fundamentals of nuclear physics, has been well written and gives the reader just a glimpse of each of the facets of the background which he will require if he intends making a comprehensive study of the field.

A valiant attempt to review the enormous amount of published work on the occurrence and distribution of uranium and thorium in various geologic sites has been made in the second chapter and, with several tables included summarizing the most recently determined abundances of uranium in various rock types, has resulted in a useful compendium of current knowledge of this subject. The concluding section on the geochemical balance in the hydrosphere is of particular importance, as great interest is at present being shown in this problem.

Chapter three is a short descriptive section on the abundance of potassium in nature and would have been better included in the previous chapter under a new heading. It is well to reiterate the caution of the author of this section that the decay constants of potassium have not been accurately determined and the values stated should be treated with reserve.

Rare gases, fission in nature, and heat from radioactivity are discussed in the next two chapters and form a useful introduction to a study of these topics.

Chapter six discusses radiation damage and energy storage, dealing particularly with the determination of the age of zircons by means of changes in their physical properties due to radiation damage. A section on thermoluminescence with some later duplication has won its way into the chapter by virtue of being a secondary effect of nuclear radiations. Considering the present state of knowledge of radiation damage relative to crystal structures, this chapter should be regarded as a preliminary report of investigations at present in progress.

Hydrocarbons formed by the effects of radioactivity are the basis of the discussion in the next chapter, the author concluding that even under the most favorable conditions the amounts generated are small.

Chapter eight on geophysical exploration by nuclear methods outlines in very

readable manner the most important aspects of the application of Geiger-Müller and scintillation counters to geophysical prospecting and assaying.

A description of nuclear logging methods as applied to the petroleum industry, mineral exploration, and soil studies completes the chapter. Sufficient description of instrumentation is given in this and the introductory chapter to allow the reader to grasp the general principles of the field equipment used.

Chapter nine on the determination of absolute age as related to rocks and minerals opens with a quotation from a nineteenth century issue of "Science" and the editor is to be congratulated on the aptness of his choice. Repetition of such a quotation will surely act as a solace to the wise and a caution to the ignorant.

> "The fascinating impressiveness of rigorous mathematical analysis, with its atmosphere of precision and elegance, should not blind us to the defects of the premises that condition the whole process."

The authors who have contributed to this large chapter, realizing the truth of this quotation, have in several instances warned the reader against drawing too many inferences from the stated ages. All the ages published in this volume rely on empirical data, such as radioactive decay constants and certain accepted decay schemes, which may be in grave error. A brief examination of the table giving the branching ratios of potassium is sufficient to show the somewhat variable state of affairs when ratios from 0.085 to 0.131 are stated for the same constant. A description is given of most of the age methods under current investigation, with perhaps over emphasis on the problems relating to helium age and the distribution of helium in rocks. Various selected ages are collected in the form of a table.

The final chapter on the origin of the earth consists of a review of past theories and a presentation of recent theories, together with the author's views on this subject. As a brief résumé of the topic, it forms an ample contribution.

Extensive bibliography and index complete the volume.

Some criticism may be leveled at certain sections which contain a wealth of detail, much of which appears to be redundant in a volume aimed at educating the "graduate student and practicing geologist." Whether lengthy tables relating to age determinations and isotopic abundances should be in the body of the text or in an appendix is a matter of opinion. Being required to pass by nine pages of tables before concluding a sentence imposes rather a strain on the free passage of information to the reader.

The importance of this book, however, lies in the fact that it constitutes an interim report on current investigations in the field of nuclear geology. The contributing authors are, for the most part, actively engaged in research in the topics which they have discussed, so that the reader is assured of having available recent information regarding any of these subjects.

With this fact in mind, the volume can be recommended to all those who are interested in geophysics, geochemistry, and allied fields and as a "must" on the shelves of geochronologists.

P. M. Jeffery
University of Western Australia,
Nedlands, Western Australia.
(Guest Investigator, Carnegie Institution,
Washington, D.C., 1955)

LETTERS TO EDITOR

THE MEASUREMENT OF THE ATMOSPHERIC DENSITY DISTRIBUTION BY THE SEARCHLIGHT TECHNIQUE

In recent issues of this JOURNAL, Elterman[1,2] has published results of the determination of atmospheric densities through an analysis of the measurements of the light scattered from a searchlight beam. The theoretical analysis presented by Elterman differs from that developed by the authors. The effect of these differing analyses upon the final results is so large that it appears worth while to submit this new one for comparison with that given by Elterman.

The light arriving at P (Fig. 1) is

$$\frac{I_0}{(r_1 \tan \varphi_1)^2} e^{-\tau l_1}$$

where I_0 is the light per cm^2 leaving the searchlight, τ is the extinction coefficient along r_1, l_1 is the equivalent path length along r_1, and r_1 and φ_1 are given in Figure 1.

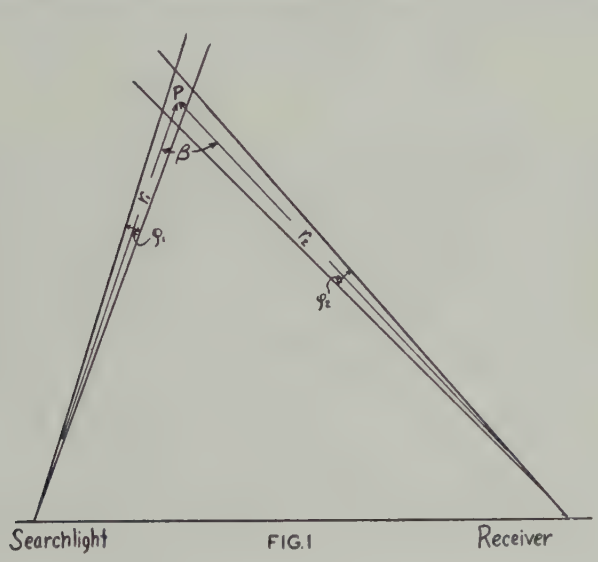

FIG. 1

Of the light arriving at the intersection of the searchlight and receiver cones, the fraction

$$\frac{2\pi^2\alpha^2 n}{\lambda^4} \frac{6(1+\rho)}{6-7\rho} \left[1 + \frac{1-\rho}{1+\rho} \cos^2 \beta\right] V$$

is scattered, where $\alpha = (\mu - 1)/n$, μ is the index of refraction of air, n is the number of molecules per cc, λ is the wavelength of the light, ρ is the depolarization coefficient

[1] L. Elterman, J. Geophys. Res., **56**, 509-520 (1951).
[2] L. Elterman, J. Geophys, Res., **59**, 351-358 (1954).

for air, β is given in Figure 1, and V is the volume of the intersection of the two cones.

The light arriving at R per cm^2 is the fraction $r_2^{-2}\, e^{-\tau l_2}$ of the light leaving the volume V where l_2 is the equivalent path length along r_2 .

Combining terms, the light arriving at R per cm ^{2} is

$$I_S = \frac{2I_0 V\pi\alpha^2 n}{(r_1 \tan\varphi_1)^2\lambda^4 r_2^2}\,\frac{6(1+\rho)}{6-7\rho}\left[1+\frac{1-\rho}{1+\rho}\cos^2\beta\right]e^{-\tau(l_1+l_2)} \quad \ldots\ldots\ldots (1)$$

If we adopt Elterman's suggestion of using the density at some height, h_1 , as a reference level to calibrate the meter reading, equation (1) reduces to

$$I_S = \frac{K_1 V n}{r_1^2 r_2^2}\left[1+\frac{1-\rho}{1+\rho}\cos^2\beta\right]e^{-\tau(l_1+l_2)} \quad \ldots\ldots\ldots\ldots\ldots (2)$$

This compares with Elterman's corresponding equation

$$I_S = K_2 n(1+\cos^2\beta) \quad \ldots\ldots\ldots\ldots\ldots\ldots\ldots (3)$$

The depolarizing term $1-\rho/1+\rho = 0.94$ and results in a small difference between the two equations. The chief point to be considered—does

$$\frac{V}{r_1^2 r_2^2}\, e^{-\tau(l_1+l_2)} \approx \text{CONSTANT}$$

If this is true, then equations (1) and (3) are of the same form. We will first discuss $e^{-\tau(l_1+l_2)}$. Elterman assumes this to be constant as long as point P is above 10 km. This is approximately true as long as the angle of elevation of the receiver θ is constant. But in the geometry used by Elterman, this angle changed throughout the range 35° to 90°. In relatively clear air, this would produce errors of approximately 10 per cent, using the values of τ given by Van de Hulst.[3] Incidentally, the extinction coefficients for clear air given in reference 1 differ by a factor of more than 13 from those usually given in the literature (see, for example, reference 3).

The evaluation of V is not a trivial problem. Maxfield and Selfridge[4] have determined V for the base-line and geometrical conditions that the authors intend to use. For these conditions, $V/r_1^2 r_2^2 \neq$ constant. No computations have been made for the base-line and angles of the searchlight beam and receiver cone given in reference 1.

EDWARD V. ASHBURN AND L. G. LAMARCA
MICHELSON LABORATORY,
U.S. NAVAL ORDNANCE TEST STATION,
Inyokern, China Lake, California, February 24, 1955
(Received February 28, 1955)

[3]H. C. Van de Hulst, The Atmosphere of the Earth and Planets, edited by Gerard P. Kuiper The University of Chicago Press, Chicago, Ill. (1949).

[4]J. Maxfield and R. G. Selfridge, Technical Note, Naval Ordnance Test Station, Inyokern, China Lake, Calif. (in press).

REPLY TO COMMENTS BY ASHBURN AND LaMARCA

Equation (1) submitted by Ashburn and LaMarca is in a general form meant to apply to all types of searchlight scene geometry and for all conditions of the atmosphere. As indicated by the writers, "the evaluation of V (the scattering volume) is not a trivial problem." This was recognized early in the investigation of the searchlight technique. It was then felt that if a suitable searchlight scene geometry was chosen, the approach used by Johnson, Meyer, Hopkins, and Mock (J. Optical Soc. Amer., **29**, 1939), which dispenses with the need for a specific evaluation of V, would yield results of sufficient accuracy. Thus, the equation used in the recent searchlight scattering work is not a generalized equation but entails the scattering volume requirement that "the opposing extremities are very nearly equal, both angularly and in length" (p. 510, ref. 1). In this respect, the searchlight scene geometry chosen (base-line 21.5 km, beam divergence 1°.25, beam elevation 60°) satisfactorily meets this requirement for the altitudes of measurement. The close agreement with radiosonde densities bears out the justification of this approach (Fig. 1, ref. 2). In line with these volume considerations, the criticism is made by Ashburn and LaMarca that their expression $V/r_1^2r_2^2$ is not constant but should be constant for the searchlight scene geometry used in the recent work. This criticism is unwarranted, since the writers indicate that no computations of $V/r_1^2r_2^2$ were made for the base-line and angles used; nor can such computations be conducted here due to their reference 4 being unpublished.

Relative to inclusion of a transmission term, it should be remembered that the recent work was conducted with the measuring instrumentation approximately two miles above sea-level in the dry atmosphere of New Mexico. Operations were carried out on clear nights only (p. 353, ref. 2). Under these conditions, it would well be in order to assume an exceptionally clear air which could be characterized by an extinction coefficient 0.1 (or smaller) of that for "relatively clear air" mentioned by Ashburn and LaMarca. The specialized operating conditions chosen is the basis for the assumption that the transmission does not vary significantly for the geometry used.

The comment that the extinction coefficients given "differ by a factor of more than 13 from those usually given in the literature" is based on a misunderstanding of the derivation and purpose of the curves in Figure 2, reference 1. The curves were not meant to provide extinction coefficients which the writers have calculated from the spectral transmissions at 40 km. Extinction coefficients so calculated would vary critically with assumed troposphere conditions. These curves were used only to show that within the spectral range of the detector the flux remaining in the beam does not vary appreciably above 10 km for a model atmosphere. Calculation with any reasonable troposphere conditions would result in a family of curves very similar in shape to those shown in Figure 2, reference 1. In this instance, *it is the flat characteristic of the curves which is important rather than the actual transmission values.* Actually, values of extinction coefficients were never presented nor applied to produce density distributions.

Louis Elterman

Geophysics Research Directorate,
Air Force Cambridge Research Center,
Cambridge 39, Massachusetts, April 28, 1955
(Received May 6, 1955)

MEASUREMENT OF THE ARRIVAL ANGLE OF "WHISTLERS"

Storey[1] has recently suggested that the atmospheric noises known as "whistlers" are due to signals from electrical disturbances in the atmosphere which have traveled along the lines of the earth's magnetic field from one hemisphere to the other.

One possible means of investigating this theory is to measure the direction of arrival of the "whistlers." If this is the same as the direction of the geomagnetic field at the measuring site, then considerable support for Storey's theory would result.

The direction of arrival of the "whistlers" can be determined by a phase-measuring method which has been used at higher frequencies.[2] Consider three aerials A, B, C placed at the corners of a triangle in which $AB = BC = d$ and angle ABC is a right-angle. If a plane wave of length λ is received at an azimuth angle α (measured from the AB direction) and an angle of elevation δ, then the phase differences ϕ_1 , ϕ_2 between the signals in the aerial pairs $A - B$, $B - C$, respectively, can be shown to be

$$\phi_1 = \frac{2\pi d}{\lambda} \cos \alpha \cos \delta$$

$$\phi_2 = \frac{2\pi d}{\lambda} \sin \alpha \cos \delta$$

$$\tan \alpha = \frac{\phi_2}{\phi_1} \quad \text{and} \quad \cos \delta = \frac{\lambda}{2\pi d} \sqrt{\phi_1^2 + \phi_2^2}$$

If, for simplicity, α is made zero and it is assumed that ϕ_1 can be measured to $\pm$ 1°, then the resulting errors in δ for various values of d/λ and δ are shown in Table 1.

TABLE 1—*Error in* δ *for* 1° *error in* ϕ_1

d/λ \ δ	60°	70°	80°
	°	°	°
0.05	±4.2	±4.0	±3.5
0.15	±1.4	±1.3	±1.2
0.25	±0.9	±0.8	±0.5

It will be seen that reasonably accurate results should be obtained for a base-line of length $d/\lambda \geq 0.15$. If Storey's theory is correct, only one pair of aerials along the direction of the horizontal component of the geomagnetic field is required. Since the vertical angle of arrival will be approximately constant, the phase-angle ϕ_1 can be determined simply. The signals from the two aerials are passed through narrow band filters having identical phase/frequency characteristics, and one of

[1]L. R. O. Storey, Phil. Trans. R. Soc., A, **246**, 113 (1953).

[2]W. Ross, E. N. Bramley, and G. E. Ashwell, Proc. Inst. Elec. Eng., **98**, Pt. 3, 294 (1951).

them is, in addition, passed through a calibrated variable phase-shifter; the resulting signals are applied to the x and y plates of a cathode-ray tube. The phase-angle between the two signals is determined by adjusting the phase-shifter on consecutive whistlers until the ellipse on the cathode-ray tube collapses into a line. With sufficient gain in each channel, a measuring accuracy of better than 1° should be attainable.

Due to the frequency variations in the whistlers, there is an optimum band-width for maximum effective selectivity. Barber and Ursell[3] have shown that the optimum band-width will be equal to the square root of the rate of change of frequency. Thus, assuming a rate of frequency change of 2.5 kc/sec^2, the optimum filter band-width is 50 cycles/sec. If the centre frequency of the filters is 3 kc/sec (chosen as a compromise between rate of change of frequency and length of base-line required), then this will give an uncertainty in δ (when $\alpha = 0$) of less than 1° for values of δ greater than 60°.

Thus, it seems that confirmation of Storey's theory could be obtained by the use of a pair of aerials spaced 15 km apart ($d/\lambda = 0.15$ at 3 kc/sec) along the direction of the horizontal component of the geomagnetic field. The signals from these are relayed, by radio link or other suitable means, to a simple phase-measuring device, and after taking account of the propagation times the vertical arrival angle is determined. If this is approximately constant and equal to the angle of dip, then the theory would appear to be substantially proved. If not, the use of a further aerial, suitably placed, should enable the directions of arrival to be determined and thus throw further light on the problems.

D. D. Crombie

Dominion Physical Laboratory,
Lower Hutt, New Zealand, June 21, 1955
(Received July 5, 1955)

[3]N. F. Barber and F. Ursell, Phil. Mag., **39**, 345 (1948).

NOTES

(24) *New ionospheric and seismological stations in Peru*—A new ionospheric station belonging to the Instituto Geofísico de Huancayo, to be known as the *Talara* station, was installed during the month of October, 1954, in the section known as Negritos (lat. 4° 37′.9 south, long. 81° 18′.4 west). The installation was carried out by the Instituto's personnel and was made possible through a small grant from the Department of Terrestrial Magnetism, Carnegie Institution of Washington, and material aid from the National Bureau of Standards. The equipment consists of the latest type C-3 ionosonde. Continuous operation began in January, 1955. Mr. Gonzalo Fernandez, of the Instituto's staff, was appointed engineer-in-charge of the station. The Instituto received from the International Petroleum Company as a gift the laboratory building, and it has also purchased from the same Company a residence for the observer and his family.

A new experimental seismological station has been completed in *Iquitos* (lat. 3° 45′.8 south, long. 73° 15′.3 west) on a provisional basis. An oil-damped Benioff vertical seismograph, formerly installed at the Huancayo station (replaced by a late model Benioff vertical), was installed by the Instituto's staff during April, 1955, and began operations on April 15, 1955. The equipment is still being adjusted for proper sensitivity, although traffic interference may eventually prove to be excessive at the present site. Should results obtained from this single seismograph prove of value, plans call for a permanent installation at another site already chosen. The equipment is being cared for by the Saint Augustine Fathers, who have graciously offered not only their services but also provided the room where the pier and dark-room have been built. The permanent installation will also include two horizontal seismographs.

The seismological station installed at *Lima* in 1908 was turned over to the Instituto at the beginning of this year. The equipment, consisting of two horizontal and one vertical Wiechert seismograph, has been overhauled completely by the Instituto's staff and has begun to operate satisfactorily within its inherent limitations. Mr. Jorge Caballero, of the Instituto's Lima office, is in charge of the station.

(25) *Merger of solar research activities*—With the ever-broadening scope of solar research, Harvard University and the Smithsonian Institution have agreed to combine the facilities of the Harvard Observatory and the Astrophysical Observatory of the Smithsonian Institution, under the directorship of Dr. Fred L. Whipple. Headquarters of the research work of the two will be located in close proximity to the Harvard Observatory in Cambridge, Massachusetts. The Smithsonian solar stations in Chile and California and the Harvard coronograph stations at Climax, Colorado, and Sacramento Peak, New Mexico, will be maintained.

(26) *Proposed publication of catalogue of geomagnetic storms, 1874-1954*—H. W. Newton and H. F. Finch, in a recent article on "Solar activity and geomagnetic storms 1954" appearing in *The Observatory* (Vol. 75, No. 884, 37-38, 1955), announced the proposed publication by the Royal Greenwich Observatory, during 1955 if possible, of two catalogues of storms in a volume to be entitled "Greenwich sunspot and geomagnetic data 1874-1954."

(27) *Centennial of death of Karl Friedrich Gauss (1777-1855)*—The year 1955 marks the hundredth anniversary of the death of Karl Friedrich Gauss, one of the world's greatest mathematicians. During 1830-1840, he became interested in mathematical physics, embracing electromagnetic theory, terrestrial magnetism, and the theory of attraction according to Newton's law. He carried out much experimental work on terrestrial magnetism and invented, among other things, the bifilar magnetometer.

(28) *New determination of the height of Mount Everest*—In Technical Paper No. 8 of the Survey of India, 23 pages, 1954, B. L. Gulatee, director of the Geodetic and Research Branch, gives the newly determined height of Mount Everest as 29,028 ± 10 feet. This is a timely announcement, in view of the recent actual conquest of Mount Everest. Whereas previous deductions of height appear to have involved some errors, these latest measurements, carried out during 1952-54, used a more rigorous technique involving a relatively complicated series of facts and ideas. Geodetic observations had to be carried out close to the peak to get quantitative figures for the distortion of the mean sea-level and the tilt of the vertical produced by the colossus. A fortunate cancellation of effects makes the new value of 29,028 feet agree closely with older values (29,002 and 29,141 feet).

(29) *Electronic data-processing machine for weather prediction*—An International Business Machine, Model 701, is about to begin turning out daily weather charts at the Joint Numerical Weather Prediction unit (joint effort of the USAF Air Weather Service, US Naval Aerology branch, and US Weather Bureau) at Suitland, Maryland. Mathematical formulas based on the dynamics of the earth's atmosphere are the basis of this new system. Electronically calculated, the movement of the air masses which cause weather variations can be predicted with reasonable accuracy. Charts produced by the computer, the first regular numerical predictions in North America, will be used at the start by the National Weather Analysis center. Eventually they will be transmitted via facsimile networks throughout the United States for use in individual weather station charts. The data are in the form of predictions of pressures expected at various heights (at approximately 3,000, 10,000, and 23,000 feet) over the United States in the next 24 and 36 hours.

(30) *Larger radio telescope for Harvard University*—Four years after the first detection of 21-cm radio emission from interstellar neutral hydrogen, at Harvard University by H. I. Ewen and E. M. Purcell, Harvard has been granted funds by the National Science Foundation to construct and operate a large radio telescope—a parabolic reflector 60 feet in diameter. Its construction will require about a year. The new instrument will supplement rather than replace the present smaller one. The 60-foot one will have approximately three times the resolving power of the 25-foot antenna, allowing positions of radio sources to be determined within about half a degree. One important task for the 60-foot dish will be the examination of Milky Way areas where small, dense, dark clouds, rich in neutral hydrogen, abound.

(31) *New radio telescope for the Department of Terrestrial Magnetism, Carnegie Institution of Washington*—The trustees of the Carnegie Institution of Washington have granted funds towards the construction of a large radio telescope. Contract

has been given to the D. S. Kennedy Company, of Cohasset, Massachusetts, to fabricate a 60-foot paraboloid. The paraboloid will be so constructed that a 12-foot rim can be attached later, making a total diameter of 84 feet, focal length 25 feet. Distortion tests on a similar paraboloid have shown that the dish is so rigid that under gravity and small wind load the deviation from the paraboloid will be approximately one millimeter.

(32) *Meeting of International Geological Congress*—The twentieth session of the International Geological Congress took place in Mexico City, September 4-11, 1955. Some of the topics treated at the meetings were (1) vulcanology of the Cenozoic, (2) the Mesozoic of the western hemisphere and its world-wide correlations, (3) the geology of petroleum, (4) relations between tectonics and sedimentation, (5) modern ideas on the origin of mineral deposits, and (6) applied geophysics.

(33) *Conference on airglow and aurrorae*—A conference on airglow and aurorae was held at the Queen's University, Belfast, Ireland, September 6 and 7, 1955, immediately following the Dublin assembly of the International Astronomical Union. Prof. S. Chapman presided. The primary purpose of the conference was to provide observers and theoretical workers actively engaged in the field with an opportunity of meeting and exchanging views on problems of common interest.

(34) *Geomagnetic activities of the United States Coast and Geodetic Survey*—Two volumes of the MHV series of publications were issued, giving magnetic hourly values and reproductions of magnetograms for College, 1950, and for Cheltenham, 1952.

Lt. Rojana Hongprasith and Capt. Vera Suvannus of Thailand and Sr. Sergio Ferraes G. of Mexico have been studying the methods and procedures of the U.S. Coast and Geodetic Survey in office and field work in geomagnetism.

Six student trainees in geophysics have been employed by the U.S. Coast and Geodetic Survey for the summer months of 1955, as a first step in the recruiting program for geophysicists to be used in the International Geophysical Year. The students, who have finished their junior year in college, are expected to develop an interest in geomagnetism that will lead them back to the Survey next year for more intensive training in magnetic field work.

Mr. Joel B. Campbell, of the Cheltenham Magnetic Observatory, U.S. Coast and Geodetic Survey, will be in charge of the field operations of the International Geophysical Year program in geomagnetism. His time is now divided between the observatory and the I.G.Y. planning.

(35) *Personalia*—Sir *Edward Bullard* is resigning from the directorship of the National Physical Laboratory, Teddington, England, which he has held since 1950. He will return to Cambridge University as a Fellow of Caius College, to undertake research in geophysics. He will, therefore, pursue his former interests of the earth sciences, to which he has made important contributions.

The National Science Foundation has established an Office for the International Geophysical Year. The new office will be headed by Dr. *J. Wallace Joyce*, who has been a member of the staff of the Assistant Secretary of Defense for Applications Engineering.

GEORGE HARTNELL, 1871–1955

Word has been received of the death of George Hartnell at Wyoming, New York, on May 20, 1955, following several months' illness. He was born at Bergen, New York, on March 21, 1871, and attended Lafayette College at Easton, Pennsylvania. After several years devoted to optical manufacturing, he joined the staff of the United States Coast and Geodetic Survey in 1908. Three years later, he was placed in charge of the Cheltenham Magnetic Observatory, holding this trust through a lengthy period of ever-increasing responsibility attaching to the activities of this key observatory. At the same time, he conducted important theoretical and practical studies on deflection observations, variometer scale-values and temperature compensation, and related topics.

Mr. Hartnell's unstinting devotion to the advancement of geophysics is commemorated in the pages of this JOURNAL and elsewhere by numerous accounts of magnetic storms, by technical papers, and by official publications. After his retirement (noted in *Terr. Mag.*, vol. 46, pp. 254-255, 1941), he took an active part in developing the geology, the botany, and the rich historical material of his native region.

He was married in 1908 to Lillian A. Freeman, whose death preceded his own by two months. He is survived by his four children, Mrs. Wirt F. Smith of Washington, D.C., Mrs. Edward K. Gladding of New Castle, Delaware, George F. Hartnell of Fredericksburg, Virginia, and Freeman H. Hartnell of Corning, New York, and by two grandchildren.

LIST OF RECENT PUBLICATIONS

By W. E. Scott

Department of Terrestrial Magnetism,
Carnegie Institution of Washington,
Washington **15**, *D. C.*

(Received June 28, 1955)

A—*Terrestrial Magnetism*

Ahmed, S. J., and W. E. Scott. Time relationship of small magnetic disturbances in arctic and antarctic. J. Geophys. Res., **60**, No. 2, 147-154 (1955).

Akimoto, S. Magnetic properties of ferromagnetic minerals contained in igneous rocks. Japanese J. Geophys., **1**, No. 2, 31 pp. (May, 1955).

Asami, E. Reverse and natural magnetism of the basaltic lavas at Kawajiri-misaki, Japan. J. Geomag. Geoelectr., **6**, No. 3, 145-152 (1954).

Bartels, J. The contrast between geomagnetic **S** and **L** at Huancayo. Indian J. Met. Geophys., **5**, special geomagnetic number, 69-74 (1954).

Bartels, J., and J. Veldkamp. International data on magnetic disturbances, fourth quarter, 1954. J. Geophys. Res., **60**, No. 2, 219-224 (1955).

Beiser, A. On an interplanetary magnetic field. J. Geophys. Res., **60**, No. 2, 155-159 (1955).

Beiser, A. Solar-terrestrial time delays. J. Geophys. Res., **60**, No. 2, 161-164 (1955).

Chapman, S. Notes on the theory of magnetic storms. Indian J. Met. Geophys., **5**, special geomagnetic number, 33-40 (1954).

Coulomb, J. Variation séculaire par convergence ou divergence à la surface du noyau. Ann. Géophys., **11**, No. 1, 80-82 (1955).

Einarsson, T., and T. Sigurgeirsson. Rock magnetism in Iceland. Nature, **175**, 892 (May 21, 1955). [Letter to Editor.]

Ferraro, V. C. A. On the emission of electric currents from the sun. Indian J. Met. Geophys., **5**, special geomagnetic number, 157-160 (1954).

Fleming, J. A. International aspects of geomagnetism in India. Indian J. Met. Geophys., **5**, special geomagnetic number, 41-50 (1954).

Giorgi, M., e F. Molina. Campo normale e variazione secolare media degli elementi magnetici in Sicilia. Ann. Geofis., Roma, **7**, No. 4, 521-537 (1954).

Inglis, D. R. Theories of the earth's magnetism. Rev. Modern Phys., **27**, No. 2, 212-248 (1955).

Junge, C. Bai-Untersuchungen am Geophysikalischen Observatorium Collm. Beitr. Geophysik, **64**, Heft 3, 173-193 (1955).

Kakioka Magnetic Observatory. Report of the Kakioka Magnetic Observatory, geomagnetism, 1942, 1943. Kakioka, No. 19, 112 pp. + 10 pls. (1954). 30 cm.

Knapp, D. G. The synthesis of external magnetic fields by means of radial internal dipoles. Ann. Géophys., **11**, No. 1, 83-90 (1955).

Lewis, R. P. W. The geomagnetic post-perturbation effect. J. Atmos. Terr. Phys., **6**, Nos. 2/3, 129-132 (1955).

Lewis, R. P. W., and D. H. McIntosh. The relation between the geomagnetic field and range disturbance in various latitudes. Indian J. Met. Geophys., **5**, special geomagnetic number, 51-62 (1954).

Lowes, F. J. Secular variation and the non-dipole field. Ann. Géophys., **11**, No. 1, 91-94 (1955).

Madagascar. Quelques mesures de la déclinaison magnétique dans le sud et l'ouest de Madagascar, par le R. P. Louis Cattala; and Recherches sur la variation de la déclinaison magnétique à Madagascar, par le R. P. Charles Poisson. Service Géologique, Tananarive, 15 pp. + 21 pls., min. (1955). 32 cm.

Malurkar, S. L. Transients of magnetographs and instantaneous values from recordings. Proc. Nat. Inst. Sci. India, **20**, No. 5, 567-569 (1954).

McDonald, K. L. Geomagnetic secular variations at the core-mantle boundary. Salt Lake City, University of Utah, Tech. Rep. No. 15, 23 pp. + 6 figs., mim. (March 15, 1955).

Meyer, O., and D. Voppel. Ein Theodolit zur Messung des erdmagnetischen Feldes mit der Förstersonde als Nullfeldindikator. D. Hydrogr. *Zs.*, **7**, Heft 3/4, 73-77 (1955).

Miguel, L. de. Saltos bruscos en corrientes telúricas y su relacion con los impulsos bruscos del campo magnético terrestre. Rev. Geofísica, **13**, No. 50, 155-167 (1954).

Nagata, T., and S. Abe. Notes on the distribution of SC* in high latitudes. Rep. Ionosphere Res. Japan, **9**, No. 1, 39-44 (1955).

Nagata, T., and N. Fukushima. Characteristics of polar magnetic storms. Indian J. Met. Geophys., **5**, special geomagnetic number, 75-88 (1954).

Néel, L. Some theoretical aspects of rock-magnetism. Adv. Phys., **4**, No. 14, 191-243 (1955).

Nicholls, G. D. The mineralogy of rock magnetism. Adv. Phys., **4**, No. 14, 113-190 (1955).

Olczak, T. Secular variation of the magnetic declination at Gdańsk. Acta Geophys. Polonica, **3**, No. 1, 27-31 (1955). [In English.]

Pramanik, S. K., and M. K. Ganguli. Sunspots and geomagnetic variation. Indian J. Met. Geophys., **5**, special geomagnetic number, 161-178 (1954).

Princep, J. M. Distribución diurna de los tipos fundamentales de bahias geomagnéticas en Tortosa, Cheltenham, Tucson y San Juan. Rev. Geofíscia, **13**, Nos. 51 and 52, 217-231 (1954).

Rikitake, T., and I. Yokoyama. Volcanic activity and changes in geomagnetism. J. Geophys. Res., **60**, No. 2, 165-172 (1955).

Runcorn, S. K. A relationship between the geomagnetic secular variation rates. J. Geophys. Res., **60**, No. 2, 231 (1955). [Letter to Editor.]

Runcorn, S. K. Core motions and reversals of the geomagnetic field. Ann. Géophys., **11**, No. 1 73-79 (1955).

Runcorn, S. K. Rock magnetism—geophysical aspects. Adv. Phys., **4**, No. 14, 244-291 (1955).

Sen Gupta, P. K. Magnetic storms and solar *M*-regions. Indian J. Met. Geophys., **5**, special geomagnetic number, 179-188 (1954).

Simon, P. Éruptions chromosphériques particulièrement importantes et activité géomagnétique. Paris, C.-R. Acad. sci., **240**, No. 10, 1056-1058 (1955).

Slaucitajs, L. El origen físico del campo geomagnético. Observatorio Astronómico de la Universidad Nacional de Eva Perón, Serie especial No. 19, 31 pp. (1954). 26 cm.

Takeuchi, H., and Y. Shima. On a self-exciting process in magneto-hydrodynamics (III). J. Phys. Earth, **2**, No. 1, 5-26 (1954). [Also in Geophys. Notes, Tokyo, **7**, No. 2, 1954.]

Teoloyucan, Observatorio Magnético de. Valores magnéticos correspondientes al. 2°. Semestre de 1953. Universidad Nacional de Mexico, Instituto de Geofísica, 23 pp., mim. (1953). 27 cm.

United States Coast and Geodetic Survey. Magnetograms and hourly values, Cheltenham, Maryland, 1952. Washington, D.C., U.S. Coast Geod. Surv., No. MHV-Ch52, 149 pp. (1954). 25 cm.

United States Coast and Geodetic Survey. Magnetograms and hourly values, College, Alaska, 1950. Washington, D.C., U.S. Coast Geod. Surv., No. MHV-Co50, 200 pp. (1954).

Veldkamp, J., and J. G. Scholte. Some remarks on the equatorial electrojet, as revealed by the analysis of solar flare effects. Indian J. Met. Geophys., **5**, special geomagnetic number, 203-212 (1954).

Vestine, E. H. Relations between flucatuations in the earth's rotation, the variation of latitude, and geomagnetism. Ann. Géophys., **11**, No. 1, 103 (1955).

B—*Terrestrial Electricity*

Chalmers, J. A., and W. W. Mapleson. Point discharge currents from a captive balloon. J. Atmos. Terr. Phys., **6**, Nos. 2/3, 149-159 (1955).

Kakioka Magnetic Observatory. Report of the Kakioka Magnetic Observatory, geoelectricity, 1941-1945. Kakioka, No. 18, 274 pp. (1954). 30 cm.

Miguel, L. de. Aparato contador automatico de iones. Instituto Geogràfico y Catastral, Observatorio Central Geofísico de Toledo, 15 pp. (1954). 23 cm.

Müller-Hillebrand, D. Charge generation in thunderstorms by collision of ice crystals with graupel, falling through a vertical electric field. Tellus, **6**, No. 4, 367-381 (1954).

Pierce. E. T. Electrostatic field-changes due to lightning discharges. Q. J. R. Met. Soc., **81**, No. 348, 211-228 (1955).

Pierce, E. T. The development of lightning discharges. Q. J. R. Met. Soc., **81**, No. 348, 229-240 (1955).

Smith, L. G. The electric charge of raindrops. Q. J. R. Met. Soc., **81**, No. 347, 23-47 (1955).

Srivastava, C. M., and S. R. Khastgir. On the maintenance of current in the stepped leader stroke of a lightning discharge. J. Sci. Industr. Res., New Delhi, B, **14**, No. 1, 34-35 (1955). [Letter to Editor.]

Telford, J. W., N. S. Thorndike, and E. G. Bowen. The coalescence between small water drops. Q. J. R. Met. Soc., **81**, No. 348, 241-250 (1955).

C—*Cosmic Rays*

Graham, J. W., and S. E. Forbush. Solar flare and magnetic storm effects in cosmic-ray intensity near the geomagnetic N pole. Phys. Rev., **98**, No. 5, 1348-1349 (1955).

Kitamura, M. What types of magnetic storm are accompanied by the decreases of the intensity of cosmic rays? Indian J. Met. Geophys., **5**, special geomagnetic number, 153-156 (1954).

Neher, H. V., and E. A. Stern. "Knee" of the cosmic-ray latitude curve. Phys. Rev., **98**, No. 3, 845-846 (1955). [Letter to Editor.]

Pomerantz, M. A. Latitude effect of cosmic radiation at low altitudes. Phys. Rev., **98**, No. 1, 105-106 (1955).

Powell, C. F. The primary cosmic radiation. Observatory, **75**, No. 884, 14-27 (1955). [The Halley lecture, Oxford, May 4, 1954.]

D—*Upper Air Research*

Aitchison, G. J., and G. L. Goodwin. Ionospheric self-interaction of radio waves at vertical incidence. Nuovo Cimento, Ser. decima, **1**, No. 4, 722-725 (1955).

Appleton, E., and W. J. G. Beynon. An ionospheric attenuation equivalence theorem. J. Atmos. Terr. Phys., **6**, Nos. 2/3, 141-148 (1955).

Ashburn, E. V. Photometry of the aurora. J. Geophys. Res., **60**, No. 2, 205-211 (1955).

Auroral Physics, Conference on. Proceedings of the Conference on Auroral Physics, July 23-26, 1951, at London, Ontario, Canada (edited by N. C. Gerson, chairman, T. J. Keneshea, and R. J. Donaldson, Jr.). Air Force Cambridge Res. Center, Geophys. Res. Papers No. 30, 459 pp. (July 1954). 28 cm. [The conference was jointly sponsored by the Geophysics Research Directorate of the USAF Cambridge Research Center and the Department of Physics of the University of Western Ontario, Canada.]

Banerji, R. B. The mechanism of fading of 150 kc pulses. Pennsylvania State University, Ionosphere Res. Lab., Sci. Rep. No. 71, 29 pp., mim. (Nov. 15, 1954). 28 cm.

Baral, S. S. Studies on the sunrise effect in regions *E* and *F*. J. Atmos. Terr. Phys., **6**, Nos. 2/3, 160-170 (1955).

Bibl, K., R. Busch, K. Rawer, et K. Suchy. La nomenclature ionospherique et les conventions pour le dépouillement. J. Atmos. Terr. Phys., **6**, Nos. 2/3, 69-87 (1955).

Booker, H. G., and J. T. deBettencourt. Theory of radio transmission by tropospheric scattering using very narrow beams. Proc. Inst. Radio Eng., **43**, No. 3, 281-290 (1955).

Bullough, K., and T. R. Kaiser. Radio reflections from aurorae—II. J. Atmos. Terr. Phys., **6**, No. 4, 198-214 (1955).

Cox, J. W., and K. Davies. Statistical studies of polar radio blackouts. Can. J. Phys., **32**, 743-756 (Dec., 1954).

Dyce, R. VHF auroral and sporadic-*E* propagation from Cedar Rapids, Iowa, to Ithaca, New York. Inst. Radio Eng. Trans. on Antennas and Propagation, **AP-3**, No. 2, 76-80 (1955).

Forbush, S. E., and E. H. Vestine. Ionospheric magnetic fields during marked decrease in cosmis rays. Indian J. Met. Geophys., **5**, special geomagnetic number, 113-116 (1954).

Gerson, N. C. Sporadic *E* propagation. J. Atmos. Terr. Phys., **6**, Nos. 2/3, 113-116 (1955).

Hagg, E. L., and G. H. Hanson. Motion of clouds of abnormal ionization in the auroral and polar regions. Can. J. Phys., **32**, 790-798 (Dec., 1954).

Heisler, L. H. A panoramic ionospheric recorder for the study of travelling disturbances in the ionosphere. Aust. J. Appl. Sci., **6**, No. 1, 1-6 (1955).

Hirono, M., and H. Maeda. Geomagnetic distortion of the *F*2 region on the magnetic equator. J. Geomag. Geoelectr., **6**, No. 3, 127-144 (1954).

International Council of Scientific Unions, Joint Commission on Radio-Meteorology. Proceedings of the third meeting held at Brussels, August 16-18, 1954. Secrétariat Général de l'U.R.S.I., Bruxelles, 30 pp. (1955). 24 cm. [This publication may be obtained from the General Secretariat of the U. R. S. I., 42 rue des Minimes, Brussels, Belgium, at the following price: 25 Belgian francs, or 4 shillings, or $0.50 U.S., postpaid.]

Johnson, C. Y., and E. B. Meadows. First investigation of ambient positive-ion composition to 219 km by rocket-borne spectrometer. J. Geophys. Res., **60**, No. 2, 193-203 (1955).

Karandikar, R. V. Search for discontinuities in the brightness of the twilight sky. J. Optical Soc. Amer., **45**, No. 5, 389-392 (1955).

Kato, S. On the solar Lyman beta radiation and the ionosphere. J. Geomag. Geoelectr., **6**, No. 3, 153-156 (1954). [Letter to Editor.]

Kim, C. C., and C. Dickerman. On the analysis of experimental recombinance data using a non-uniform recombinance model proposed by Chapman. J. Geophys. Res., **60**, No. 2, 229-230 (1955). [Letter to Editor.]

Landseer-Jones, B. C. The significance of a nonterrestrial magnetic field in neutral stream theories of the aurora. J. Atmos. Terr. Phys., **6**, No. 4, 215-226 (1955).

Meek, J. H., and A. G. McNamara. Magnetic disturbances, sporadic *E*, and radio echoes associated with the aurora. Can. J. Phys., **32**, 326-329 (May, 1954).

Meinel, A. B. The morphology of the aurora. Proc. Nat. Acad. Sci., **40**, No. 10, 943-950 (1954).

Minnis, C. M. Ionospheric behaviour at Khartoum during the eclipse of 25th February 1952. J. Atmos. Terr. Phys., **6**, Nos. 2/3, 91-112 (1955).

Nicolet, M. Meteor ionization and the nighttime *E* layer. Pennsylvania State University, Ionosphere Res. Lab., Sci., Rep. No. 72, 25 pp., mim. (Nov. 30, 1954). 28 cm.

Oguti, T., and T. Nagata. Model experiments of the screening effect of the ionosphere. Rep. Ionosphere Res. Japan, **8**, No. 4, 171-184 (1954).

Osborne, B. W. Horizontal movements of ionization in the equatorial *F*-region. J. Atmos. Terr. Phys., **6**, Nos. 2/3, 117-123 (1955).

Parkinson, R. W. The nighttime lower ionsphere as deduced from a theoretical and experimental investigation of coupling phenomena at 150 kc/sec. Pennsylvania State University, Ionospheric Res. Lab., Sci. Rep. No. 73, 65 pp., mim. (Dec. 15, 1954). 28 cm.

Parkinson, R. W. Instrumentation for the continuous measurement of certain ionospheric echo characteristics. Rev. Sci. Instr., **26**, No. 4, 319-323 (1955).

Pfister, W., J. C. Ulwick, and R. J. Marcou. Further remarks on bifurcation in the *E*-layer. Phys. Rev., **97**, No. 4, 1183-1184 (1955).

Phillips, G. J. An apparatus for recording time-delays between radio fading characteristics. J. Atmos. Terr. Phys., **6**, Nos. 2/3, 124-128 (1955).

Saha, K. R. Atmospheric turbulence and diffusion—Part II. Indian J. Met. Geophys., 5, No. 4, 297-304 (1954).

St. Amand, P., H. B. Pettit, F. E. Roach, and D. R. Williams. On a new method of determining the height of the nightglow. J. Atmos. Terr. Phys., **6**, No. 4, 189-197 (1955).

Sato, T. On anomalous variations of maximum electron density and its height in the *F*2 region of the ionosphere. J. Geomag. Geoelectr., **6**, No. 3, 99-119 (1954).

Sato, T., and T. Namikawa. On latitudinal distributions of diurnal and semi-diurnal components of h' *F*2 of the ionosphere. J. Geomag. Geoelectr., **6**, No. 3, 157-159 (1954). [Letter to Editor.]

Seddon, J. C., and J. E. Jackson. Absence of bifurcation in the *E*-layer. Phys. Rev., **97**, No. 4, 1182-1183 (1955).

Skinner, N. J., and R. W. Wright. Some geomagnetic effects in the equatorial F_2-region. J. Atmos. Terr. Phys., **6**, No. 4, 177-188 (1955).

Straker, T. W. The ionosphere propagation of radio waves of frequency 16 kc/s over short distances. Proc. Inst. Radio Eng., B, **102**, No. 3, 396-399 (1955). [Digest of an Institution monograph.]

Vegard, L. Intensity variations of auroral hydrogen lines and the influence of the solar proton radiation on the auroral luminescence. Geofys. Pub., Oslo, **19**, No. 4, 10 pp. (1955).

Vegard, L., and G. Kvifte. Theory and observations of the enhancement of auroral hydrogen lines with increasing distance from the magnetic axis point. Geofys. Pub., Oslo, **19**, No. 2, 10 pp. + 1 pl. (1954).

Vegard, L., G. Kvifte, A. Omholt, and S. Larsen. Studies of the twilight sodium lines from observations at Oslo and Tromsö, and results of auroral spectrograms from Oslo. Geofys. Pub., Oslo, **19**, No. 3, 22 pp. + 6 pls. (1955).

Warwick, C. S. Flare height and association with SID's. Astroph. J., **121**, No. 2, 385-390 (1955).

Yerg, D. G. Notes on correlation methods for evaluating ionospheric winds from radio fading records. J. Geophys. Res., **60**, No. 2, 173-185 (1955).

E—*Radio Astronomy*

Burke, B. F., and K. L. Franklin. Observations of a variable radio source associated with the planet Jupiter. J. Geophys. Res., **60**, No. 2, 213-217 (1955).

Christiansen, W. N., and J. A. Warburton. The sun in two-dimensions at 21 cm. Observatory, **75**, No. 884, 9-10 (1955).

Eshleman, V. R., P. B. Gallagher, and A. M. Peterson. Continuous radar echoes from meteor ionization trails. Proc. Inst. Radio Eng., **43**, No. 4, 489 (1955).

Greenhow, J. S., and E. L. Neufeld. The diffusion of ionized meteor trails in the upper atmosphere. J. Atmos. Terr. Phys., **6**, Nos. 2/3, 133-140 (1955).

Hartz, T. R. A solar noise outburst of January 15, 1955. Nature, **175**, 908-909 (May 21, 1955). [Letter to Editor.]

Hewish, A. The irregular structure of the outer regions of the solar corona. Proc. R. Soc., **228**, No. 1173, 238-251 (1955).

Kraus, J. D. Distribution of radio brightness across the Andromeda nebula. Nature, **175**, 502-503 (March 19, 1955).

Morgan, W. W. The spiral structure of the galaxy. Sci. Amer., **192**, No. 5, 42-48 (1955).

O'Brien, P. A., and E. Tandberg-Hanssen. Distribution of radio-frequency brightness across the solar disk at a wavelength of 60 cm. Observatory, **75**, No. 884, 11-13 (1955).

Sen, H. K. Nonlinear theory of space-charge wave in moving, interacting electron beams with application to solar radio noise. Phys. Rev., **97**, No. 4, 849-855 (1955).

Tandberg-Hanssen, E. On the correlation between radio-frequency radiation from the sun and solar activity. Astroph. J., **121**, No. 2, 367-375 (1955).

Walsh, D., and Hanbury Brown. A radio survey of the great loop in Cygnus. Nature, **175**, 808-809 (May 7, 1955).

Wild, J. P. Radio waves from the sun. Sci. Amer., **192**, No. 6, 40-44 (1955).

F—*Earth's Crust and Interior*

Båth, M. The density ratio at the boundary of the earth's core. Tellus, **6**, No. 4, 408-414 (1954).

Bullard, E. C. Introduction to a discussion on "Movements in the earth's core and electrical conductivity." Ann. Géophys., **11**, No. 1, 49-52 (1955).

Bullen, K. E. Physical properties of the earth's core. Ann. Géophys., **11**, No. 1, 53-64 (1955).

Ewing, M., J. L. Worzel, D. B. Ericson, and B. C. Heezen. Geophysical and geological investigations in the Gulf of Mexico, Part I. Geophysics, **20**, No. 1, 1-18 (1955).

Flint, R. F., and M. Rubin. Radiocarbon dates of pre-Mankato events in eastern and central North America. Science, **121**, 649-658 (May 6, 1955).

Gutenberg, B. Channel waves in the earth's crust. Geophysics, **20**, No. 2, 283-294 (1955).

Hawkes, L. Evolution of the earth. Nature, **175**, 575-576 (April 2, 1955). [Résumé of a joint discussion of the Geological and Royal Astronomical Societies, held at Burlington House on

February 2 to consider problems discussed by the late Dr. G. M. Lees in his presidential address to the Geological Society in 1953—"The evolution of a shrinking earth" (Q. J. Geol. Soc., **109**, 217-257, 1953).]

Howell, B. F., Jr., and D. Budenstein. Energy distribution in explosion-generated seismic pulses. Geophysics, **20**, No. 1, 33-52 (1955).

Hughes, H. The pressure effect on the electrical conductivity of peridot. J. Geophys. Res., **60**, No. 2, 187-191 (1955).

Jacobs, J. A. Inside the earth. J. R. Astr. Soc. Can., **49**, No. 3, 97-113 (1955).

Powers, H. A. Composition and origin of basaltic magma of the Hawaiian Islands. Geochim. et Cosmochim. Acta, **7**, Nos. 1/2, 77-107 (1955).

Reinhardt, H.-G. Steinbruchsprengungen zur Erforschung des tieferen Untergrundes (Grundlagen, bisherige Ergebnisse und Ausführungsmoglichkeiten in der DDR). Freiberger Forschungshefte, **C15** (Geophysik), 92 pp. (1954). 24 cm.

Revelle, R., and W. Munk. Evidence from the rotation of the earth. [As relating to geophysical discussion on "Movements in the earth's core and electrical conductivity."] Ann. Géophys., **11**, No. 1, 104-108 (1955).

Rikitake, T. Electrical conductivity of the earth's core. Ann. Géophys., **11**, No. 1, 95-97 (1955).

Runcorn, S. K. The electrical conductivity of the earth's mantle. Trans. Amer. Geophys. Union, **36**, No. 2, 191-198 (1955).

Runcorn, S. K., and D. C. Tozer. The electrical conductivity of olivine at high temperatures and pressures. Ann. Géophys., **11**, No. 1, 98-102 (1955).

Urey, H. C. Distribution of elements in the meteorites and the earth and the origin of heat in the earth's core. Ann. Géophys., **11**, No. 1, 65-72 (1955).

Wahlstrom, E. E. Petrographic mineralogy. John Wiley and Sons, Inc., New York, 408 pp. (1955).

G—*Miscellaneous*

Alfvén, H. Magneto-hydrodynamic waves and solar prominences. Indian J. Met. Geophys., **5**, special geomagnetic number, 133-136 (1954).

Babcock, H. W., and H. D. Babcock. The sun's magnetic field, 1952-1954. Astroph. J., **121**, No. 2, 349-366 (1955).

Chapman, S. Scientific programme of the International Geophysical Year 1957-58. Nature, **175**, 402-406 (March 5, 1955).

Conseil International des Unions Scientifiques. Huitième Rapport, Commission pour l'Étude des Relations entre les Phénomènes Solaires et Terrestres. Paris, J. and R. Sennac, 184 pp. (1954). 20 cm.

Das, A. K. Solar radiation in the far ultraviolet and some related geophysical phenomena. Indian J. Met. Geophys., **5**, special geomagnetic number, 141-152 (1954).

Dungey, J. W. Solar electrodynamics. J. Atmos. Terr. Phys., **6**, Nos. 2/3, 88-90 (1955).

Ebro, Observatorio del. Heliofísica (1952 and 1953). Tortosa, Bol. Observatorio del Ebro, **40**, 47 pp. (1954), and **41**, 35 pp. (1955). 25 cm.

Japan. Geophysical papers dedicated to Professor Mankichi Hasegawa by his friends and pupils on his sixtieth birthday, January 2nd, 1954. Sixty contributions, ~ 1,000 pp. (1954). 25 cm. Bd.

Malurkar, S. L. The solar flare effect at Alibag on June 13th, 1951. Ann. Geofis., Roma, **7**, No. 2, 215-219 (1954).

Parker, E. N. The formation of sunspots from the solar toroidal field. Astroph. J., **121**, No. 2, 491-507 (1955).

Redman, R. O., and Z. Suemoto. Temperature and turbulence in the chromosphere. Mon. Not. R. Astr. Soc., **114**, No. 5, 524-539 (1955).

Schove, D. J. The sunspot cycle, 649 B.C. to A.D. 2000. J. Geophys. Res., **60**, No. 2, 127-146 (1955).

Smyth, M. J. Photoelectric investigations of solar corpuscular radiation, II. Mon. Not. R. Astr. Soc., **114**, No. 5, 503-513 (1955).

Warwick, J. W. Heights of solar flares. Astroph. J., **121**, No. 2, 376-384 (1955).

NOTICE

When available, single unbound volumes can be supplied at $6 each and single numbers at $2 each, postpaid.

Charges for reprints and covers

Reprints can be supplied, but prices have increased considerably and costs depend on the number of articles per issue for which reprints are requested. It is no longer possible to publish a schedule of reprint charges, but if reprints are requested approximate estimates will be given when galley proofs are sent to authors. Reprints without covers are least expensive; standard covers (with title and author) can be supplied at an additional charge. Special printing on covers can also be supplied at further additional charge.

Fifty reprints, without covers, will be given to institutions paying the publication charge of $8 per page.

Alterations

Major alterations made by authors in proof will be charged at cost. Authors are requested, therefore, to make final revisions on their typewritten manuscripts.

Orders for back issues and reprints should be sent to Editorial Office, 5241 Broad Branch Road, N.W., Washington 15, D.C., U.S.A.

Subscriptions are handled by The Editorial Office, 5241 Broad Branch Road, N.W., Washington 15, D.C., U.S.A.

CONTENTS—Concluded